AD_____

Award Number: DAMD17-01-1-0382

TITLE: The Role of Fps in Tumor-Associated Angiogenesis

PRINCIPAL INVESTIGATOR: Waheed Sangrar, Ph.D.
Peter A. Greer, Ph.D.

CONTRACTING ORGANIZATION: Queen's University
Kingston Ontario Canada K7L 3N6

REPORT DATE: July 2004

TYPE OF REPORT: Annual Summary

PREPARED FOR: U.S. Army Medical Research and Materiel Command
Fort Detrick, Maryland 21702-5012

REPORT DOCUMENTATION PAGE

Form Approved
OMB No. 074-0188

1. AGENCY USE ONLY (Leave blank)	2. REPORT DATE	3. REPORT TYPE AND DATES COVERED
	July 2004	Annual Summary (1 Jul 01-30 Jun 04)

4. TITLE AND SUBTITLE
The Role of Fps in Tumor-Associated Angiogenesis

5. FUNDING NUMBERS
DAMD17-01-1-0382

6. AUTHOR(S)
Waheed Sangrar, Ph.D.
Peter A. Greer, Ph.D.

7. PERFORMING ORGANIZATION NAME(S) AND ADDRESS(ES)
Queen's University
Kingston Ontario Canada K7L 3N6

E-Mail: ws4@post.queensu.ca

8. PERFORMING ORGANIZATION REPORT NUMBER

9. SPONSORING / MONITORING AGENCY NAME(S) AND ADDRESS(ES)
U.S. Army Medical Research and Materiel Command
Fort Detrick, Maryland 21702-5012

10. SPONSORING / MONITORING AGENCY REPORT NUMBER

11. SUPPLEMENTARY NOTES

12a. DISTRIBUTION / AVAILABILITY STATEMENT
Approved for Public Release; Distribution Unlimited

12b. DISTRIBUTION CODE

13. ABSTRACT (Maximum 200 Words)

Fps and Fer are members of a unique family of cytoplasmic tyrosine kinases. Transgenic expression of Fps in mice (*fps*^{MF}) gave rise to hyper-vascularity and multi-focal hemangiomas implicating this kinase in angiogenic regulation. This phenotype suggested that tumorigenesis and metastases may be promoted in these mice and conversely, inhibited in *fps* loss-of-function mice. Surprisingly, we observed early onset of tumors in *fps* loss-of-function mice (relative to *wild type*) suggesting that Fps has a tumor suppressor-like function. Characterization of the vessels in *fps*^{MF} mice showed that their vessels were leaky, and that vascularity was increased approximately 1.7-fold. In addition, it was shown that the vascular defects in these mice correlated with VEGF- and PDGF-activation of gain-of-function Fps in endothelial cells. Numerous hematological and hemostatic defects associated with the angiogenic phenotype were also observed. Interestingly, these abnormalities were reminiscent of Kasabach Merritt Syndrome and disseminated intravascular coagulation. Collectively, these data suggested that the vascular abnormalities in *fps*^{MF} mice are a result of a defect/delay in vascular maturation. As well, they suggest that Fps influences the processes of angiogenesis and hemostasis through regulatory effects on the endothelium.

14. SUBJECT TERMS
Transgenic mice, breast cancer, tumorigenesis, angiogenesis, Tyrosine kinase, cytokines, oncogenes, hemangioma, metastases

15. NUMBER OF PAGES
114

16. PRICE CODE

17. SECURITY CLASSIFICATION OF REPORT	18. SECURITY CLASSIFICATION OF THIS PAGE	19. SECURITY CLASSIFICATION OF ABSTRACT	20. LIMITATION OF ABSTRACT
Unclassified	Unclassified	Unclassified	Unlimited

Table of Contents

INTRODUCTION

Fps and its closely related homologue Fer are the sole members of a unique family of cytoplasmic tyrosine kinases. Genetic analysis of *fps* loss-of-function mice suggested a role for Fps in inflammation[1]. Transgenic expression of an activated form of Fps (MFps) gave rise to mice (fps^{MF} mice) with pronounced hyper-vascularity which implicated this kinase in angiogenic mechanisms[2]. This led to the hypothesis that tumorigenesis and or metastases may be enhanced in fps^{MF} mice and repressed in *fps* loss-of-function mice. Other studies had suggested a role for Fps in vesicular trafficking and in signaling downstream of growth factors and cytokines[3,4]. Hence it was also hypothesized that Fps may regulate angiogenesis through regulation of signaling pathways potentiated by angiogenic factors and/or through modulation of the expression profiles of extracellular proteases implicated in angiogenesis. Fps therefore held promise as a novel target for anti-angiogenic therapies.

Based on accumulating evidence that angiogenesis and hemostasis are inter-related processes[5], it was speculated that Fps may influence the processes of coagulation or fibrinolysis. This had potential implications for intervention strategies in thrombotic complications sometimes associated with advanced highly-vascularized tumors, including those of the breast.

PROGRESS ASSOCIATED WITH STATEMENT OF WORK

Obj. #1: Assessment of the effect of *fps* and *fer* allelic variant on tumorigenesis in a mouse breast tumor model.

(a) Breeding pairs which produced offspring that generate tumors in $fps^{-/-}$ (*fps* null), fps^{KR} and fps^{MF} genetic backgrounds were generated in the 1st year. We also generated breeding pairs which gave rise to tumorigenic mice in a transgenic *fps* over-expressing background (fps^{TG})[6].

(b) We have observed an early onset of tumorigenesis in loss-of-function *fps* genetic backgrounds ($fps^{-/-}$ and fps^{KR}). This early onset could be rescued as suggested by normal onset times of tumors in a fps^{TG} mice. The results of these studies have been presented in a recently submitted manuscript[7].

We were unable to generate sufficient number of tumorigenic mice with a fps^{MF} genetic background. We suspect that embryos of this genotype are dying *in utero*[8]. Due to time and labor constraints the number of tumorigenic mice with fps^{KR}/fps^{DR} and fer^{DR} genetic backgrounds that were generated were insufficient for a complete study. Preliminary indications suggest that like $fps^{-/-}$ and fps^{KR} mice, tumor onset occurs early in fps^{KR}/fps^{DR} and fer^{DR} genetic backgrounds.

(c) Lung metastases was monitored in tumorigenic mice harboring fps^{0} and fps^{KR} alleles. We have completed this assessment and were unable to observe significant differences in the number of metastasized nodules in lungs from *wt* and *fps* loss-of-function mice.

Obj. #2: Assessment of the endothelial cell (EC) immortalizing ability of *fps* relative to the known EC immortalizing/transforming agent polyoma middle T(PymT).

(a) pMSCV-based retroviruses encoding PymT, *fps*, fps^{KR} and fps^{MF} were successfully generated in the 1st year.

(b) Primary cells from day 12 yolk-sacs of *wt* mice were transduced with the retroviruses generated in Obj. #2a and subject to puromycin drug selection. Some indications of PyMT-mediated transformation were observed, however immortalized cell lines could not be generated by infection with any of the *fps* constructs. As stated last year, difficulties were encountered with infection efficiencies. We suspect that viral-mediated transfer may not be an optimal method for expression in primary cultures because of their low proliferative potential. This has led us to consider Lentiviral-based approaches, which enable excellent infection efficiencies of

non-cycling cells. Lentiviral-based delivery systems are currently under development and will be utilized as an alternative method to assess the EC immortalizing ability of Fps.

Obj. #3: Generation of EC lines from different *fps* genetic backgrounds for *in vitro* studies.

(a) pMSCV-based retroviruses encoding PymT and SV40-T were generated in the 1st year.

(b) As stated in the previous report, difficulties were encountered generating sufficient numbers of EC populations using explant and flow-cytometry-based cell sorting methods. We have since then began developing a magnetic cell-sorting approach for generating EC lines. Cell populations which are enriched for ECs have been acquired as suggested by flow cytometry using antibodies against the endothelial specific markers, CD31 and CD105. We are now optimizing this method in order to obtain more homogeneous preparations of EC cells.

Obj. #4: Assessment of the role of Fps in angiogenesis *in vitro*.

(a) Methods enabling visualization of neovascularization from fibrin-immobilized aorta and yolk-sacs were established.

(b) Work performed in the 1st year did not indicate any difference in neovascularization between *wt* and fps^{MF} mice in yolk-sac explants. Examination of neovascularization from aortic explants also showed no significant differences between the two genotypes. These results are preliminary and await further confirmation however, they are consistent with evidence suggesting that the vascular defects in fps^{MF} mice may be due to defects in angiogenic remodeling rather than neovascularization (See Reportable Outcomes/Published in [8]).

(c) Low priority was given to assessment of angiogenesis using implanted perforated polycarbonate chambers since there were no significant indications of differences in neovasularization of explants between *wt* and fps^{MF} mice (Obj. #4b).

(d) The completion of Obj. #3b is required for testing the ability of immortalized ECs to form tubules in fibrin-gels.

(e) C166 cell lines expressing myc-epitope-tagged forms of kinase-inactive Fps (FpsKR), myristoylated (activated) Fps (MFps) and Fps were generated in the 1st year.

(f) Studies with the cell lines in Obj. 4e showed that C166 lines expressing FpsKR or Fps lose their ability to spontaneously form tubule-like arrangements in culture. We are currently testing to see if this abrogation is influenced by VEGF. These same lines also display reduced proliferation and sensitivity to PDGF-induced signaling. These results comprise part of a study currently under preparation for publication (See Reportable Outcomes).

Obj. #5: Assessment of coagulation and fibrinolytic parameters in fps^{MF} mice.

(a) Standardized PT and APTT assays have been completed. These and other hemostatic parameters have been incorporated in a recently published manuscript describing the association between the angiogenic phenotype of fps^{MF} mice and various hemostatic and hematological abnormalities (see Reportable Outcomes/Key Accomplishments)[9].

(b) *In vitro* clot lysis assays have been completed and these results have been incorporated in a recently published manuscript[9].

Obj. #6: Examination of proteolytic expression profiles of cell lines expressing Fps.

(a) MMP expression appears to be normal in macrophages isolated from fps^{MF} mice.

(b) Examination of uPA and MMP-2/-9 activity of cell cultures of immortalized ECs will be done upon completion of Obj. #3.

Obj. #7: The role of Fps in signaling pathways potentiated by VEGF, bFGF and thrombin.

(a) Activation of (M)Fps downstream of the thrombin receptor occurs in C166 cells implicating this kinase in endothelial responses to thrombotic events. This observation is consistent with our observations of Fps activation in response to thrombin in platelets([10] / See also Outcomes).

An earlier study demonstrated that Fps is activated in response to basic-fibroblast growth factor (bFGF) in ECs[11]. Our studies showed that C166 cells are insensitive to bFGF. The reason for the discrepancy with the earlier study may be due to the use of different cell lines.

In the previous report, we mentioned that platelet-derived growth factor (PDGF) and vascular endothelial growth factor (VEGF) treatment of C166 cells activates MFps but not Fps. These and other results characterizing the vascular phenotype of *fps*^{MF} mice have been recently published[8] (see Reportable Outcomes/Key Accomplishments).

(b) We have nearly established a consistent method for establishing endothelial cultures from mice (Obj. #3). We will then use these cultures to investigate the role of Fps in signaling pathways initiated by VEGF, PDGF and thrombin; we have opted not to study bFGF given the inert response of (M)Fps in response to this growth factor.

KEY RESEARCH ACCOMPLISHMENTS

(1) Relative to *wt* backgrounds, an early onset of tumorigenesis was observed in *fps*^{0} and *fps*^{KR} genetic backgrounds. Remarkably, mutational analyses of the tyrosine kinome in colorectal cancers detected 4 Fps tumor-specific single-mutation variants in the kinase domain[12]. We have recently generated Fps constructs which incorporate these same mutations and have shown that 3 of them negatively influence kinase activity while the other has no effect. These results suggested that Fps may have tumor suppressor-like properties. These results have been very recently submitted for publication[7].

(2) The work from Obj. #7 has led to a published report on the characterization of the vascular defects in *fps*^{MF} mice[8]. The work also shows that MFps but not Fps is activated in response to PDGF and VEGF and that this may be associated with the development of their vascular defects.

(3) Macrophages are important modulators of angiogenesis and we speculated that Fps may modulate angiogenesis through alteration of their function. During the course of our studies on proteolytic expression profiles of macrophages we made observations which showed that myelopoietic function, and subsequently erythropoietic function was perturbed in these animals. These data concurred with earlier data implicating Fps in hematopoiesis and formed the basis of two publications in Experimental Hematology[13,14] Altered hematopoietic regulation as a contributing factor to the development of the hyper-vascular phenotype remains a definite possibility in *fps*^{MF} mice.

(4) Assessment of hemostatic and hematological parameters of *fps*^{MF} mice – including those proposed in Objective 5a and 5b – led to the characterization of phenotypes that are strongly associated with the angiogenic phenotype. This has led to the publication of a manuscript[9] which shows that many of the *fps*^{MF} phenotypes are reminiscent of hemostatic disorders such as Kasabach Merritt Syndrome (KMS) and disseminated intravascular coagulation (DIC). This study suggests that Fps influences both angiogenic and hemostatic function through regulatory effects on the endothelium. Thus, *fps*^{MF} mice may constitute an important model for the studying the inter-relationships between hemostasis and angiogenesis[5].

REPORTABLE OUTCOMES

Promotion: Asst.(adjunct) Professor, Queen's Univ (See previous report). Renewed to June 05.

Publications:

Manuscripts in preparation

1) **W. Sangrar** and P.A. Greer. Activated Fps regulates sensitivity of the MAP kinase cascade to growth factors in endothelial cells (August 2004).

Manuscripts submitted

2). **W. Sangrar**, R.A. Zirngibl, Y. Gao, W. Muller, Jia, Z and P.A. Greer. An identity crisis for *fps/fes*: Oncogene or tumor-supressor? (Submitted to Nature July 2004). (APPENDED)

Published Manuscripts

3). **W. Sangrar**, Y.Gao, B.Bates, R. Zirngibl, P.A.Greer. (2004) Activated Fps/Fes tyrosine kinase regulates erythroid differentiation and survival. *Experimental Hematology (In press)*. (APPENDED)

4). **W. Sangrar**, Y.A. Senis, J. Samis, Y. Gao, M. Richardson, D.H. Lee, and P.A. Greer. (2004) Hemostatic and hematological abnormalities in gain-of-function *fps/fes* transgenic mice are associated with the angiogenic phenotype. *J Thromb Haemost (In press)*. (APPENDED)

5). **W. Sangrar,** J. Mewburn, S.G. Vincent, J.T. Fisher and P.A. Greer. (2004) Vascular defects in gain-of-function fps/fes transgenic mice correlate with PDGF- and VEGF-induced activation of mutant Fps/Fes kinase in endothelial cells. *Journal of Thrombosis and Haemostasis.* 2, 820-832. (APPENDED)

6). **W. Sangrar**, Y. Gao, R. Zirngibl, M. Scott, P.A Greer. (2003) The *fps/fes* proto-oncogene regulates hematopoietic lineage output. *Experimental Hematology.* **31**, 1259-67. (APPENDED)

7). Y.A. Senis, **W. Sangrar**, R.A. Zirngibl, A.W.B. Craig, D.H. Lee and P.A. Greer. (2003) Fps and Fer become tyrosine phosphorylated following collagen and thrombin induced activation of platelets. *J Thromb Haemost* **1**, 1062-1070. (APPENDED)

Abstracts

1). **W. Sangrar**, Y. Gao, R.A. Zirngibl, M.L. Scott, P.A. Greer. The Fps/Fes tyrosine kinsae regulates hematopoietic lineage output. 43rd ASCB, San Fran. CA, USA. Dec. 13-17, 2003.

2). **W. Sangrar**, Y. Senis, M. Richardson and P.A. Greer. Abnormalities of platelet morphology and function in hyper-vasuclar gain-of-function *fps/fes* mice. 94th Annual AACR meeting, Washington DC, USA. July 11th-14th, 2003.

3). **W. Sangrar**, J. Mewburn, Y. Senis, R.A. Zirngibl, Man Y. Tse, S.G. Vincent, M.L. Scott, S.C. Pang, D.H. Lee, J.T. Fisher and P.A. Greer. Mice expressing gain-of-function Fps/Fes are characterized by vascular malformation, aberrant levels of circulating blood cells and potential defects in endothelial, platelet and macrophage function. *Breast Cancer Era of Hope Meeting*, Orlando, Florida, September 25th-28th, 2002.

4). **W. Sangrar**, R.A. Zirngibl, J. Mewburn, Y.A. Senis, C. Chapler, D.H.Lee and P.A. Greer. A murine transgenic line expressing a myristoylated form of Fps/Fes is characterized by disorganized hyper-vascular patterning and peripheral blood defects. *Blood* **98**, 31a. *43rd Annual A.S.H. Meeting.* Orlando, Florida, 7th-12th December, 2001.

5). Y.Senis, R. Zirngibl, **W. Sangrar**, N. Peterson, D.Lee, P.Greer. Fps and Fer are expressed in human and mouse platelets and become tyrosine phosphorylated following collagen and thrombin stimulation. *Blood* **98**, 26a. *43rd A.S.H.* Orlando, Florida, 7th-12th Dec. 2001.

6). **W.Sangrar**, R.Zirngibl, K.Williams, W. Muller and P.Greer. Early mammary tumour development in Polyomavirus-Middle-T transgenic mice which harbor null or kinase-inactivated *fps* alleles. *Signaling in Normal and Cancer Cells.* Banff, Alberta. March 2001.

CONCLUSIONS

Our investigations suggested that Fps has tumor suppressor-like properties[7]. This was unexpected given that Fps and other members of the tyrosine kinase family were previously characterized as dominant-acting oncoproteins. We also extensively characterized the vascular phenotype of *fps*^{MF} mice and showed that VEGF and PDGF could activate gain-of-function Fps in endothelial cells[8]. Activation was not detected with wild-type Fps suggesting that modification of PDGF- and VEGF-signaling by activated Fps contributes to the vascular phenotype. As expected, numerous hematological and hemostatic defects were observed in *fps*^{MF} mice. Interestingly, these defects were reminiscent of those observed in pathologies associated with vascular aberrations such as KMS and DIC. These data supported a role for Fps in influencing angiogenesis and hemostasis through regulatory effects on the endothelium[9] and have led to the hypothesis that the vascular defects in these mice are a result of a delay/defect in vascular maturation/remodeling. Lastly, it was found that activated Fps promotes myeloid output, but mildly retards erythroid output. The significance of this regulation to their angiogenic phenotype is as yet unclear.

REFERENCES

1. Zirngibl RA, Senis Y, Greer PA: Enhanced endotoxin-sensitivity in Fps/Fes-null mice with minimal defects in hematopoietic homeostasis. Mol Cell Biol 2002, 22:2472-2486
2. Greer P, Haigh J, Mbamalu G, Khoo W, Bernstein A, Pawson T: The Fps/Fes protein-tyrosine kinase promotes angiogenesis in transgenic mice. Mol Cell Biol 1994, 14:6755-6763.
3. Zirngibl R, Schulze D, Mirski SE, Cole SP, Greer PA: Subcellular localization analysis of the closely related Fps/Fes and Fer protein-tyrosine kinases suggests a distinct role for Fps/Fes in vesicular trafficking. Exp Cell Res 2001, 266:87-94
4. Greer PA: Closing in on the biological functions of Fps/Fes and Fer. Nature Reviews Molecular Cell Biology 2002, 3:278-289
5. Browder T, Folkman J, Pirie-Shepherd S: The hemostatic system as a regulator of angiogenesis. J Biol Chem 2000, 275:1521-1524
6. Greer P, Maltby V, Rossant J, Bernstein A, Pawson T: Myeloid expression of the human c-fps/fes proto-oncogene in transgenic mice. Mol Cell Biol 1990, 10:2521-2527.
7. Sangrar W, Zirngibl R, Gao Y, Muller W, Jia Z, Greer P: An identity crisis for *fps/fes*: Oncogene or tumour-suppressor? Submitted to Nature July 2004
8. Sangrar W, Mewburn J, Vincent S, Fisher J, Greer P: Vascular defects in gain-of-function fps/fes transgenic mice correlate with PDGF- and VEGF-induced activation of mutant Fps/Fes kinase in endothelial cells. J Thromb Haemost 2004, 2:820-832
9. Sangrar W, Senis Y, Samis J, Gao Y, Richardson M, Lee DH, Greer PA: Hemostatic and hematological abnormalities in gain-of-function fps/fes transgenic mice are associated with the angiogenic phenotype. Journal of Thrombosis and Haemostasis 2004 In Press
10. Senis YA, Sangrar W, Zirngibl RA, Craig AWB, Lee DH, Greer PA: Fps/Fes and Fer Nonreceptor Protein-Tyrosine Kinases Regulate Collagen- and ADP-Induced Platelet Aggregation. Journal of Thrombosis and Haemostasis 2003, 1:1062-1070
11. Kanda S, Lerner EC, Tsuda S, Shono T, Kanetake H, Smithgall TE: The nonreceptor protein-tyrosine kinase c-Fes is involved in fibroblast growth factor-2-induced chemotaxis of murine brain capillary endothelial cells. J Biol Chem 2000, 275:10105-10111.
12. Bardelli A, Parsons DW, Silliman N, Ptak J, Szabo S, Saha S, Markowitz S, Willson JK, Parmigiani G, Kinzler KW, Vogelstein B, Velculescu VE: Mutational analysis of the tyrosine kinome in colorectal cancers. Science 2003, 300:949
13. Sangrar W, Gao Y, Zirngibl R, Scott M, Greer P: The fps/fes proto-oncogene regulates hematopoietic lineage output. Experimental Hematology 2003, 31:1259-1267
14. Sangrar W, Gao Y, Bates B, Zirngibl RA, Greer PA: Activated Fps/Fes tyrosine kinase regulates erythroid differentiation and survival. Experimental Hematology 2004 In Press

APPENDED DOCUMENTS

(1.) W. Sangrar, R.A. Zirngibl, Y. Gao, W. Muller, Jia, Z and P.A. Greer. An identity crisis for *fps/fes*: Oncogene or tumor-supressor? (Submitted to Nature, July 2004)

(2.) W. Sangrar, Y. Gao, B. Bates, R. Zirngibl, P. A. Greer. (2004) Activated Fps/Fes tyrosine kinase regulates erythroid differentiation and survival. *Experimental Hematology (In press)*

(3.) W. Sangrar, Y.A. Senis, J. Samis, Y. Gao, M. Richardson, D.H. Lee, and P.A. Greer. (2004) Hemostatic and hematological abnormalities in gain-of-function *fps/fes* transgenic mice are associated with the angiogenic phenotype. *Journal of Thrombosis and Haemostasis (In press)*

(4.) W. Sangrar, J. Mewburn, S.G. Vincent, J.T. Fisher and P.A. Greer. (2004) Vascular defects in gain-of-function *fps/fes* transgenic mice correlate with PDGF- and VEGF-induced activation of mutant Fps/Fes kinase in endothelial cells. *Journal of Thrombosis and Haemostasis.* 2, 820-832

(5.) W. Sangrar, Y. Gao, R.A Zirngibl, M.L. Scott, P.A Greer. (2003) The *fps/fes* proto-oncogene regulates hematopoietic lineage output. *Experimental Hematology.* 31, 1259-67

(6.) Y.A. Senis, **W. Sangrar**, R.A. Zirngibl, A.W.B. Craig, D.H. Lee and P.A. Greer. (2003) Fps/Fes andFer non-receptor protein-tyrosine kinases regulate collagen- and ADP-induced platelet aggregation. *Journal of Thrombosis and Haemostasis.* **1**, 1062-1070.

APPENDIX 1

An identity crisis for *fps/fes*: Oncogene or tumour-suppressor?

Waheed Sangrar*, Ralph A. Zirgnibl[†], Yan Gao*, William J. Muller[§], Zongchao Jia[†] and Peter A. Greer*[†‡].
*Queen's University Cancer Research Institute, Division of Cancer Biology and Genetics
[‡]e-mail: greerp@post.queensu.ca
[†]Department of Biochemistry, Queen's University
[§]Molecular Oncology Group, McGill University Health Center

Corresponding author information:
Dr. Peter A. Greer
Queen's University Cancer Research Institute
Botterell Hall, Room A309
Ontario, Canada, K7L 3N6
Tel: (613) 533-2813
Fax: (613) 533-6830
e-mail: greerp@post.queensu.ca

An identity crisis for *fps/fes*: Oncogene or tumour-suppressor?

Fps/Fes proteins encoded by avian (*fps*) or feline (*fes*) retroviral oncogenes were among the first members of the protein-tyrosine kinase family to be characterized as dominant-acting oncoproteins (reviewed in[1]). Addition of retroviral Gag sequences or other experimentally induced mutations activated the transforming potential of Fps/Fes, it therefore seemed reasonable to expect activating somatic mutations might someday be found in human cancers. Genetic evidence that inactivating *fps/fes* mutations contributes to cancer now suggests a novel and unexpected tumour-suppressor role for Fps/Fes.

Until recently, mutations in *fps/fes* had not been found in human tumours. This changed last year when a mutational analysis of the tyrosine kinome in a panel of 182 colorectal cancers identified four somatic mutations in *fps/fes*[2]. The authors speculated that these mutations in the catalytic domain could have activated Fps/Fes and thereby contributed to malignancy. Biochemical analysis reveals that three of them (V743M, S759F and M704V) abolished kinase activity, while the fourth (R706Q) had no apparent effect (Fig. 1b). For comparison we included a K588R mutation in the ATP-binding fold that was previously shown to disrupt kinase activity[3]. A hypothetical structural model of Fps/Fes was generated using crystal structures of other tyrosine kinases (Fig. 1c) and used to predict the effects of the three inactivating mutations (V754M, S759F and M704M) on the catalytic domain. All three were predicted to introduce substantial conformational changes that could account for loss of activity. In contrast, the R706 residue is located in the flexible activation loop (Fig. 1c, clear loop) where one might expect the conservative R706Q substitution to be more easily tolerated. This biochemical analysis demonstrated that these mutations inactivated, rather than activated Fps/Fes; and therefore argued against a classical oncogenic role for these *fps/fes* mutations in cancer. On the contrary, these results raised the interesting possibility that Fps/Fes might have a tumour-suppressor function. We addressed this by examining the effect of targeted *fps/fes* mutations on tumour progression in mice. Remarkably, breast tumour onset in a MMTV-polyoma virus middle T (Py-mT) transgenic mouse model occurred significantly earlier in mice targeted with either null ($fps^{-/-}$) or kinase-inactivating ($fps^{KR/KR}$) mutations (Fig. 1a, right). Furthermore, a *fps/fes* transgene (fps^{Tg}) restored tumour onset kinetics to the WT profile in targeted $fps^{-/-}$ mice (Fig. 1, left, $fps^{-/-}fps^{Tg}$).

These observations provide novel genetic evidence that Fps/Fes acts as a tumour-suppressor. This is certainly surprising because all previous indications suggested it was more likely to contribute to cancer as a dominant-acting oncoprotein. It remains to be determined what the molecular function of Fps/Fes is in epithelial cells, how kinase-inactivating or null mutations might contribute to transformation, or how Fps/Fes might attenuate tumourigenesis. Interestingly, the related Fer kinase was recently shown to play a role in maintaining adherens junctions [4]. This contributes to an evolving model predicting that loss-of-function mutations in genes encoding adherens junction proteins or components of the Wnt pathway could contribute to epithelial tumours. In light of the observations reported here, we suggest that Fps/Fes should also be considered as a potential tumour-suppressor in epithelial tissues.

Figure 1

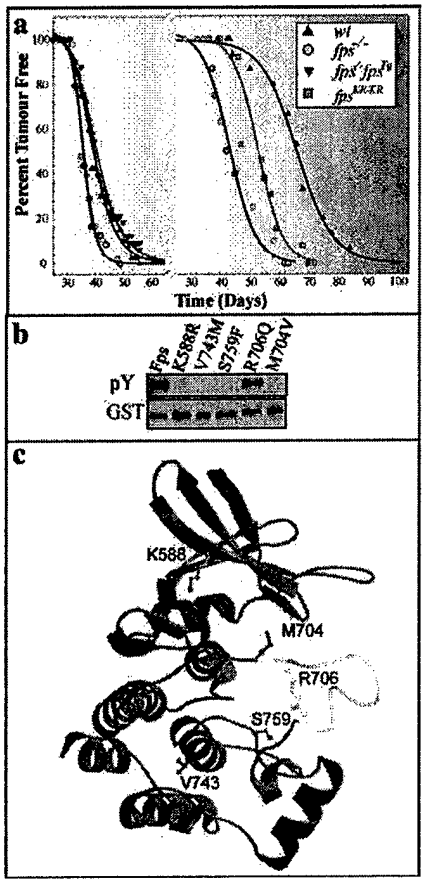
a
Percent Tumour Free
Time (Days)
wt
fps-/-
fps-/-fpsFu
fpsKK-KR
b
Fps
K588R
V743M
S759F
R706Q
M704V
pY
GST
c
K588
M704
R706
S759
V743

Figure 1. Disruption of *fps/fes* correlated with earlier tumour onset. **a,** Time to tumour onset was assessed by physical palpitation in a MMTV-Py-MT transgenic mouse model of breast cancer in the indicated *fps/fes* genetic backgrounds. Two independent experiments were performed by different investigators (left and right). Tumours appeared sooner in $fps^{-/-}$ mice than in wild type (WT) mice (left panel: WT, n = 40; $fps^{-/-}$, n = 57; P = 0.017). A rescue transgene (fps^{Tg}) restored tumour onset to the WT profile in the $fps^{-/-}$ background (left panel: $fps^{-/-}$, n = 57; $fps^{-/-}$ fps^{Tg}, n = 33; P = 0.003). Mice targeted with a kinase-inactivating K588R mutation ($fps^{KR/KR}$) also displayed earlier tumour onset relative to WT mice (right: WT, n = 24; $fps^{KR/KR}$, n = 21; $P = 5.2 \times 10^{-5}$). Interestingly, although onset times were earlier, the rates of tumour growth were unaltered in $fps^{KR/KR}$ or $fps^{-/-}$ relative to WT mice. **b,** GST fusion proteins containing the SH2 and kinase domains of WT Fps (Fps) or the indicated missense mutations were isolated on glutathione agarose beads and incubated with ATP to allow autophosphorylation. The proteins were then analyzed by immunoblotting with anti-pY (pY) and anti-GST (GST). **c,** A hypothetical structure was generated by threading the human Fps/Fes protein sequence onto the solved structures of Src and other related tyrosine kinases. The positions of the mutated side-chains are indicated.

REFERENCES

1. Greer, P. Closing in on the biological functions of Fps/Fes and Fer. *Nat Rev Mol Cell Biol* **3**, 278-89. (2002).
2. Bardelli, A. et al. Mutational analysis of the tyrosine kinome in colorectal cancers. *Science* **300**, 949 (2003).
3. Senis, Y. et al. Targeted disruption of the murine fps/fes proto-oncogene reveals that Fps/Fes kinase activity is dispensable for hematopoiesis. *Mol Cell Biol* **19**, 7436-46 (1999).
4. Xu, G. et al. Continuous association of cadherin with {beta}-catenin requires the non-receptor tyrosine-kinase Fer. *J Cell Sci* **117**, 3207-3219 (2004).

APPENDIX 2

Activated Fps/Fes tyrosine kinase regulates erythroid differentiation and survival

Running Title: Erythroid defects in gain-of-function *fps* transgenic mice

Waheed Sangrar[1,2], Yan Gao[1], Barbara Bates[1], Ralph Zirngibl[1], and Peter A. Greer[1,2*].

[1]Division of Cancer Biology and Genetics, Queen's University Cancer Research Institute, [2]Department of Pathology and Molecular Medicine, Queen's University, Kingston, Ontario, K7L3N6, Canada

*To whom correspondence should be addressed: Dr. Peter A. Greer, PhD, Division of Cancer Biology and Genetics, Queen's University Cancer Research Institute, Botterell Hall, Room A309, Kingston, Ontario, K7L3N6, Canada. Tel: (613) 533-2813; FAX: (613) 533-6830; Email: greerp@post.queensu.ca.

Table of contents category: Erythropoiesis

Abstract (words): 250
Word count (excluding references, figure legends, and tables): 4148

Abstract

Objective. A substantial body of evidence implicates the cytoplasmic protein tyrosine kinase Fps/Fes in regulation of myeloid differentiation and survival. In this study we wished to determine if Fps/Fes also plays a role in the regulation of erythropoiesis.

Methods. Mice tissue-specifically expressing a "gain-of-function" mutant *fps/fes* transgene (*fps*^{MF}) encoding an activated variant of Fps/Fes (MFps) were used to explore the *in vivo* biological role of Fps/Fes. Erythropoiesis in these mice was assessed by hematological analysis, lineage marker analysis, bone-marrow colony assays and biochemical approaches.

Results. *fps*^{MF} mice displayed reductions in peripheral red cell counts. However, there was an accumulation of immature erythroid precursors, which displayed increased survival. Fps/Fes and the related Fer kinase were both detected in early erythroid progenitors/blasts and in mature red cells. Fps/Fes was also activated in response to erythropoietin (Epo) and stem cell factor (Scf), two critical factors in erythroid development. In addition, increased Stat5A/B activation and reduced Erk1/2 phosphorylation was observed in *fps*^{MF} primary erythroid cells in response to Epo or Scf, respectively.

Conclusions. These data support a role for Fps/Fes in regulating the survival and differentiation of erythroid cells through modulation of Stat5A/B and Erk kinase pathways induced by Epo and Scf. The increased numbers and survival of erythroid progenitors from *fps*^{MF} mice, and their differential responsiveness to Scf and Epo, implicates Fps/Fes in the commitment and survival of multi-lineage progenitors to the erythróid lineages. The anemic phenotype in *fps*^{MF} mice suggests that down-regulation of Fps/Fes activity might be required for terminal erythroid differentiation.

Introduction

Erythropoietin (Epo) and stem cell factor (Scf) play diverse roles in regulating erythropoiesis through effects on survival, proliferation and differentiation of erythroid progenitor cells. These effects are mediated by intracellular signaling via their cognate receptors, the erythropoietin receptor (EpoR), and c-kit, respectively. These receptors and their ligands have been shown to be critical for erythroid development by the association of mutations in their genes with failed gestation and severe reductions in fetal liver colony-forming unit erythroid (CFU-E) progenitors [1,2]. Although the critical requirements of these ligand-receptors pairs are well acknowledged, the cellular and molecular mechanisms through which they exert such wide and dynamic effects on erythropoiesis are still poorly understood.

Fps/Fes (hereafter referred to as Fps) and Fer form a unique subfamily of cytoplasmic protein-tyrosine kinases which are structurally distinguished from members of the Src, Abl, Btk, Jak, Zap70 or Fak subfamilies (reviewed in [3]). Fps and Fer contain a central Src-homology 2 (SH2) domain and a C-terminal tyrosine kinase domain. The unique structural features of Fps and Fer include an N-terminal Fer/CIP-4 (Cdc42 interacting protein-4) homology (FCH) domain [4], which is thought to play a role in cytoskeletal interactions, and an adjacent coiled-coil domain involved in homotypic oligomerization [5]. The high degree of homology between Fps and Fer suggests that these kinases have similar biological functions [3].

Early studies showed that *fps* mRNA was detectable in adult and embryonic undifferentiated progenitors of the erythroid lineage and in both differentiated and undifferentiated progenitors of the granulomonocytic lineage [6,7]. *In vitro* studies have shown that Fps is expressed in cells of the myeloid lineage and that it might promote differentiation and survival of myeloid cells [3,8-14]. Studies have also shown that Fps is phosphorylated upon

engagement of a wide array of hematopoietic growth factor and cytokine receptors and this has suggested a role in myelopoiesis. Fps has been implicated in signaling downstream from a number of cytokine receptors including those for GM-CSF, Epo, IL-3, and IL-4; and those which employ the common gp130 subunit, such as IL-6, oncostatin M, ciliary neurotrophic factor, IL-11 and leukemia inhibitor factor [15-22]. Sensitivity to these cytokines suggested an *in vivo* role for Fps in regulating differentiation and survival pathways in granulomonocytic and erythroid development, as well as other lineages.

Subsequent genetic experiments have not completely substantiated the earlier *in vitro* observations. Surprisingly, a knock-in mutation in mice which abolished Fps kinase activity ($fps^{KR/KR}$) did not give rise to any overt defects in hematopoiesis [23]. Following that, two independent studies on *fps*-null ($fps^{-/-}$) mice generated contradictory results. One study suggested enhanced myelopoiesis [24], while the second study reported only minimal effects including decreased circulating levels of granulocytes and monocytes which were rescued by a *fps* transgene ($fps^{-/-Tg}$) [25]. Subsequent analysis of a gain-of-function *fps* transgenic line (fps^{MF} mice) revealed increased circulating levels of granulocytes and monocytes [26]. In addition, progenitor colony assays showed a dramatic increase in the number of CFU-GM and CFU-GEMM in the bone-marrow of fps^{MF} mice. Taken together, these results suggested that Fps might regulate lineage determination at the level of multi-potential progenitor cells (CFU-GEMM) and further downstream at the level of the bipotential granulomonocytic progenitor (CFU-GM) [26]. Furthermore, decreases in circulating levels of lymphocytes and bone-marrow mature B-cell levels suggested that Fps might also act on early multi-lineage progenitors to promote myeloid expansion at the expense of the lymphoid lineage [26]. Expression of Fps in multi-lineage progenitors was also supported by the observed kinetics of *fps*-directed Cre-

mediated excision of a loxP flanked PIGA gene in all hematopoietic lineages [27]. Collectively, these genetic data were consistent with a role for Fps in promoting granulomoncytic output through influencing the differentiation and survival parameters of both early and late myeloid progenitors [26].

Transgenic expression of a gain-of-function variant of Fps (MFps) gave rise to mice with pronounced hyper-vascularity and multi-focal hemangiomas [28,29]. This *fps*^{MF} transgene consisted of the complete human *fps/fes* locus including *cis*-acting sequences shown to direct tissue-specific expression [29-31]. The additional fifteen base-pairs of sequence introduced into the *fps*^{MF} transgene relative to the wild type gene resulted in a N-terminally myristoylated Fps protein (MFps), which may behave as a gain-of-function mutant by virtue of enhanced association with the plasma membrane. The *fps*^{MF} mice displayed a skewing of hematopoietic output towards the granulomonocytic lineage [26]. In this study, we have made novel observations showing that Fps (and Fer) are expressed in primary erythroid cells and that they remain detectable in terminally differentiated red blood cells (RBC). Secondly, we have extended previous observations made in cell lines by demonstrating Fps and MFps activation downstream of the EpoR in primary erythroid cells. Thirdly, we report for the first time that Fer is activated downstream of Epo, and that Fps, MFps and Fer are tyrosine phosphorylated in response to Scf stimulation in primary erythroid cells. Lastly, we argue that the data support a model where activated Fps regulates erythroid survival and differentiation by modulation of Epo and Scf signaling.

Methods

Mice

Transgenic mice (fps^{MF}) tissue-specifically over-expressing myristoylated Fps (MFps) in an in-bred CD-1 background were housed at the Animal Care Facility at Queen's University, Kingston Ontario. Derivation and genotyping of this line has been described [29]. All procedures were approved by the Queen's University Animal Care Committee in accordance with the regulations set forth by the Canadian Council on Animal Care.

Colony assays

Methyl cellulose progenitor assays were performed as previously described [26]. Briefly, methyl cellulose was supplemented with two different cocktails of recombinant cytokines (R&D Systems, Minneapolis, MN): One cocktail consisted of 50 ng/ml Stem cell factor (Scf), 5 ng/ml IL-3, 10 ng/ml IL-6, 10 ng/ml Tpo, 1 U/ml Epo and 5 ng/ml GM-CSF and the second cocktail consisted of 1 U/ml Epo and 5 ng/ml GM-CSF.

Isolation and stimulation of primary erythroid cells.

Primary erythroid cells were isolated from spleens of phenyl-hydrazine (PHZ)-treated wild type (*wt*) and fps^{MF} mice as described elsewhere [32,33]. Splenocytes (70-120 x 10^6 cells/ml) were subsequently starved in α-MEM (Gibco) containing 0.5% fetal bovine serum (Gibco) for 2-6 hours. Cells were resuspended in serum-free α-MEM (Gibco) prior to stimulation with 200 ng/ml of Scf (R&D Systems Inc.), or with 50 U/ml of Epo (R&D Systems Inc.) for 0-60 min at 37°C. Stimulations were terminated by transferring aliquots of 10 X 10^6 cells into lysis buffer (50 mM Hepes, 150 mM NaCl, 10% glycerol, 1% Triton-X 100, 1.5 mM EGTA, 10 mM sodium pyrophosphate, 100 mM NaF, pH 7.4) containing the protease inhibitors leupeptin (10 μg/ml) and aprotinin (10 μg/ml). In all cases, volumes containing equal numbers of lysed cells (10 x

10^6) were immunoprecipitated with anti-FpsQE or anti-FerLA rabbit polyclonal antibody [7] and/or blotted directly with anti-FpsQE antibody. Anti-FpsQE is cross-reactive for Fps and Fer, and is referred to in the text and figures as anti-Fps/Fes, while anti-FerLA is Fer specific and is referred to as anti-Fer. In some experiments, blots were probed with the following antibodies according to manufacturer instructions: anti-phospho(p)-Stat5A/B, anti-Stat5A, (Upstate Biotechnology, Lake Placid, NY); anti-Erk1/2, anti-pErk1/2 (Cell Signaling, Beverly, MA).

Bone marrow and spleen flow cytometry

Spleen flow cytometry was performed as previously described [25]. Erythroid progenitors derived from untreated or PHZ-treated *wt* and fps^{MF} mice were detected in bone marrow and spleen using R-PE-conjugated rat anti-mouse Ter119 and FITC-conjugated rat anti-mouse CD44 monoclonal antibodies (BD PharMingen, San Diego, CA). FITC-conjugated Annexin V (BD PharMingen) was used to detect apoptotic cells.

Red blood cell preparations

Whole blood was collected and platelet rich plasma (PRP) was obtained as described [34,35]. Platelets were then extracted from PRP by centrifugation (6 min, 1000 x *g*, 22°C) and subsequently lysed in red blood cell lysis buffer (RBC-LB: 25 mM HEPES, 225 mM NaCl, 1% (v/v) Nonidet P-40, pH 7.4). After platelet separation, the remaining RBC suspension was counted and subsequently lysed 1:10 in RBC-LB plus inhibitors. Samples were then analyzed by Western blotting using anti-Fer or anti-Fps/Fer. Typically, contaminating platelet and leukocytes levels in RBC suspensions were 1.100 ± 0.004 % and 0.05 ± 10^{-4} %, respectively.

Results

Anemia and accentuated erythropoieis in fps^{MF} mice

Hematological analyses of peripheral blood revealed that fps^{MF} mice have reduced levels of RBCs and reticuloctyes, suggesting that erythropoietic output was impaired (Table 1). The basis for this mild anemia was explored by measuring erythroid progenitor cell numbers in the bone marrow using methyl cellulose colony assays (Table 1). Colony forming units erythroid (CFU-E) were actually increased in fps^{MF} mice relative to *wt* mice when assayed in the presence of a heterogeneous cytokine cocktail consisting of Scf, Epo, IL-3, IL-6, Tpo, Epo and GM-CSF (Table 1; $p = 0.03$). However, similar numbers of CFU-E were detected using a more restricted cytokine cocktail consisting of only Epo and GM-CSF. Burst forming units erythroid (BFU-E) were not significantly different in bone marrow from fps^{MF} mice relative to *wt* mice when assayed either in the presence of the heterogeneous cytokine cocktail or the more restricted cytokine mixture (Table 1). Notably, no apparent differences in the morphology or size of CFU-E or BFU-colonies were observed.

We next performed lineage analysis of erythroid cells in the bone marrow and spleens using flow cytometry. Using the erythroid-specific marker Ter119 we observed a 1.5-2.1-fold ($p \leq 0.01$) elevation in erythroid populations in both the bone marrow (Figure 1, panels A and B) and spleens (Figure 1, panels C and D) of fps^{MF} relative to *wt* mice. This initial analysis revealed an anemic state in fps^{MF} mice, accompanied by indications of increased erythropoiesis in the bone marrow and spleens.

Accentuated erythropoiesis persists in fps^{MF} mice under conditions of experimentally induced hemolysis.

We next considered the possibility that the observed increases in erythroid progenitor levels might represent a compensatory response to anemia. In order to evaluate erythropoiesis under comparable physiological conditions, we chemically induced severe hemolytic anemia by treating the mice with PHZ [36]. Dramatic increases in the number of $Ter119^+/CD44^+$ double positive erythroid progenitor populations were observed in response to PHZ-induced erythroid stimulation in both *wt* and fps^{MF} mice (Figure 2). Even under these conditions, there were increased numbers of erythroid progenitors in fps^{MF} mice (Figure 2; $p = 0.045$). This showed that the erythropoietic compensatory response capacity was intact in fps^{MF} mice, and the relatively accentuated state of erythropoiesis in fps^{MF} mice persists even under these stressed conditions.

Enhanced survival of erythroblasts in fps^{MF} mice

Epo has been proposed to protect committed erythroid progenitors from undergoing apoptosis [37,38]. The apoptotic index of splenocytes isolated from PHZ-treated *wt* mice was high (60.7%) and was likely attributable to withdrawal of Epo during preparation for flow-cytometry (Figure 3A). However, under these same conditions, the apoptotic index of splenocytes isolated from PHZ-treated fps^{MF} mice was comparatively reduced (38.3%), suggesting that increases in erythroid progenitor levels in fps^{MF} mice might be related to an increase in their survival capacity (Figure 3B). In order to confirm that these staining patterns were erythroid specific, we next tested the annexin V staining profiles of $Ter119^+$ splenocytes. This analysis confirmed that the observed global decreases in apoptosis in fps^{MF} splenocytes were specifically associated with erythroid populations (Figure 3, panels C and D).

Increased early erythroblast populations in fps^{MF} mice

To further investigate the basis of the observed increase of erythroid progenitors in fps^{MF} mice, we utilized a forward scatter analyses which has previously been used as an indicator of erythroid maturation [39,40]. This technique revealed two $Ter119^+$ populations in splenocytes from PHZ-challenged mice (Figure 4A; scatter plot). A high forward scatter population (*II*) corresponding to larger, immature, erythroid cells (potentially late CFU-Es to early blasts); and a low forward scatter population (*I*) corresponding to smaller, more mature cells. Interestingly, splenocytes from PHZ-treated fps^{MF} mice exhibited a dramatic increase in the $Ter119^+$ immature high-forward scatter population (*II*; $p < 10^{-3}$) and a concomitant decrease in the more mature low-forward scatter population (*I*; $p < 10^{-3}$) (Figure 4B; scatter plot). This shift in cellularity between mature and immature populations was striking, and was readily observable in individual *wt* and fps^{MF} mice (Figure 4, compare *wt* panels C-F to fps^{MF} panels G-J). These results were consistent with the observed increase in CFU-E colonies and as well, with the increase of $Ter119^+$ erythroid precursors in the bone marrow and spleen. Together these data strongly argued for an expansion of immature erythroid populations in fps^{MF} mice.

We next determined whether the observed increases in survival indices of fps^{MF} erythroid-specific progenitors seen in Figure 3 was specifically attributed to either population *I* or population *II*. Decreased apoptotic indices in fps^{MF} relative to *wt* cells were seen in both populations *I* and *II*, suggesting that the increased survival of erythroid progenitors in fps^{MF} mice was not specifically associated with either immature or more mature erythroid progenitor cells (Figure 4, panels A,B; histograms).

Fps, MFps and Fer are expressed in primary erythroid cells and are tyrosine phosphorylated in response to Epo and Scf

While Fps protein expression has been demonstrated in erythroleukemic cell lines such as TF-1 [15], there has been no direct evidence of Fps expression in primary erythroid cells. The observed expansion and survival of erythroid progenitors in fps^{MF} mice strongly suggested that Fps might be expressed in these cell types. We sought to confirm this by Western blotting analysis of splenocytes obtained from PHZ-treated mice. Fps, MFps and Fer expression was detected in these highly-enriched primary erythroid precursor preparations (Figure 5A).

Epo and Scf are critical for erythropoiesis and have been shown to cooperatively mediate erythroid development [41]. Differences in progenitor levels and erythroblast maturation in fps^{MF} mice led us to examine whether MFps and Fps are activated in Epo and Scf signaling pathways. Stimulation of primary erythroid cells with either Epo or Scf (Figure 5B and 6A, respectively) produced a time-dependent increase in tyrosine phosphorylation levels of Fps, MFps and Fer. The activation profiles of Fps and Fer were similar, with highest levels of tyrosine phosphorylation seen at the latest time point explored (40 min) with both agonists. Differences were also observed in the Epo- and Scf-induced global tyrosine phosphorylation profiles in *wt* and fps^{MF} erythroid cells. The kinetics of Epo-induced tyrosine phosphorylation changes in several proteins appeared different between *wt* and fps^{MF} erythroid cells (Figure 5C); and the Scf-induced changes in global tyrosine phosphorylation were reduced in fps^{MF} erythroid cells (Figure 6B).

fps^{MF} erythroid cells displayed enhanced Stat5A/B activation in response to Epo and reduced Erk1/2 activation in response to Scf

Genetic and *in vitro* studies have previously implicated Fps in Stat5 signaling in myeloid cells [23,24,42,43]. In addition, Stat5 has been shown to play significant roles in the regulation of erythropoiesis through its effects on survival [39]. We therefore compared Stat5 activation in response to Epo and Scf in *wt* and fps^{MF} splenocytes. No overt differences in the kinetics or magnitude of Scf-induced Stat5A/B were observed (data not shown). However, we observed a trend towards hyper-phosphorylation of total Stat5A/B in fps^{MF} mice in response to Epo (Figure 5C). Figure 5D shows quantified Stat5A/B activation profiles from three independent experiments. These observations suggested that Stat5 hyper-phosphorylation might contribute to the reduced apoptosis of $Ter119^{+}$ cells shown in Figures 3 and 4.

The kinetics of activation of the MAP kinase pathway was also assessed by monitoring Erk1/2 activation. In response to Epo, the kinase activation profile of Erk1/2 was transient in *wt* and fps^{MF} splenocytes, and the overall magnitude of activation was comparable (Figure 5C). In contrast, Erk1/2 activation in response to Scf was diminished in fps^{MF} mice (Figure 6C and D). This was consistent with a reduction in global phosphotyrosine signals in response to Scf in fps^{MF} splenocytes (Figure 6B). These data suggested that MFps might specifically dampen the Scf response of the MAP kinase pathway.

Fps, MFps and Fer tyrosine kinases are expressed in mature red blood cells

Detection of Fps, MFps and Fer in primary erythroid precursors suggested that residual levels of these kinases might persist in red blood cells (RBC). Initial immunoprecipitation and western blotting analysis of RBC preparations using antibody specific for Fps and Fer (Fps/Fer) showed that Fps, MFps and Fer were all expressed (Figure 7A, left). Immunoprecipitation with an

antibody specific for Fer followed by probing with the anti-Fps/Fer antibody confirmed the slower migrating band to be Fer (Figure 7A, right). The identity of this band as Fer was further substantiated by immunoblotting SCLs prepared from *fps*$^{-/-}$ red cells, and detecting only the slower migrating Fer protein in *fps*$^{-/-}$ cells (Figure 7B). MFps migrated at a position intermediate to Fps and Fer (Figure 7A and B). This migration position has been previously observed in platelets (Figure 7C) and macrophages (not shown). In addition, MFps expression in RBCs was found to be several-fold higher than endogenous Fps (Figure 7B) which was consistent with a transgene copy number that is elevated approximately 5-fold relative to endogenous *fps* [29].

It was possible that the Fps and Fer signals detected in RBC preparations originated from small amounts of contaminating platelets, which we have previously shown to express this kinase [35]. We therefore repeated this analysis using quantities of purified platelets which corresponded in number to contaminating levels empirically determined to be present in *wt* RBC preparations (1.100 ± 0.004 % platelets; n = 4). Western blotting analyses using anti-FpsQE antibody showed that Fps and Fer were undetectable in lanes containing contaminating equivalents of purified platelets (Figure 7D, lanes labeled *P*). In contrast, readily detectable Fps and Fer levels were seen in the RBC preparations loaded in adjacent lanes (Figure 7D, lanes labeled R; n = 3 per genotype) confirming that Fps and Fer signals were specific to RBCs.

Discussion

Immunophenotyping analysis showed increased numbers of $Ter119^+/CD44^+$ erythroid progenitors in the bone marrow and spleen of fps^{MF} mice. We postulate that these apparent promoting effects of fps^{MF} on erythropoiesis were a direct and expected consequence of the upstream CFU-GEMM multi-lineage progenitor expansion that was previously reported [26] (Figure 8). A statistically significant increase in the number of CFU-E colonies correlated with potential expansion of the CFU-GEMM population (Table 1). Importantly, $Ter119^+/CD44^+$ erythroid precursor levels remained elevated in fps^{MF} animals after severe hemolytic anemia was induced to nullify potential feedback stress-erythropoiesis effects. Under these conditions, FACS forward scatter analysis revealed a major expansion of immature erythroblast populations with elevated survival indices, suggesting that the erythropoietic response capacity was not only intact, but was accentuated in fps^{MF} mice. Collectively, these data pointed to a role for MFps in promoting early erythroid development up to and around the CFU-E and early erythroblast stages via positive effects on their survival. Hence, the previously reported granulomonocytic lineage-directing effects of MFps might also extend laterally to the erythroid lineage (Figure 8). However, a reduction in peripheral fps^{MF} reticulocyte and red-cell counts suggested that a block in differentiation might be present somewhere past the late-CFU-E and/or the early blast stages (Figure 8). Expansion of presumptive late CFU-Es and/or early immature blasts (population *II*) in fps^{MF} mice, accompanied with reductions in more mature blasts (population *I*) represented a likely position for such a block (Figure 4). Coupled with reduced red cell output, the similarity in survival potential between populations *I* and *II,* argued that the shift in cellularity towards early progenitors in fps^{MF} mice was a consequence of impaired differentiation rather than survival. Collectively then, our data are consistent with an erythroid-lineage promoting effect

which originates from expanded populations of CFU-GEMM and extends to stages at or around the CFU-E and early blast (Figure 8). Subsequent to this step, MFps might also impart a mild-delay or block in erythroid differentiation immediately after the late CFU-E/early blast stage (Figure 8). In support of this, we previously reported a statistically significant increase in RBCs in *fps*$^{-/-}$ mice, which was corrected with a wild type *fps* transgene [44]. We speculate that these early promotion effects may be through MFps modulation of SCF/c-Kit signaling, which is required for BFU-E to CFU-E differentiation [45], and further downstream through effects on CFU-E survival.

GM-CSF-induced Stat5 signaling was compromised in *fps*$^{KR/KR}$ mice, which were targeted with a kinase-inactivating mutation; and conversely, enhanced in *fps*^{MF} mice [23,26]. Interestingly, Stat5 activation has also been shown to be involved in Epo-induced survival during erythroid development. This has been suggested by the minimal requirement of the Stat5-pY(343) binding site for efficient EpoR function [46], by the anemic and apoptotic erythoid cell phenotypes of Stat5A$^{-/-}$/Stat5B$^{-/-}$ mice [39], and by the constitutively active state of Stat5 in Epo-independent erythroid cell lines [47]. Here, we report for the first time that Fps (and Fer) are activated in response to Epo in primary erythroid cells, and that Stat5A/B are hyper-responsive to Epo in *fps*^{MF} mice. These results suggest a potential molecular basis for MFps-mediatated promotion of early erythropoiesis in which the survival of immature erythroid cells is accentuated by a mechanism involving cytokine-induced hyper-phosphorylation of Stat5A/B.

Epo and its cognate receptor the EpoR have been shown to be crucial for the survival of CFU-E progenitors [1,48]. Other studies have shown that Epo-mediated effects on survival were restricted to stages post-CFU-E, from the proerythroblast stage through until the basophilic erythroblast stage [1,38,48,49]. These stage-specific Epo-dependent survival effects correlated

well with the observed increases in CFU-E numbers and with the increased survival indices of populations *I* and *II* in *fps*^{MF} mice. Interestingly, early erythroblasts from Stat5A$^{-/-}$/Stat5B$^{-/-}$ exhibited reduced survival which was postulated to account, at least in part, for a block in their differentiation towards more mature blasts [39]. An expansion of population *II* in *fps*^{MF} mice corresponded with positive effects on survival and increases in Stat5A/B phosphorylation. However, this positive effect on survival was not exclusive to presumptive CFU-Es/early blasts but extended also to mature blasts. This is consistent with a role for Fps in specifically regulating Epo-dependent survival of CFU-Es, as well as immature and mature blasts.

Epo and GM-CSF alone were not sufficient to promote enhanced CFU-E development in *fps*^{MF} mice suggesting potential roles for other cytokines in this effect. In this regard, IL-3, GM-CSF and Scf have all been implicated in erythroid progenitor generation and proliferation. However, genetic studies subsequently showed that IL-3 and GM-CSF were not required, or play redundant roles in erythropoiesis [50-52]. Hence, although these cytokines can activate Fps in myeloid cells, they might not significantly contribute to promoting CFU-E development. On the other hand, Scf and its cognate receptor c-kit have been shown to be essential for CFU-E generation [45] suggesting that the accentuated CFU-E phenotype in *fps*^{MF} mice might also involve signaling pathways triggered by Scf. In this context, the novel observation that Fps (and Fer) is activated in response to Scf, and that this response is heightened in the case of MFps, is compelling. Coupled with the importance of Scf in promoting BFU-E to CFU-E differentiation [2,45], these data directly implicate Fps in Scf-mediated signaling events that regulate development of this progenitor.

Our data also suggested that Erk1/2 phosphorylation was compromised in response to Scf in *fps*^{MF} mice primary erythroid cells. Scf can induce rapid tyrosine phosphorylation of Erk1/2

[53] and its prolonged or sustained activation has been associated with differentiation [54-57]. Consistent with this, we observed sustained activation of Erk1/2 in both *wt* and fps^{MF} mice; however, the magnitude of this sustained Erk1/2 response was reduced in fps^{MF} mice, and this alteration might underlie the apparent block or delay in erythroid differentiation in fps^{MF} mice. In this regard, numerous other studies have positively correlated reduced Erk1/2 activation with impaired differentiation in erythroid cells [58,59] while others have specifically linked Scf-signaling with delays in differentiation in a manner which is independent of effects on survival [60,61]. These reports support the possibility that the increased proportion of population *II* in fps^{MF} splenocytes reflects an MFps-mediated enhancement of an Scf-induced delay or block in differentiation that is independent of effects on survival. Indeed the similarity in the apoptotic index of both populations *I* and *II* argue in favor of this. Although these results collectively support a block in differentiation sometime after late CFU-Es or early blasts, we cannot rule-out the possibility that the observed differences in Epo- and Scf-induced signaling reflects different states of maturation of these splenocytes. Nor can we completely exclude the possibility that the anemia in fps^{MF} mice might in part be due to accelerated RBC turnover arising from destruction of subpopulations of defective red cells [62].

In closing, our data support a role for Fps in regulating early erythroid survival and late erythroid differentiation through modulation of Epo and Scf signaling. The promoting effects of MFps might be a consequence of upstream expansion of multi-lineage progenitors such as the CFU-GEMM, consistent with a lineage-regulating role for this kinase [26]. In addition, the detection of Fps (and Fer) in RBCs suggests a role for this kinase in erythrocytes. Numerous kinases have been implicated in signaling processes which regulate erythrocyte glycolysis, cell

shape, potassium and chloride ion transport and cell-volume [63]. Thus, a potential novel role for Fps or Fer in in erythrocytes is intriguing and remains to be explored.

Acknowledgements

We would like to thank the following organizations and individuals: Derek Schulze and Matt Gordon for technical assistance with flow cytometry. W.S. was supported by a fellowship award from the US Department of Defense Breast Cancer Research Program (Grant ID: BCRP – DAMD17-0110382). This study was funded by a grant from National Cancer Institute of Canada (Grant # 012183), with funds from the Canadian Cancer Society.

Table 1: Red cell counts and colony assays

Parameter	*wild-type* (*n*)	fps^{MF} (*n* / *p*-value)
Red Blood Cells (10^{12}/l)	9.1± 0.1 (28)	**7.8 ± 0.1** (22 / $<10^{-10}$)
Reticulocytes (10^{9}/l)	259.5 ± 9.1 (28)	**213.2 ± 10.8** (22 / $<10^{-2}$)
Hemoglobin (g/l)	145.1 ± 1.6 (28)	**132.3 ± 1.9** (22 / $<10^{-5}$)
Hematocrit (ml/l)	461 ± 4 (28)	**438 ± 7** (22 / <0.01)
*CFU – Erythroid (CFU-E) (per 50,000 cells)	154 ± 4 (4)	**211 ± 10** (4 / 0.013)
*BFU – Erythroid (BFU-E) (per 50,000 cells)	12 ± 1 (4)	22 ± 10 (4 / 0.40)
**CFU - Erythroid (CFU-E) (per 50,000 cells)	173 ± 13 (4)	143 ± 13 (4 / 0.14)
**BFU – Erythroid (BFU-E) (per 50,000 cells)	4 ± 1 (4)	5 ± 1 (4 / 0.61)

Hematological parameters of *wild-type* (4.3 ± 0.2 mo; $n = 28$) and fps^{MF} (4.2 ± 0.2 mo; $n = 22$) mice were determined on a Sysmex XE-2100 automated hematological counter. *Bone marrow methyl cellulose assays were supplemented with a cocktail of recombinant cytokines (R&D Systems, Minneapolis, MN) containing 50 ng/ml Steel factor (SF), 5 ng/ml IL-3, 10 ng/ml IL-6, 10 ng/ml Tpo, 1 U/ml Epo and 5 ng/ml GM-CSF. ** Bone marrow methyl cellulose assays were supplemented with a more restricted cocktail of recombinant cytokines 1 U/ml Epo and 5 ng/ml GM-CSF. Data are presented as mean ± standard error of the mean (SEM) along with P-values (*p*) and the number of animals used in the analyses (*n*). Statistically significant parameters are bolded.

Figure 1.

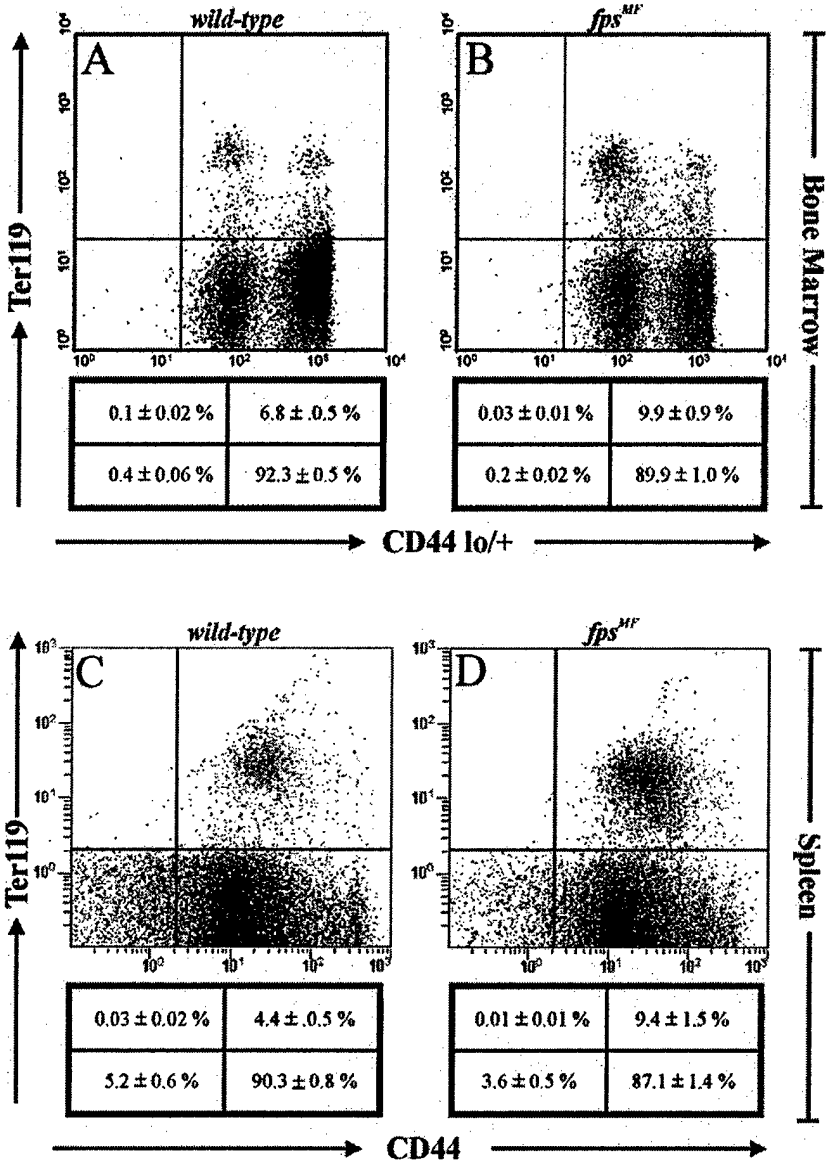
wild-type
fps^MF
A
B
Ter119
Bone Marrow
0.1 ± 0.02 %
6.8 ± .0.5 %
0.4 ± 0.06 %
92.3 ± 0.5 %
0.03 ± 0.01 %
9.9 ± 0.9 %
0.2 ± 0.02 %
89.9 ± 1.0 %
CD44 lo/+
wild-type
fps^MF
C
D
Ter119
Spleen
0.03 ± 0.02 %
4.4 ± .0.5 %
5.2 ± 0.6 %
90.3 ± 0.8 %
0.01 ± 0.01 %
9.4 ± 1.5 %
3.6 ± 0.5 %
87.1 ± 1.4 %
CD44

Figure 2

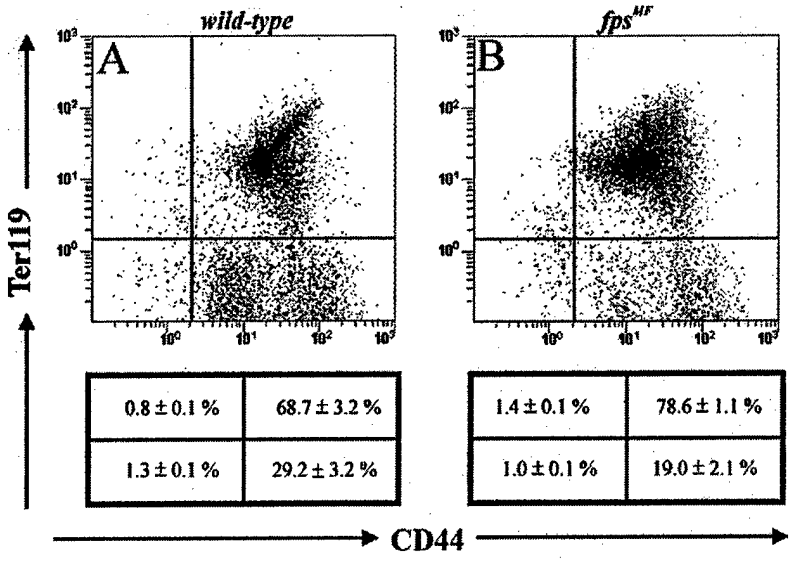
wild-type
fps^MF
A
B
Ter119
CD44
0.8 ± 0.1 %
68.7 ± 3.2 %
1.3 ± 0.1 %
29.2 ± 3.2 %
1.4 ± 0.1 %
78.6 ± 1.1 %
1.0 ± 0.1 %
19.0 ± 2.1 %

Figure 3

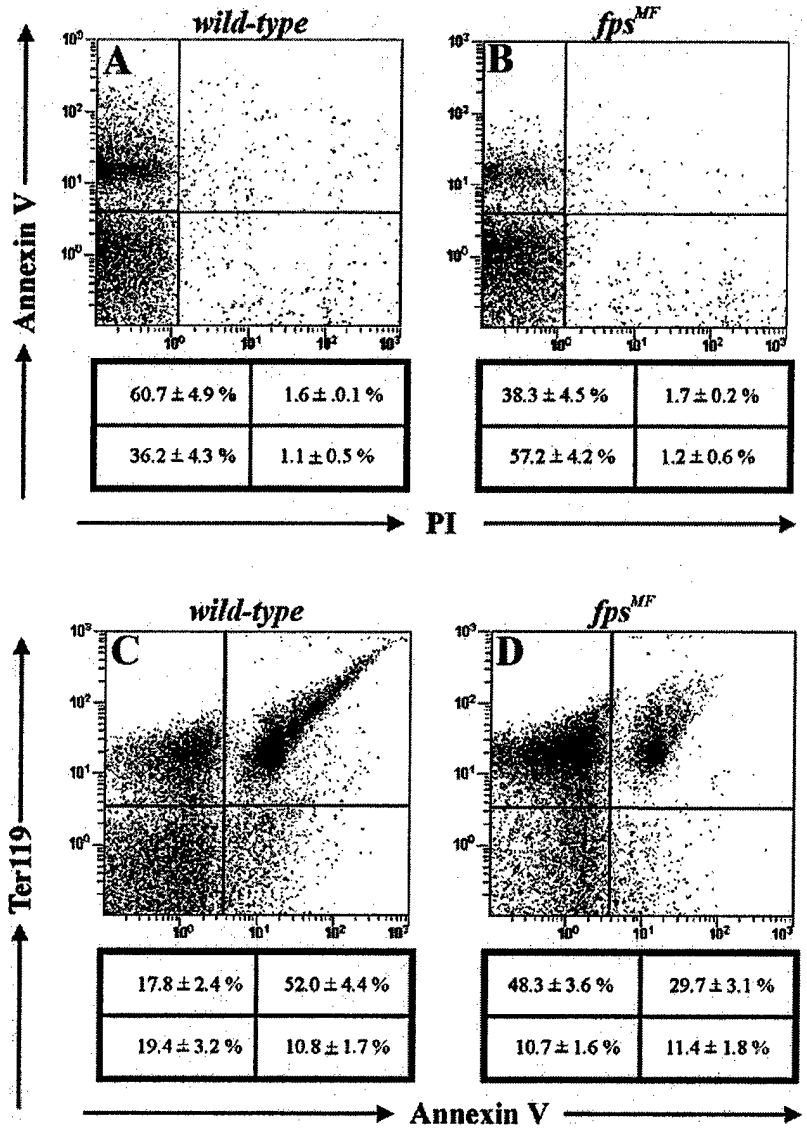
wild-type
A
fps^MF
B
Annexin V
60.7 ± 4.9 %
1.6 ± .0.1 %
36.2 ± 4.3 %
1.1 ± 0.5 %
38.3 ± 4.5 %
1.7 ± 0.2 %
57.2 ± 4.2 %
1.2 ± 0.6 %
PI
wild-type
C
fps^MF
D
Ter119
17.8 ± 2.4 %
52.0 ± 4.4 %
19.4 ± 3.2 %
10.8 ± 1.7 %
48.3 ± 3.6 %
29.7 ± 3.1 %
10.7 ± 1.6 %
11.4 ± 1.8 %
Annexin V

Figure 4

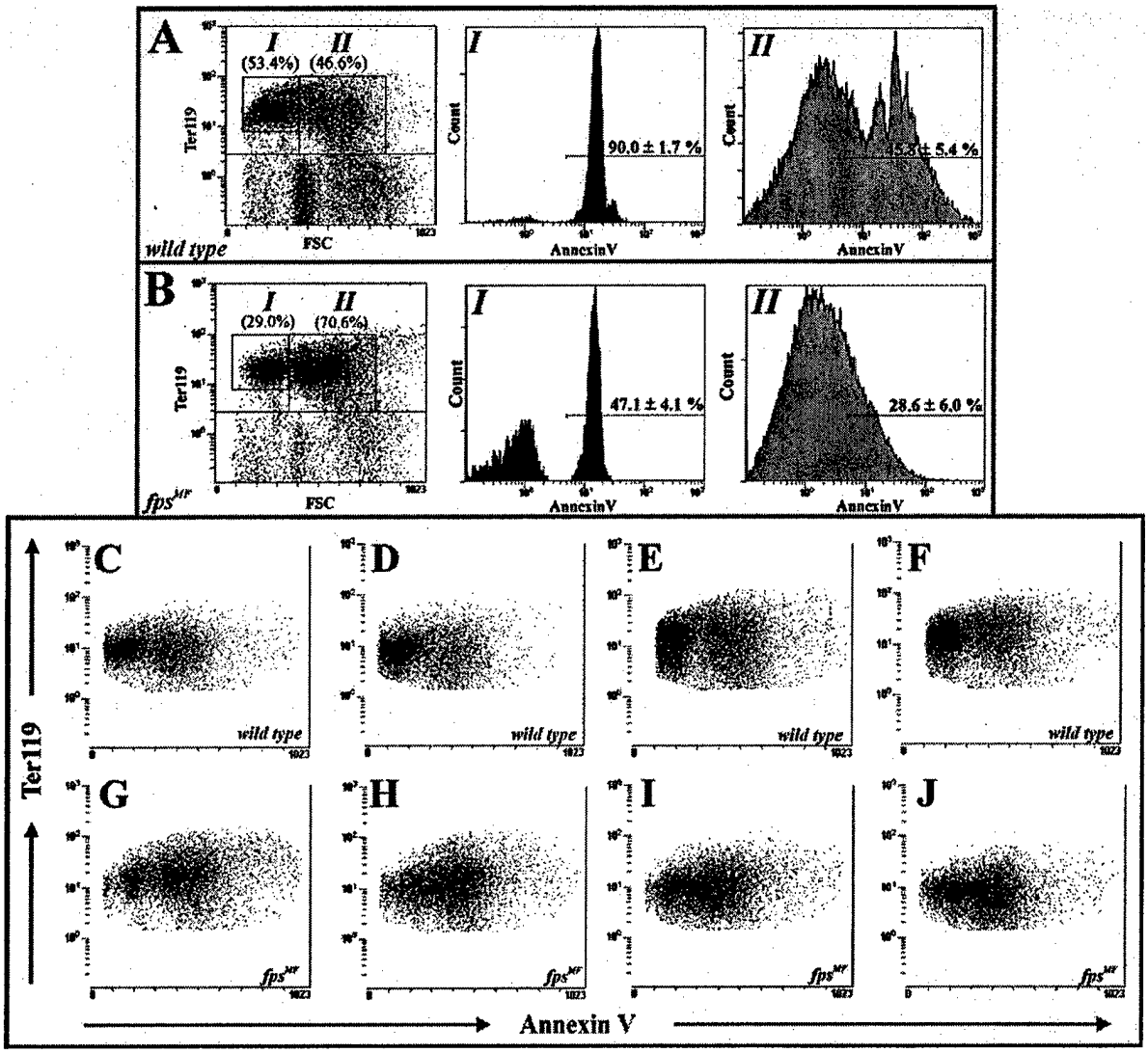
A
I
II
(53.4%)
(46.6%)
Ter119
FSC
wild type
Count
90.0 ± 1.7 %
AnnexinV
15.3 ± 5.4 %
B
(29.0%)
(70.6%)
47.1 ± 4.1 %
28.6 ± 6.0 %
fps^MF
C
D
E
F
G
H
I
J
Ter119
Annexin V

Figure 5

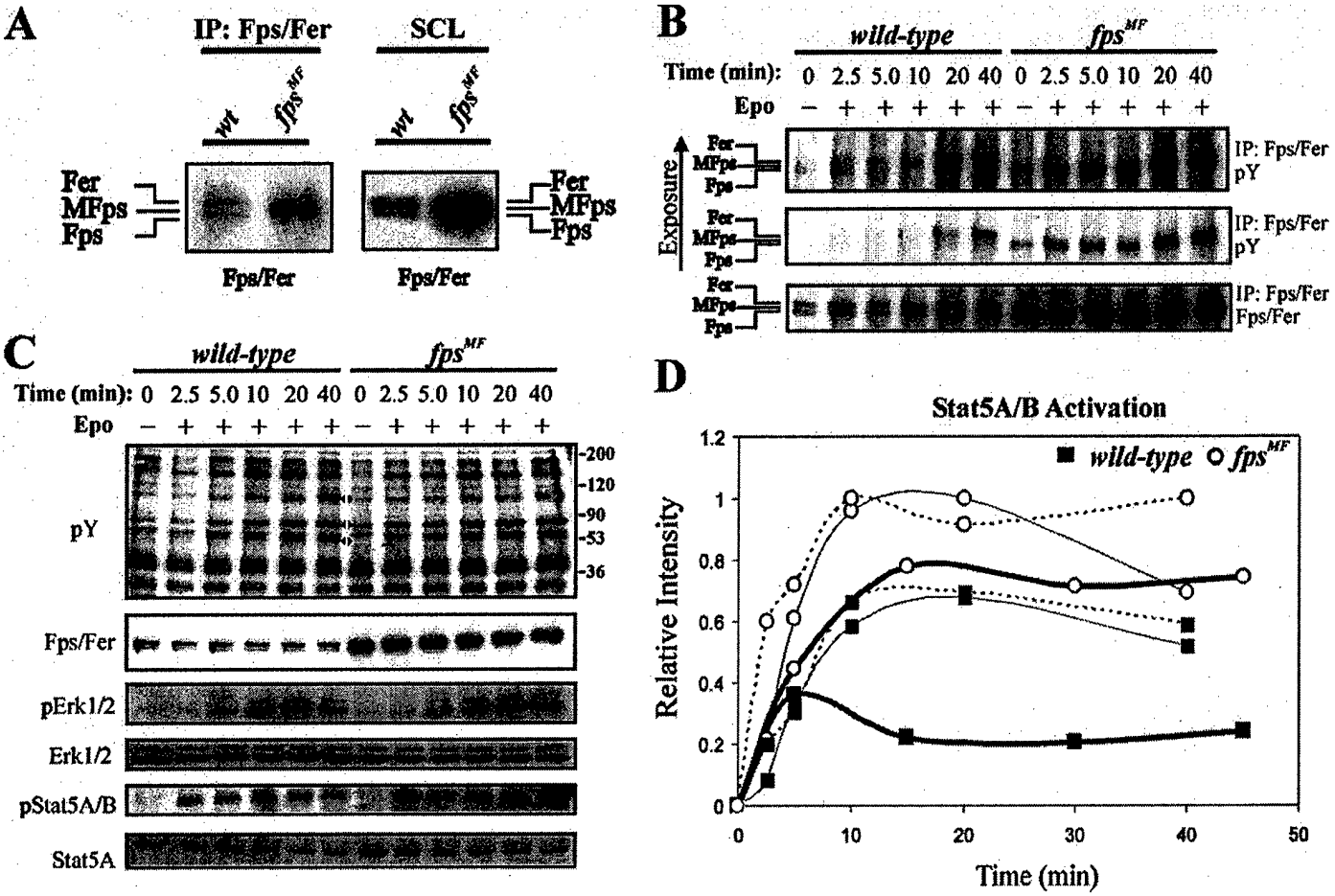
A
IP: Fps/Fer
SCL
wt
fps^MF
Fer
MFps
Fps
Fps/Fer
B
wild-type
fps^MF
Time (min): 0 2.5 5.0 10 20 40 0 2.5 5.0 10 20 40
Epo
Exposure
IP: Fps/Fer pY
IP: Fps/Fer pY
IP: Fps/Fer Fps/Fer
C
wild-type
fps^MF
Time (min): 0 2.5 5.0 10 20 40 0 2.5 5.0 10 20 40
Epo
pY
200
120
90
53
36
Fps/Fer
pErk1/2
Erk1/2
pStat5A/B
Stat5A
D
Stat5A/B Activation
wild-type
fps^MF
Relative Intensity
Time (min)

Figure 6

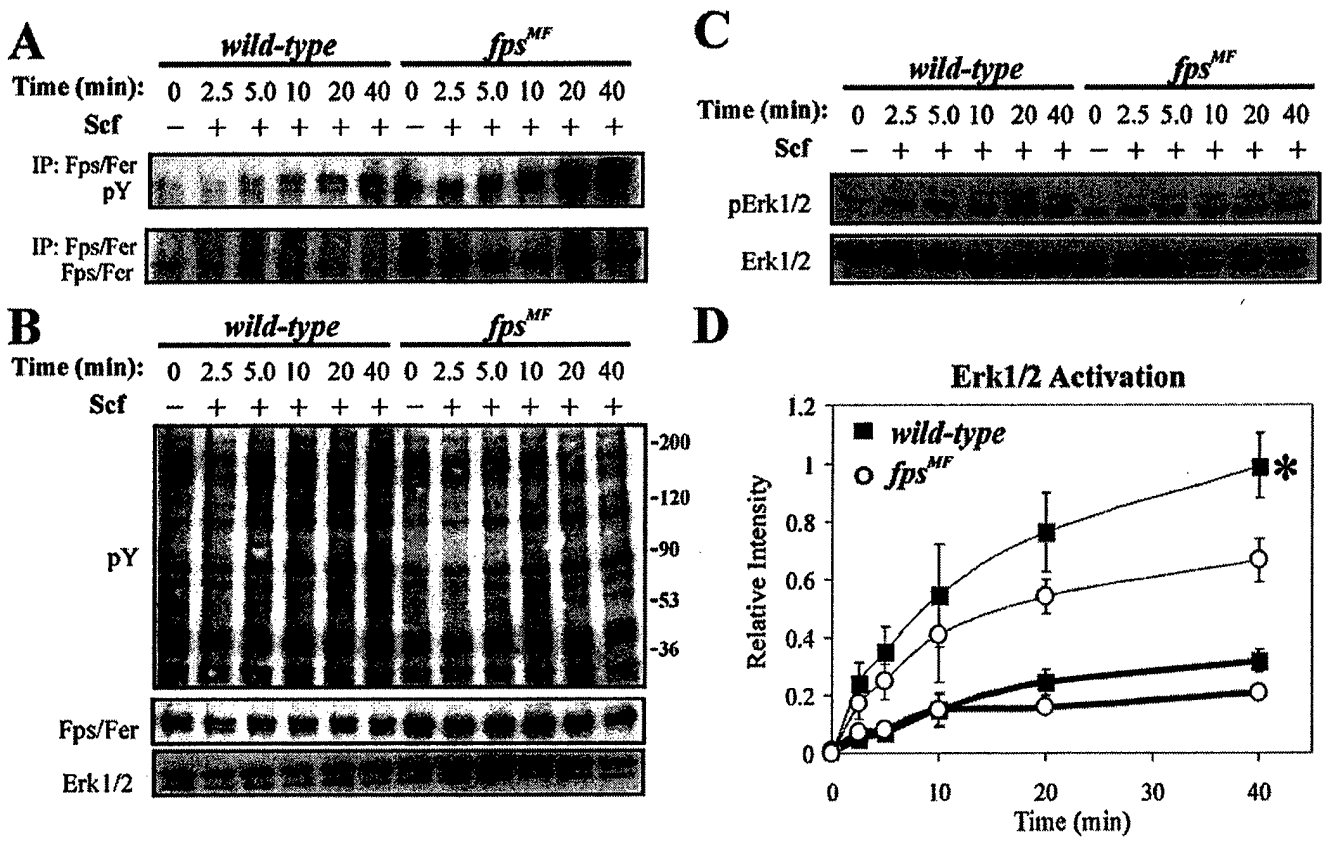
A
wild-type
fps^MF
Time (min): 0 2.5 5.0 10 20 40 0 2.5 5.0 10 20 40
Scf – + + + + + – + + + + +
IP: Fps/Fer pY
IP: Fps/Fer Fps/Fer
B
wild-type
fps^MF
Time (min): 0 2.5 5.0 10 20 40 0 2.5 5.0 10 20 40
Scf – + + + + + – + + + + +
pY
-200
-120
-90
-53
-36
Fps/Fer
Erk1/2
C
wild-type
fps^MF
Time (min): 0 2.5 5.0 10 20 40 0 2.5 5.0 10 20 40
Scf – + + + + + – + + + + +
pErk1/2
Erk1/2
D
Erk1/2 Activation
wild-type
fps^MF
Relative Intensity
1.2
1
0.8
0.6
0.4
0.2
0
0
10
20
30
40
Time (min)
*

Figure 7

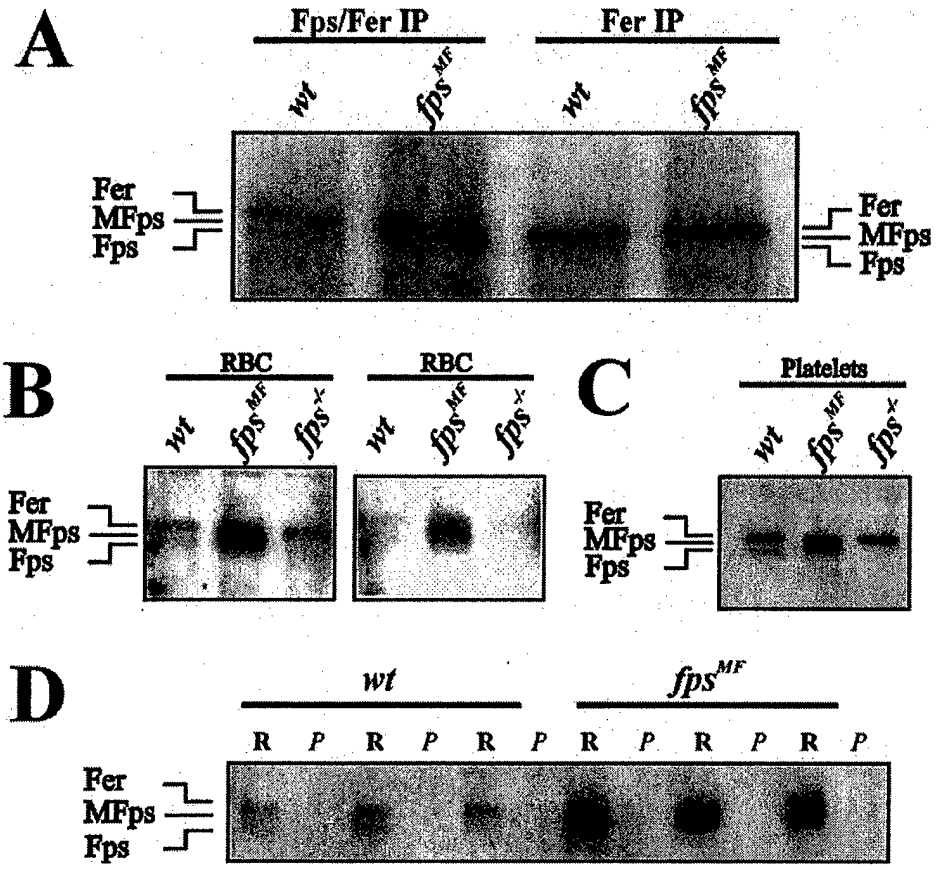
A
Fps/Fer IP
Fer IP
wt
fps^MF
wt
fps^MF
Fer
MFps
Fps
Fer
MFps
Fps
B
RBC
RBC
wt
fps^MF
fps^-
wt
fps^MF
fps^-
Fer
MFps
Fps
C
Platelets
wt
fps^MF
fps^-
Fer
MFps
Fps
D
wt
fps^MF
R P R P R P R P R P R P
Fer
MFps
Fps

Figure 8

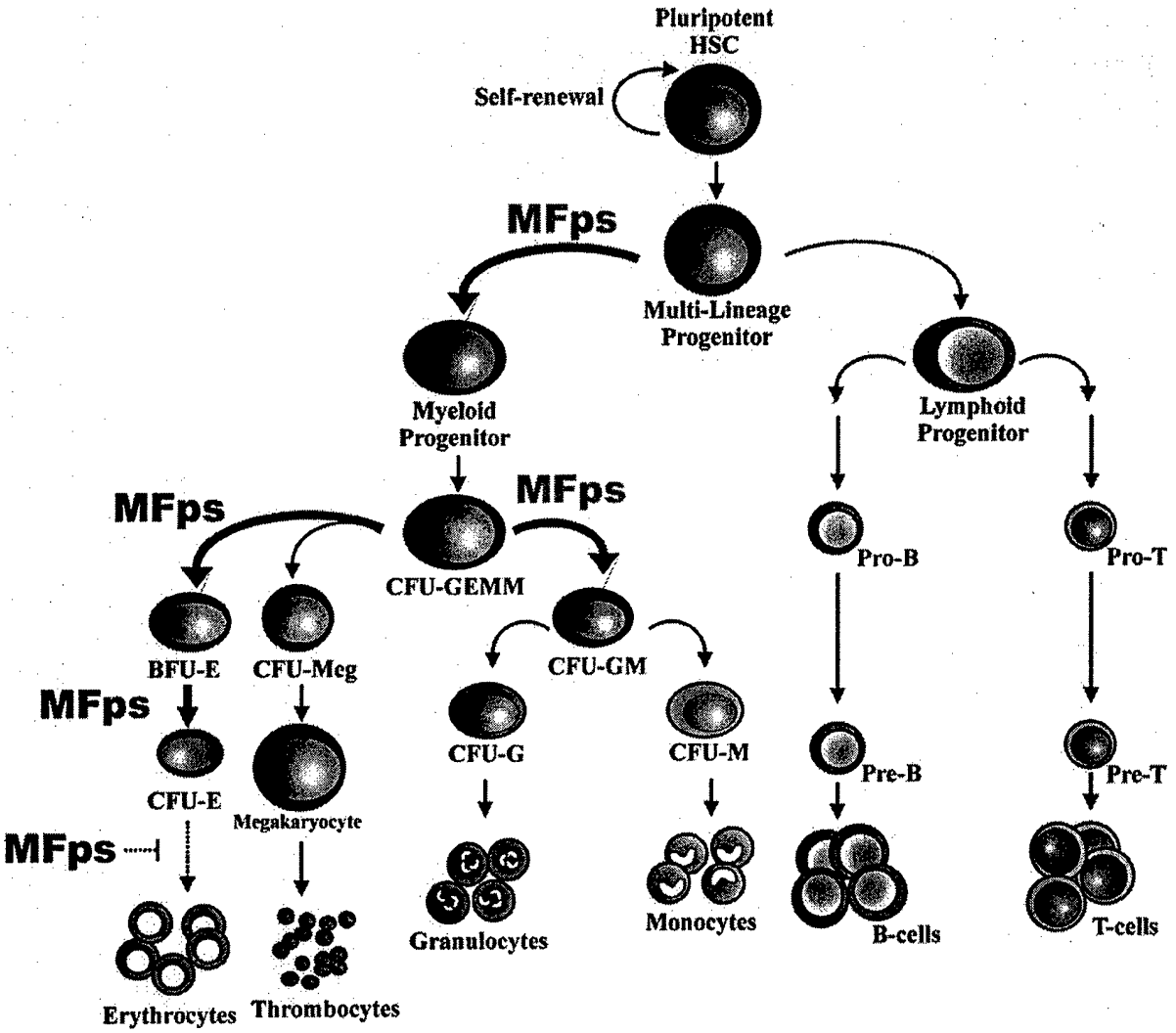
Pluripotent
HSC
Self-renewal
MFps
Multi-Lineage
Progenitor
Myeloid
Progenitor
Lymphoid
Progenitor
MFps
MFps
CFU-GEMM
BFU-E
CFU-Meg
CFU-GM
MFps
CFU-G
CFU-M
Pro-B
Pro-T
CFU-E
Megakaryocyte
Pre-B
Pre-T
MFps
Granulocytes
Monocytes
B-cells
T-cells
Erythrocytes
Thrombocytes

Figure 1. Flow cytometry analysis of erythroid progenitors in spleen and bone marrow. Bone marrow isolated from *wt* (A) and *fps*^{MF} (B) mice (2.9 ± 0.2 mo.) was stained with the erythroid marker Ter119 and analyzed by flow cytometry. Bone marrow from *fps*^{MF} mice contained increased Ter119^{+}CD44$^{lo/+}$ erythroid progenitor populations compared to *wt* mice (n = 28; p < 0.009). Splenocytes isolated from *wt* (C) and *fps*^{MF} (D) mice (2.8 ± 0.4 mo.) were similarly analyzed. Increased levels of erythroid progenitors (Ter119^{+}CD44^{+}; n = 8; p = 0.01) were observed in the spleens of *fps*^{MF} mice.

Figure 2. Flow cytometry analysis of erythroid progenitors from PHZ-treated mice. Erythroid progenitors isolated from spleens of PHZ-treated *wt* (A) and *fps*^{MF} (B) mice were stained with the erythroid markers Ter119 and analyzed by flow cytometry. Under stressed conditions, Ter119^{+}CD44$^{lo/+}$ erythroid progenitor populations were increased in *fps*^{MF} compared to *wt* mice (*wt*: 68.7 ± 3.2%; *fps*^{MF}: 78.6 ± 1.9%; n = 4; p = 0.044).

Figure 3. Decreased apoptosis in erythroid cells from *fps*^{MF} mice. Splenocytes isolated from PHZ-treated *wt* (4.5 ± 0.2 mo; n = 5) and *fps*^{MF} mice (4.3 ± 0.3 mo; n = 6) were stained with apoptotic and erythroid markers and analyzed by flow cytometry. Splenocytes from *fps*^{MF} (B) mice have decreased AnnexinV^{+}/PI^{-} staining profiles relative to *wt* mice (A) (p = 0.008). The Ter119^{+} erythroid population in *fps*^{MF} (D) splenocytes exhibited decreased AnnexinV^{+} staining compared to the same population from *wt* (C) mice (p = 0.004).

Figure 4. Accumulation and increased survival of immature erythroblasts in *fps*^{MF} mice. Splenocytes isolated from PHZ-treated *wt* (4.5 ± 0.2 mo; $n = 5$) and *fps*^{MF} mice (4.3 ± 0.3 mo; $n = 6$) were analyzed by flow cytometry using Ter119 to stain erythroid cells. Representative forward scatter spectrum of Ter119^{+} splenocytes isolated from PHZ-treated *wt* (A; left) or *fps*^{MF} (B; left) mice showed 2 distinct populations labeled *I* and *II*. Population *II* corresponds to early, immature erythroid cells, while population *I* corresponded to later, more mature erythroblasts. Analysis of 5 *wt* mice (A; left) showed that populations *I* and *II* represented 53.4 ± 2.8% and 46.6 ± 5.0% of Ter119^{+} cells, respectively. In *fps*^{MF} splenocytes (B; left) population *I* decreased to 29.0 ± 1.5% ($n = 5$; $p = 2.1 \times 10^{-4}$) and population *II* increased to 70.6 ± 1.6% ($n = 6$ $p = 2.1 \times 10^{-4}$). Profiles from individual *wt* (panels C-F) and *fps*^{MF} mice (panels G-J) better illustrate the differential shift in populations *I* and *II*. The Ter119^{+} cells in populations *I* and *II* were separately assessed for Annexin V staining. Analysis of 5 *wt* mice showed that 90.0± 1.7% of population *I* and 45.8 ± 5.4% of population *II* stained positive for Annexin V (A; middle, and right). The number of Annexin V positive cells from 6 *fps*^{MF} mice in populations *I* and *II* decreased to 47.1 ± 4.1% ($p = 3.6 \times 10^{-5}$) and 28.6 ± 4.9% (0.045), respectively (B; middle, and right).

Figure 5. Fps, MFps and Fer are expressed in primary erythroid cells and are phosphorylated in response to Epo. (A) Anti-Fps/Fer IPs and soluble cell lysates (SCL) from primary erythroid cells were probed with anti-Fps/Fer to detect the indicated Fps, MFps and Fer proteins. Both Fps and Fer were detected in anti-Fps/Fer IP and SCL samples from *wt* cells. In *fps*^{MF} cells, the more abundant MFps protein obscures Fps and Fer. (B) Splenocytes from PHZ-treated mice were stimulated with Epo (50 U/ml) for the indicated times. Immunoprecipitation with anti-Fps/Fer

followed by blotting with anti-phosphotyrosine (anti-pY) antibodies revealed that Fps, MFps and Fer were inducibly tyrosine phosphorylated by Epo stimulation. Stripping and reblotting with anti-Fps/Fer confirmed equivalent loading and also demonstrated a high degree of over-expression of MFps relative to endogenous *wt* Fps and Fer. (C) Immunoblotting analysis of SCLs of *wt* and *fps*^{MF} erythroid cells stimulated with Epo (50 U/ml) for the indicated times using anti-pY (pY), anti-Fps/Fer, anti-phosphoStat5A/B (pStat5A/B), anti-Stat5A (Stat5A), anti-phospho Erk1/2 (pErk1/2) and anti-Erk1/2 (Erk1/2). The phosphorylation profiles of several protein(s) (pY panel; arrowheads) were different in *fps*^{MF} mice. Epo-induced activation profiles of Erk1/2 were similar in *wt* and *fps*^{MF} cells, whereas Stat5A/B phosphorylation was enhanced in *fps*^{MF} relative to *wt* cells. (D) Quantification of three independent experiments showing enhanced Stat5A/B phosphorylation. The intensity data shown represent the relative ratios of phosphorylated Stat5A/B to total Stat5A. Dotted, medium and heavy line weights represent profiles from individual experiments on *wt* (■) or *fps*^{MF} (○) cells.

Figure 6. Fps, MFps and Fer are tyrosine phosphorylated in response to Scf in primary erythroid cells. Splenocytes from PHZ-treated *wt* and *fps*^{MF} mice were stimulated with Scf for the indicated times. (A) Fps, MFps and Fer were immunoprecipitated with anti-Fps/Fer and immunoblotted with anti-pY (pY). Scf stimulation resulted in inducible tyrosine phosphorylation of Fps, MFps and Fer. Stripping and reprobing with anti-Fps/Fer confirmed equivalent loading. (B) Immunoblotting analysis of SCLs of *wt* and *fps*^{MF} splenocytes stimulated with Scf (200 ng/ml) using anti-pY (pY), anti-Fps/Fer and anti-Erk1/2. (C) Immunoblotting analysis of SCLs of *wt* and *fps*^{MF} splencytes stimulated with Scf (200 ng/ml) for the indicated times using anti-phosphoErk1/2 (pErk1/2) and anti-Erk1/2 (Erk1/2). Scf-induced activation profiles of Erk1/2

were diminished in *fps*^{MF} erythroid cells in response to Scf. (D) Mean ± SEM values of three independent experiments in which enhanced Erk1/2 phosphorylation was observed. The intensity data shown represent the relative ratios of phosphorylated Erk1/2 to total Erk1/2. Light and heavy line weights represent Erk2 and Erk1 activation profiles, respectively; *wt* (■); *fps*^{MF} (○) (*$p \leq 0.05$).

Figure 7. Fps and Fer tyrosine kinases are expressed in RBCs. (A) Fps, MFps and Fer from *wt* or *fps*^{MF} RBC preparations were immunoprecipitated together (Fps/Fer IP), or Fer was immunprecipitated alone (Fer IP). Fps, MFps and Fer were then detected by immunoblotting with anti-Fps/Fer. (B) Fps, MFps and Fer were detected in enriched RBCs (SCLs) from *wt*, *fps*^{MF} or *fps*$^{-/-}$ mice by immunoblotting using anti-Fps/Fer. A lighter exposure from another blot (right) more clearly depicts the migration position of Fps, MFps and Fer. (C) Fps, MFps and Fer were detected in purified platelets (SCLs) from *wt*, *fps*^{MF} or *fps*$^{-/-}$ mice by immunoblotting using anti-Fps/Fer. (D) Comparison of Fps, MFps and Fer levels from quantities of purified platelets (*P*) which are identical to the number of contaminating platelets present in enriched RBC preparations (R) (*wt*, $n = 3$; *fps*^{MF}, $n = 3$; 3.3 ± 0.25 mo). Fps, MFps and Fer were detected by immunoblotting with anti-Fps/Fer.

Figure 8. Hypothetical model for Fps involvement in lineage commitment by hematopoietic progenitors. Increased mature circulating granulocytes and monocytes, and decreased lymphoid cells in *fps*^{MF} mice suggested a role for Fps at the level of the committed multi-lineage progenitor cells [26]. Increased numbers of CFU-GEMM were consistent with that role, and increased numbers of CFU-GM suggested that this lineage-commitment role extends to the more mature bipotential granulomonocytic progenitor. The lack of a selective increase in monocytic or

granulocytic cells argued against a lineage-determining role for Fps beyond this bipotential progenitor. Increases in CFU-GEMM, CFU-E, and the proportions of early erythroid progenitors/blasts suggested that the lineage determining role extends laterally to erythroid lineage. The sphere of influence of Fps in this lineage-promotion effect involves effects on survival and extends to stages at or around CFU-Es and early blasts. However, peripheral levels of reticulocytes and red cells were reduced, suggesting that Fps might regulate erythroid differentiation at later stages of erythropoiesis.

References

1. Wu H, Liu X, Jaenisch R, Lodish HF (1995) Generation of committed erythroid BFU-E and CFU-E progenitors does not require erythropoietin or the erythropoietin receptor. Cell 83:59
2. Russell ES (1979) Hereditary anemias of the mouse: a review for geneticists. Adv Genet 20:357
3. Greer PA (2002) Closing in on the biological functions of Fps/Fes and Fer. Nature Reviews Molecular Cell Biology 3:278
4. Aspenstrom P (1997) A Cdc42 target protein with homology to the non-kinase domain of FER has a potential role in regulating the actin cytoskeleton. Curr Biol 7:479
5. Cheng H, Rogers JA, Dunham NA, Smithgall TE (1999) Regulation of c-Fes tyrosine kinase and biological activities by N- terminal coiled-coil oligomerization domains. In: Mol Cell Biol, 8335
6. Care A, Mattia G, Montesoro E, Parolini I, Russo G, Colombo MP, Peschle C (1994) c-fes expression in ontogenetic development and hematopoietic differentiation. Oncogene 9:739
7. Haigh J, McVeigh J, Greer P (1996) The fps/fes tyrosine kinase is expressed in myeloid, vascular endothelial, epithelial, and neuronal cells and is localized in the trans-golgi network. Cell Growth Differ 7:931
8. Feldman RA, Gabrilove JL, Tam JP, Moore MA, Hanafusa H (1985) Specific expression of the human cellular fps/fes-encoded protein NCP92 in normal and leukemic myeloid cells. Proc Natl Acad Sci U S A 82:2379
9. MacDonald I, Levy J, Pawson T (1985) Expression of the mammalian c-fes protein in hematopoietic cells and identification of a distinct fes-related protein. Mol Cell Biol 5:2543
10. Kim J, Feldman RA (2002) Activated Fes protein tyrosine kinase induces terminal macrophage differentiation of myeloid progenitors (U937 Cells) and activation of the transcription factor PU.1. Molecular and Cellular Biology 22:1903
11. Kim J, Ogata Y, Feldman RA (2003) Fes Tyrosine Kinase Promotes Survival and Terminal Granulocyte Differentiation of Factor-dependent Myeloid Progenitors (32D) and Activates Lineage-specific Transcription Factors. J Biol Chem 278:14978
12. Yu G, Smithgall TE, Glazer RI (1989) K562 leukemia cells transfected with the human c-fes gene acquire the ability to undergo myeloid differentiation. J Biol Chem 264:10276
13. Ferrari S, Manfredini R, Tagliafico E, Grande A, Barbieri D, Balestri R, Pizzanelli M, Zucchini P, Citro G, Zupi G, et al. (1994) Antiapoptotic effect of c-fes protooncogene during granulocytic differentiation. Leukemia 8 Suppl 1:S91
14. Ferrari S, Donelli A, Manfredini R, Sarti M, Roncaglia R, Tagliafico E, Rossi E, Torelli G, Torelli U (1990) Differential effects of c-myb and c-fes antisense oligodeoxynucleotides on granulocytic differentiation of human myeloid leukemia HL60 cells. Cell Growth Differ 1:543
15. Hanazono Y, Chiba S, Sasaki K, Mano H, Yazaki Y, Hirai H (1993) Erythropoietin induces tyrosine phosphorylation and kinase activity of the c-fps/fes proto-oncogene product in human erythropoietin-responsive cells. Blood 81:3193
16. Brizzi MF, Aronica MG, Rosso A, Bagnara GP, Yarden Y, Pegoraro L (1996) Granulocyte-macrophage colony-stimulating factor stimulates JAK2 signaling pathway and rapidly activates p93fes, STAT1 p91, and STAT3 p92 in polymorphonuclear leukocytes. J Biol Chem 271:3562

17. Hanazono Y, Chiba S, Sasaki K, Mano H, Miyajima A, Arai K, Yazaki Y, Hirai H (1993) c-fps/fes protein-tyrosine kinase is implicated in a signaling pathway triggered by granulocyte-macrophage colony-stimulating factor and interleukin-3. Embo J 12:1641
18. Linnekin D, Mou SM, Greer P, Longo DL, Ferris DK (1995) Phosphorylation of a Fes-related protein in response to granulocyte- macrophage colony stimulating factor. J Biol Chem 270:4950
19. Izuhara K, Feldman RA, Greer P, Harada N (1996) Interleukin-4 induces association of the c-fes proto-oncogene product with phosphatidylinositol-3 kinase. Blood 88:3910
20. Jiang H, Foltenyi K, Kashiwada M, Donahue L, Vuong B, Hehn B, Rothman P (2001) Fes mediates the IL-4 activation of insulin receptor substrate-2 and cellular proliferation. J Immunol 166:2627
21. Adunyah SE, Spencer GC, Cooper RS, Rivero JA, Ceesay K (1995) Interleukin-11 induces tyrosine phosphorylation, and c-jun and c-fos mRNA expression in human K562 and U937 cells. Ann N Y Acad Sci 766:296
22. Matsuda T, Fukada T, Takahashi-Tezuka M, Okuyama Y, Fujitani Y, Hanazono Y, Hirai H, Hirano T (1995) Activation of Fes tyrosine kinase by gp130, an interleukin-6 family cytokine signal transducer, and their association. J Biol Chem 270:11037
23. Senis Y, Zirngibl R, McVeigh J, Haman A, Hoang T, Greer PA (1999) Targeted disruption of the murine fps/fes proto-oncogene reveals that Fps/Fes kinase activity is dispensable for hematopoiesis. Mol Cell Biol 19:7436
24. Hackenmiller R, Kim J, Feldman RA, Simon MC (2000) Abnormal Stat activation, hematopoietic homeostasis, and innate immunity in c-fes-/- mice. Immunity 13:397
25. Zirngibl RA, Senis Y, Greer PA (2002) Enhanced endotoxin-sensitivity in Fps/Fes-null mice with minimal defects in hematopoietic homeostasis. Mol Cell Biol 22:2472
26. Sangrar W, Gao Y, Zirngibl R, Scott M, Greer P (2003) The fps/fes proto-oncogene regulates hematopoietic lineage output. Experimental Hematology 31:1259
27. Keller P, Payne JL, Tremml G, Greer PA, Gaboli M, Pandolfi PP, Bessler M (2001) FES-Cre targets phosphatidylinositol glycan class A (PIGA) inactivation to hematopoietic stem cells in the bone marrow. J Exp Med 194:581
28. Sangrar W, Mewburn J, Vincent S, Fisher J, Greer P (2004) Vascular defects in gain-of-function fps/fes transgenic mice correlate with PDGF- and VEGF-induced activation of mutant Fps/Fes kinase in endothelial cells. Journal of Thrombosis and Haemostasis 2:820
29. Greer P, Haigh J, Mbamalu G, Khoo W, Bernstein A, Pawson T (1994) The Fps/Fes protein-tyrosine kinase promotes angiogenesis in transgenic mice. Mol Cell Biol 14:6755
30. Greer P, Maltby V, Rossant J, Bernstein A, Pawson T (1990) Myeloid expression of the human c-fps/fes proto-oncogene in transgenic mice. Mol Cell Biol 10:2521
31. Heydemann A, Warming S, Clendenin C, Sigrist K, Hjorth JP, Simon MC (2000) A minimal c-fes cassette directs myeloid-specific expression in transgenic mice. Blood 96:3040
32. Mason JM, Beattie BK, Liu Q, Dumont DJ, Barber DL (2000) The SH2 inositol 5-phosphatase Ship1 is recruited in an SH2-dependent manner to the erythropoietin receptor. J Biol Chem 275:4398
33. Haq R, Halupa A, Beattie BK, Mason JM, Zanke BW, Barber DL (2002) Regulation of erythropoietin-induced STAT serine phosphorylation by distinct mitogen-activated protein kinases. J Biol Chem 277:17359

34. Law DA, Nannizzi-Alaimo L, Ministri K, Hughes PE, Forsyth J, Turner M, Shattil SJ, Ginsberg MH, Tybulewicz VL, Phillips DR (1999) Genetic and pharmacological analyses of Syk function in alphaIIbbeta3 signaling in platelets. Blood 93:2645
35. Senis YA, Sangrar W, Zirngibl RA, Craig AWB, Lee DH, Greer PA (2003) Fps/Fes and Fer Nonreceptor Protein-Tyrosine Kinases Regulate Collagen- and ADP-Induced Platelet Aggregation. Journal of Thrombosis and Haemostasis. 1:1062
36. Vannucchi AM, Bianchi L, Cellai C, Paoletti F, Carrai V, Calzolari A, Centurione L, Lorenzini R, Carta C, Alfani E, Sanchez M, Migliaccio G, Migliaccio AR (2001) Accentuated response to phenylhydrazine and erythropoietin in mice genetically impaired for their GATA-1 expression (GATA-1(low) mice). Blood 97:3040
37. Koury MJ, Bondurant MC (1990) Erythropoietin retards DNA breakdown and prevents programmed death in erythroid progenitor cells. Science 248:378
38. Kelley LL, Koury MJ, Bondurant MC, Koury ST, Sawyer ST, Wickrema A (1993) Survival or death of individual proerythroblasts results from differing erythropoietin sensitivities: a mechanism for controlled rates of erythrocyte production. Blood 82:2340
39. Socolovsky M, Nam H, Fleming MD, Haase VH, Brugnara C, Lodish HF (2001) Ineffective erythropoiesis in Stat5a(-/-)5b(-/-) mice due to decreased survival of early erythroblasts. Blood 98:3261
40. Pootrakul P, Sirankapracha P, Hemsorach S, Moungsub W, Kumbunlue R, Piangitjagum A, Wasi P, Ma L, Schrier SL (2000) A correlation of erythrokinetics, ineffective erythropoiesis, and erythroid precursor apoptosis in thai patients with thalassemia. Blood 96:2606
41. Wu H, Klingmuller U, Besmer P, Lodish HF (1995) Interaction of the erythropoietin and stem-cell-factor receptors. Nature 377:242
42. Garcia R, Yu CL, Hudnall A, Catlett R, Nelson KL, Smithgall T, Fujita DJ, Ethier SP, Jove R (1997) Constitutive activation of Stat3 in fibroblasts transformed by diverse oncoproteins and in breast carcinoma cells. Cell Growth Differ 8:1267
43. Nelson KL, Rogers JA, Bowman TL, Jove R, Smithgall TE (1998) Activation of STAT3 by the c-Fes protein-tyrosine kinase. J Biol Chem 273:7072
44. Zirngibl RA, Senis Y, Greer PA (2002) Enhanced endotoxin sensitivity in fps/fes-null mice with minimal defects in hematopoietic homeostasis. Mol Cell Biol 22:2472
45. Nocka K, Majumder S, Chabot B, Ray P, Cervone M, Bernstein A, Besmer P (1989) Expression of c-kit gene products in known cellular targets of W mutations in normal and W mutant mice--evidence for an impaired c-kit kinase in mutant mice. Genes Dev 3:816
46. Pircher TJ, Geiger JN, Zhang D, Miller CP, Gaines P, Wojchowski DM (2001) Integrative signaling by minimal erythropoietin receptor forms and c-Kit. J Biol Chem 276:8995
47. Bao H, Jacobs-Helber SM, Lawson AE, Penta K, Wickrema A, Sawyer ST (1999) Protein kinase B (c-Akt), phosphatidylinositol 3-kinase, and STAT5 are activated by erythropoietin (EPO) in HCD57 erythroid cells but are constitutively active in an EPO-independent, apoptosis-resistant subclone (HCD57-SREI cells). Blood 93:3757
48. Lin CS, Lim SK, D'Agati V, Costantini F (1996) Differential effects of an erythropoietin receptor gene disruption on primitive and definitive erythropoiesis. Genes Dev 10:154
49. Koury MJ, Bondurant MC (1988) Maintenance by erythropoietin of viability and maturation of murine erythroid precursor cells. J Cell Physiol 137:65
50. Dranoff G, Crawford AD, Sadelain M, Ream B, Rashid A, Bronson RT, Dickersin GR, Bachurski CJ, Mark EL, Whitsett JA, et al. (1994) Involvement of granulocyte-macrophage colony-stimulating factor in pulmonary homeostasis. Science 264:713

51. Stanley E, Lieschke GJ, Grail D, Metcalf D, Hodgson G, Gall JA, Maher DW, Cebon J, Sinickas V, Dunn AR (1994) Granulocyte/macrophage colony-stimulating factor-deficient mice show no major perturbation of hematopoiesis but develop a characteristic pulmonary pathology. Proc Natl Acad Sci U S A 91:5592
52. Nishinakamura R, Nakayama N, Hirabayashi Y, Inoue T, Aud D, McNeil T, Azuma S, Yoshida S, Toyoda Y, Arai K, et al. (1995) Mice deficient for the IL-3/GM-CSF/IL-5 beta c receptor exhibit lung pathology and impaired immune response, while beta IL3 receptor-deficient mice are normal. Immunity 2:211
53. Okuda K, Sanghera JS, Pelech SL, Kanakura Y, Hallek M, Griffin JD, Druker BJ (1992) Granulocyte-macrophage colony-stimulating factor, interleukin-3, and steel factor induce rapid tyrosine phosphorylation of p42 and p44 MAP kinase. Blood 79:2880
54. Qui MS, Green SH (1992) PC12 cell neuronal differentiation is associated with prolonged p21ras activity and consequent prolonged ERK activity. Neuron 9:705
55. Marshall CJ (1995) Specificity of receptor tyrosine kinase signaling: transient versus sustained extracellular signal-regulated kinase activation. Cell 80:179
56. Okuma E, Inazawa Y, Saeki K, Yuo A (2002) Potential roles of extracellular signal-regulated kinase but not p38 during myeloid differentiation of U937 cells stimulated by cytokines: augmentation of differentiation via prolonged activation of extracellular signal-regulated kinase. Exp Hematol 30:571
57. Murphy LO, Smith S, Chen RH, Fingar DC, Blenis J (2002) Molecular interpretation of ERK signal duration by immediate early gene products. Nat Cell Biol 4:556
58. Secchiero P, Melloni E, Heikinheimo M, Mannisto S, Di Pietro R, Iacone A, Zauli G (2004) TRAIL regulates normal erythroid maturation through an ERK-dependent pathway. Blood 103:517
59. Athanasiou M, Blair DG, Mavrothalassitis G (2003) ERF, an ETS-related transcriptional repressor, can induce erythroid differentiation. Anticancer Res 23:2143
60. Ogawa K, Tashima M, Toi T, Sawai H, Sawada H, Fujita J, Maruyama Y, Okuma M (1994) Inhibition of erythroid differentiation by stem cell factor in K562 cells expressing the c-kit gene. Exp Hematol 22:45
61. Muta K, Krantz SB, Bondurant MC, Dai CH (1995) Stem cell factor retards differentiation of normal human erythroid progenitor cells while stimulating proliferation. Blood 86:572
62. Sangrar W, Senis Y, Samis JA, Gao Y, Richardson M, Lee DH, Greer PA (2004) Hemostatic and hematological abnormalities in gain-of-function fps/fes transgenic mice are associated with the angiogenic phenotype. Journal of Thrombosis and Haemostasis (accepted)
63. Minetti G, Low PS (1997) Erythrocyte signal transduction pathways and their possible functions. Curr Opin Hematol 4:116

APPENDIX 3

Hemostatic and hematological abnormalities in gain-of-function *fps/fes* transgenic mice are associated with the angiogenic phenotype

Running Title: Hemostatic pathologies in activated *fps/fes* transgenic mice.

Waheed Sangrar[*,†], Yotis Senis[‡], John A. Samis[§], Yan Gao[*], Mary Richardson[**], David H. Lee[‡‡], and Peter A. Greer[*,†,§§].

[*]Division of Cancer Biology and Genetics, Queen's University Cancer Research Institute,
[†]Department of Pathology and Molecular Medicine, Queen's University, Kingston, Ontario, Canada
[‡]Department of Pharmacology, Oxford University, United Kingdom.
[§]Dept. of Biochemistry, Queen's University, Kingston, ON, Canada
[**]Department of Pathology and Molecular Medicine, McMaster University, Hamilton, Ontario, Canada
[‡‡]Department of Medicine, Queen's University, Kingston, Ontario, Canada.

[§§]To whom correspondence should be addressed: Peter A. Greer, Division of Cancer Biology and Genetics, Queen's University Cancer Research Institute, Botterell Hall, Room A309, Kingston, Ontario, K7L 3N6, Canada. Tel: (613) 533-2813; FAX: (613) 533-6830;
Email: greerp@post.queensu.ca.

Abstract: 213 words
Document (excluding figure legends and references): 3900 words

Keywords: Angiogenesis; *fps/fes*; hemangioma; thrombocytopenia, coagulation, fibrinolysis.

SUMMARY

Background. The Fps/Fes tyrosine kinase has been implicated in the regulation of hematopoiesis and inflammation. Mice expressing an activated variant of Fps/Fes (MFps) encoded by a gain-of-function mutant transgenic *fps/fes* allele (fps^{MF}) exhibited hematological phenotypes which suggested that Fps/Fes can direct hematopoietic lineage output. These mice also displayed marked hyper-vascularity and multifocal-hemangiomas which implicated this kinase in the regulation of angiogenesis.

Objective. Here we explored the potential involvement of Fps/Fes in the regulation of hemostasis through effects on blood cells and the vascular endothelium.

Methods. Hematological parameters of fps^{MF} mice were characterized by peripheral blood analysis, histology, and transmission electron microscopy. Hemostasis parameters and platelet functions were assessed by flow cytometry and measurements of activated partial thromboplastin time, prothrombin time, thrombin clot time, platelet aggregation, bleeding times and *in vitro* fibrinolytic assays.

Results. Hematological and morphological analyses showed that fps^{MF} mice displayed mild thrombocytopenia, anemia, red cell abnormalities and numerous hemostatic defects, including hypofibrinogenemia, hyper-fibrinolysis, impaired whole blood aggregation and a mild bleeding diathesis.

Conclusions. fps^{MF} mice displayed a complex array of hemostatic perturbations which are reminiscent of hemostatic disorders such as disseminated intravascular coagulation (DIC) and of hemangioma-associated pathologies such as Kasabach Merritt Phenomenon (KMS). These studies suggest that Fps/Fes influences both angiogenic and hemostatic function through regulatory effects on the endothelium.

INTRODUCTION

Fps/Fes (hereafter referred to as Fps) and Fer are members of a unique subfamily of cytoplasmic protein-tyrosine kinases which are structurally distinguished from members of the Src, Abl, Btk, Jak, Zap70 or Fak subfamilies[1]. They share structural similarities with some of the latter subfamilies, including a central Src-homology 2 (SH2) domain and a C-terminal tyrosine kinase domain. They are distinguished however, by an N-terminal Fer/CIP-4 (Cdc42 interacting protein-4) homology (FCH) domain and by adjacent coiled-coil domains. These domains are thought to mediate cytoskeletal interactions and to direct homotypic oligomerization, respectively[1,2]. The high-degree of homology between Fps and Fer suggests that these kinases have common biological roles[3].

A role for Fps in regulating angiogenesis was suggested by phenotypes in a transgenic mouse line tissue-specifically expressing an activated form of Fps (MFps) that contained a Src-like myristoylation consensus sequence at its N-terminus. This line of mice (*fps*^{MF}) displayed cavernous and capillary-type hemangiomas which were frequently associated with lymph-nodes and which persisted throughout the life-span of the animal[4]. In humans, hemangiomas are a common benign tumor of childhood in which a post-natal endothelial proliferative phase (~1 year) precedes an involution phase (2-10 years) characterized by decreased cell turn-over and vessel maturation[5-7]. Hemangiomas have been postulated to arise from delayed maturation of angioblastic tissue as suggested by the fetal-like character of their endothelial cells (EC)[8]. The presence of hemangiomas and tissue-wide hyper-vascularity in *fps*^{MF} mice suggested unregulated proliferation and/or maturation during vascular development[9]. This idea was consistent with post-natal presence of tissue-wide hypervascularity characterized by a predominance of second-order vessels and as well, with a signaling role for Fps downstream of key angiogenic

remodeling factors such as Angiopoietin 2 (Ang-2) and VEGF[9,10]. The presence of hemangiomas in these mice therefore suggested that Fps may regulate aspects of endothelial function related to vascular maturation/remodeling[9].

The initial detection of Fps in human and murine endothelial cell (EC) lines supported the possibility that Fps regulated endothelial function[11]. Subsequent isolation of spontaneously immortalized endothelial cell lines (C166 lines) from *fps*^{MF} mice further implicated Fps in regulating endothelial proliferation and survival[4,12]. Similar to immortalized ECs derived from hemangiomas, these C166 cells could spontaneously form tube-like structures in matrigel[12,13]. MFps was found to be highly expressed in C166 cells and it was selectively hyper-inducible relative to Fps in response to either VEGF or PDGF stimulation[9]. Independent studies also showed that Fps could be induced in response to fibroblast growth factor-2 (FGF-2), angiopoietin 2 (Ang-2) and VEGF[10,14,15]. A role for Fps in VEGF signaling *in vivo*, was later affirmed by a study which showed that MFps can compensate for failed vasculogenesis in Flk-1 deficient embryos[16]. Taken together, these data argued that Fps regulates endothelial function and that a dysfunctional *fps*^{MF} endothelium underlies the pro-angiogenic phenotype of these mice.

Fps has also been implicated in the regulation of hematopoiesis[3,17-19]. Early *in vitro* biochemical studies showed that Fps is expressed in cells of the myeloid lineage and that it could promote the differentiation and survival of myeloid cell lines. A recent analysis of *fps*^{MF} mice revealed elevated levels of peripheral granulocytes and monocytes and increases in bone-marrow CFU-GM and CFU-GEMM progenitors[19]. These observations supported a role for Fps in regulating myeloid sublineage determination at the level of multi-potential progenitor cells (CFU-GEMM), and at the level of the bipotential granulocytic progenitor (CFU-GM)[19].

Decreased circulating levels of lymphocytes and mature B-cells further suggested that Fps might act higher in the hematopoeitic hierarchy by promoting myeloid expansion at the expense of the lymphoid lineage[19]. This was consistent with the ability of a *fps*-directed Cre transgene to delete a loxP-flanked PIGA gene in all hematopoietic lineages[20]. These genetic data were consistent with previously proposed roles for Fps in influencing the differentiation and survival of myeloid progenitors and pointed to a role for this kinase in influencing hematopoietic output.

Previous studies have clearly documented a role for Fps in angiogenesis. In this study, we report hematological and hemostatic defects which are related to the angiogenic phenotype of fps^{MF} mice and which support a role for Fps in endothelial regulation. We demonstrate that the hyper-vascular line of fps^{MF} mice are mildly thrombocytopenic and anemic and display red cell defects characteristic of hemangioma-associated disorders and of some hemolytic anemias. In addition, a shortened activated partial thromboplastin time (aPTT), hypofibrinogenemia, hyperfibrinolysis and a mild bleeding diathesis in fps^{MF} mice suggest that these mice have abnormal coagulative and fibrinolytic function. This complex array of hemostatic defects suggests that the endothelium in fps^{MF} mice is abnormal, consistent with a role for Fps in regulating endothelial function.

METHODS

Mice

A colony of transgenic mice (*fps*^{MF}) tissue-specifically over-expressing a myristoylated form of Fps (MFps) in an in-bred CD-1 background was housed at the Animal Care Facility at Queen's University, Kingston ON. All procedures were approved by the Queen's University Animal Care Committee in accordance with the regulations set forth by the Canadian Council on Animal Care. Derivation and genotyping of this line has been previously described[4].

Histology

Spleens from *wt* and *fps*^{MF} littermates (3.5 ± 0.2 mo.) were surgically removed, sectioned and stained with hematoxylin and eosin. Spleen cross-sections of areas equivalent to a 200X field of view on a conventional light microscope were examined in triplicate for each mouse. Megakaryocytes were counted manually and data were expressed as average number of megkaryocytes per 200X field.

Collagen and convulxin stimulation of washed platelets

Washed platelets were prepared as previously described with modifications[21]. Platelet aggregation was assessed using a Chronolog Model 490 Washed Platelet Aggregometer. Three-hundred µl volumes of platelet suspensions were stimulated with collagen (4 µg/ml) or convulxin (0.16 µg/ml; Centerchem Inc., Norwalk CT) under constant stirring conditions at 37°C. Aggregation was assessed as function of changes in optical density over time.

P-selectin expression in response to collagen-related peptide (CRP) and convulxin

A range of concentrations of CRP (0 – 15 µg/ml) was added to 60 µl aliquots of blood previously diluted in Tyrodes-Hepes buffer to give 0.25-1.0x10^8 platelets/ml. FITC-conjugated anti-CD62P (FITC-CD62P; Pharmingen, Mississauga, ON) (0.1 µg) was added to each sample followed by

incubation for 10 min at 22°C. The reactions were stopped by addition of paraformaldhyde in cacodylate buffer (pH 7.2) and sampled on a Beckman Coulter Epics Altra flow cytometer. In other experiments, washed platelet suspensions (0.75-3 x 10^8 platelets/ml) containing FITC-CD62P (0.1 μg) and 2 mM $CaCl_2$ were incubated with 0-30 μg/ml CRP or 0-10 μg/ml convulxin for 10 min at 22°C and reactions were stopped and analyzed by flow cytometry as described above.

Hemostasis assays

Platelet-poor plasma (PPP) was obtained by centrifugation (1500 x *g*, 10 min) of citrated murine blood. Activated partial thromboplastin time (aPTT) and prothrombin time (PT) were measured using Automated aPTT and Simplastin Excel reagents, respectively (Oganon Taknika, Durham, NC). Briefly, PT assays were performed by adding 100 μl of Simplastin Excel (prepared as described by manufacturer) to mouse PPP diluted 1:1 in Hepes-buffered saline (HBS; 20 mM 4-(2-hydroxyethyl)-1-piperazineethanesulfonic acid, 150 mM NaCl, pH 7.4) containing 0.1% bovine serum albumin (HBS-BSA). Clotting was measured as a function of absorbance at 405 nm (A_{405}) and was monitored at 37°C at 2 sec intervals in a SpectraMax 190 microtitre plate reader (Molecular Devices, Sunnyvale, CA). For aPTT assays, a mixture containing equivalent volumes (50 μl) of aPTT reagent (prepared as described by manufacturer), plasma and HBS-BSA were pre-warmed at 37°C, and the reaction was initiated by adding 50 μl of 25 mM $CaCl_2$. Clotting was monitored as described for the PT assay. Thrombin (IIa) clot time (TCT) was assessed by adding PPP (diluted 1/5 in HBS) to microtitre wells containing aliquots of IIa and $CaCl_2$ (6 nM and 20 mM final concentrations respectively). Clotting was monitored at A_{405}, at 37°C on a SpectraMax 190 microtitre plate reader. Estimates of plasma fibrinogen were determined using a microturbidometric assay as described. [22,23]. *In vitro* fibrinolysis assays were

performed essentially as described[23]; briefly, PPP diluted in HBS containing 0.01% Tween-80, was added to microtitre wells containing recombinant human tPA (r-tPA), purified human IIa (generously provided by Dr. M. Nesheim, Queen's University, Kingston, ON) and $CaCl_2$. Final concentrations of r-tPA, IIa and $CaCl_2$ in each well were 1.1 nM, 6 nM and 20 mM, respectively. Clotting was monitored at A_{405}, at 37°C on a SpectraMax 190 microtitre plate reader.

Bleeding times

Bleeding time assays were performed as previously described[24]. Briefly, 1.5 mm of distal tail was removed from *wt* (1.9 ± 0.02 mo.) and *fps*^{MF} (1.8 ± 0.05 mo.) littermates and the tail was immediately immersed in isotonic saline equilibrated to 37°C. Bleeding time was defined as a complete cessation of observable bleeding up to a maximum time of 10 min, at which point bleeding was stopped by cauterization.

Statistical and morphometric analyses

Area analyses of RBC cross-sections was performed using Image Pro Plus morphometric analysis software; Media Cybernetics, Silverspring, Maryland, USA. Student t-tests, means, standard deviations, standard error of the means were performed using the Microsoft Excel statistical package (Microsoft, Canada).

RESULTS

Anemia and red cell damage in *fps*^{MF} mice

It has been previously shown that hemangioma induction *in vivo* is associated with the emergence and progression of anemia and red cell defects[25]. Since the hypervascular line of *fps*^{MF} mice naturally develop multifocal hemangiomas[4], we examined *fps*^{MF} peripheral blood for hematological abnormalities. Mean reductions of several hematological parameters were observed in *fps*^{MF} mice which suggested that these mice were anemic (Table 1). Reductions were observed in red blood cell (RBC) count, hematocrit, total hemoglobin, O_2 content, and O_2 capacity (Table 1). In addition, plasma bilirubin levels were elevated suggesting that this anemia might have a hemolytic component. Interestingly, RDW-SD and MCV were also elevated, pointing to the presence of red cell defects in *fps*^{MF} mice (Table 1). Subsequent examination of light micrographs of *fps*^{MF} red cell smears revealed an array of red cell defects, the most predominant of which were acanthocytes (Figure 1). A nominal increase in the number of keratocytes and schistocytes was also apparent in these *fps*^{MF} smears (Figure 1). The presence of red cell anomalies suggested that the anemia in these mice might be related either to increased red cell turnover, or to a defect in erythroid output.

Evidence of excessive red-cell fragmentation in *fps*^{MF} mice

The increase in MCV (Table 1) compelled us to further examine the size-distribution profiles of *fps*^{MF} red cells. Computer-assisted morphometric analyses of transmission electron micrographs (TEM) was employed to measure cross-sectional areas of individual RBCs (>2500) derived from three *wt* and three *fps*^{MF} mice. Consistent with an elevated MCV, a slight rightward-shift in the cross-sectional area distribution curve of *fps*^{MF} RBCs was observed (Figure 1G, lower panel). This shift amounted to a 7% and 10% increase in the mean and median of cross-sectional areas,

respectively (Figure 1G, upper panel). More, importantly, this analysis revealed a 1.7-fold increase in the frequency of areas between 0-0.5 μm^2, suggesting that an increased frequency of red-cell fragmentation was present in these mice (Figure 1G, lower panel).

Thrombocytopenia in *fps*^{MF} mice

A large body of evidence exists documenting associations between hemangiomas and thrombocytopenia[5,26-29]. Accordingly, *fps*^{MF} mice were also found to have moderate reductions in circulating platelet levels ($p < 10^{-4}$; Table 1). In addition, the platelet concentration was more varied in *fps*^{MF} mice (SD = 127.4, SEM = 29.2) compared to *wt* mice (SD = 75.1, SEM = 15.0). In this respect, one *fps*^{MF} mouse which was not included in the analysis in Table 1 had undetectable platelet levels, while the platelet concentration of 3 others in the analyzed sample, ranged from 96 x 10^9/l to 131 x 10^9/l.

Impaired Collagen- and ADP-induced whole blood aggregation in *fps*^{MF} mice

We next utilized whole blood aggregation assays to measure platelet-associated coagulation potential. These assays revealed a striking impairment in collagen- and ADP-induced whole blood platelet aggregation (data not shown). In order to determine whether these defects were associated with thrombocytopenia or with a defect intrinsic to platelets, we next examined washed platelet aggregation in response to either collagen or to the GPVI-specific agonist, convulxin. These experiments indicated that *fps*^{MF} platelets have a relatively normal intrinsic aggregation potential in response to the tested agonists (Figure 2) and this strongly suggested that the observed aggregation defects in whole blood were related, at least in part, to mouse to mouse variations in the severity of thrombocytopenia.

CRP- and convulxin-induced P-selectin expression is compromised in *fps*^{MF} platelets

We further investigated platelet function by stimulating platelets in whole blood with CRP, a GPVI specific agonist. Whole blood from *wt* mice was diluted to normalize platelet counts to levels present in *fps*^{MF} mice prior to stimulation. Flow cytometric analyses revealed reduced surface P-selectin expression in *fps*^{MF} mice (Figure 3A). To test whether this activation defect was intrinsic to *fps*^{MF} platelets or to differences in other blood factors we next extended these analyses to washed platelets stimulated with CRP or convulxin, both highly potent GPVI-specific agonists. As shown in Figure 3B and 3C, we continued to observe reduced P-selectin expression in *fps*^{MF} mice in response to either agonist. These data suggested an intrinsic *fps*^{MF} platelet defect that is related to P-selectin expression.

Increased platelet fragmentation and size in *fps*^{MF} mice

A minor, but significant increase in the mean platelet volume (MPV) of *fps*^{MF} mice was detected in the peripheral blood analysis (Table 1). Further examination of platelets by TEM provided visible evidence that *fps*^{MF} platelets were generally larger (Figure 4C and 4D) compared to *wt* platelets (Figure 4A and 4B). Also visibly apparent were increases in platelet fragments suggesting that abnormal platelet fragmentation/destruction was occurring (Figure 4C, 4D and data not shown). As with the red-cell analysis above, we next determined the size-distribution profiles of platelets in these TEM images (Figure 4E). As expected, a shift in the mean of the distribution curve for *fps*^{MF} platelets towards larger cross-sectional areas was observed (Figure 4E). Remarkably, increased platelet populations of very small platelet fragments ($< 0.4\ \mu m^2$) were also detectable by this analysis, suggesting unusually high levels of platelet fragmentation. A qualitative inspection of *fps*^{MF} platelet ultrastructure showed no marked abnormalities in mitochondria, microtubules, dense granules, α-granules or dense tubule systems.

Megakaryocytopoiesis in *fps*^{MF} mice

The presence of thrombocytopenia and of large platelets in *fps*^{MF} mice suggested that a normal compensatory platelet production response may be present in these mice. To assess this possibility, we examined megakaryocyte population levels in *fps*^{MF} mice. We opted to examine splenic megakaryocyte populations since the spleen assists the bone-marrow in platelet production[30]. Immunohistochemical inspection of spleen sections strongly suggested megakaryocytopoiesis in *fps*^{MF} mice (Compare Figure 5A to 5B). This was confirmed by semi-quantitative analysis which revealed a 3.3-fold increase in the number of megakaryocytes per unit tissue-area ($p = 0.002$).

Hemostasis defects in *fps*^{MF} mice

Vascular lesions such as hemangiomas have been frequently associated with hemostasis dysfunction and this led us to examine coagulative and fibrinolytic parameters in *fps*^{MF} mice[31-37]. Intrinsic and extrinsic coagulation were measured using aPTT and PT assays, respectively. Interestingly, we observed a significant shortening (20%) of the aPTT, but not the PT in *fps*^{MF} mice (Table 2). We next measured plasma fibrinogen levels using a microturbidometric assay[22,23]. This assay revealed that plasma fibrinogen levels were reduced by about 12% and suggested that TCTs might be prolonged (Table 2). In agreement with this, we observed a delay in TCTs in *fps*^{MF} mice compared to *wt* mice (Table 2). Fibrinolysis was then assessed by employing an *in vitro* fibrinolysis assay which utilized mouse plasma, purified tissue-plasminogen activator and thrombin[23]. A shortened lysis time (t_{50}) was observed signifying that fibrinolysis was slightly enhanced in *fps*^{MF} mice. (Table 2). Lastly, tail-bleeding assays were performed to assess the *in vivo* significance of these hemostatic defects (Figure 6). The average

bleeding time was found to be increased approximately 2.2-fold, suggesting that *fps*^{MF} mice also have a mild bleeding diathesis.

DISCUSSION

In a murine model of Kasabach Merritt Syndrome (KMS), hemangiomas induced by transgenic endothelial cell injection, resulted in the development of thrombocytopenia, anemia and several red cell structural anamolies[25]. The hemangiomas in *fps*^{MF} mice do not have vascular tumors typical of KMS[38]; however, the presentation of thrombocytopenia in these mice suggests a parallel with Kasabach Merritt Syndrome (KMS)[5,26,27,29,33]. Interestingly, other parallels with cases of KMS were also observed, included hemolytic anemia, hypofibrinogenemia and megakaryocytopoiesis[5,26,31,33,39]. This similarity of the type of hematological and hemostatic defects to those observed in cases of KMS supported the notion that these defects are secondary to hemangiomas in *fps*^{MF} mice.

Our data also showed unusual levels of red cell and platelet damage as suggested by; 1) the presence of acanthocytes, keratocytes and schistocytes; 2) by excessive red cell and platelet fragmentation (Figure 1G and 4E), and; 3) by elevated bilirubin which could be caused by increased hemolytic activity (Table 1). These data supported the idea that hemangioma-associated red cell and platelet consumption and/or destruction might underlie the observed anemia and thrombocytopenia in these mice. Indeed, platelet consumption has been hypothesized to occur as a result of the prothrombotic environment within developing hemangiomas[5,40-42]. As well, keratocytes have been associated with mechanical trauma arising in disturbed circulatory conditions such as cavernous hemangiomas, while schistocytes, have been associated with fibrin deposition – a condition also known to occur in hemangiomas[25,43,44]. The significance of acanthocytes in *fps*^{MF} mice however is unclear, although their presence has been associated with mild to severe hemolytic states[45-47]. Thus, thrombocytopenia, anemia, red cell anomalies, and perhaps other reported defects, may be secondary effects of hemangiomas in *fps*^{MF} mice.

We cannot exclude the possibility that thrombocytopenia and anemia might also be associated with decreased hematopoietic output. This possibility merits consideration given that Fps is strongly implicated in hematopoietic regulation. Earlier work using the *fps*^{MF} line of mice suggested that increased peripheral monocytic output was mediated by enhanced lineage output from early multipotential myeloid progenitors[19]. More recently we have shown that this enhancement extends laterally to promote early erythroid progenitor expansion, but that a block in differentiation further downstream (post-CFU-E) might also exist (W. Sangrar, P. Greer, unpublished results). In this case, the anemia present in these mice might be due to an MFps-mediated reduction in erythropoietic output. Interestingly, platelet and erythroid lineages have both been shown to develop from a late common megakaryocyte/erythrocyte lineage-restricted progenitor[48]; hence, it is conceivable that megakaryopoiesis/thrombopoiesis may as well be impaired in *fps*^{MF} mice. In this respect it is interesting that we have observed increases in splenic megakaryocytes numbers. While this might represent a simple compensatory response to thrombocytopenia, it might also reflect a post-megakaryoctyic defect in platelet release. Indeed, genetic studies have shown that megakaryocyte accumulation can accompany thrombocytopenia and that this can occur independently of thrombopoietic efficiency[49]. We are therefore currently using bone-marrow transplantation assays to assess the contribution of a potential defect in erythroid and platelet ontogeny to the observed anemia and thromobcytopenia in *fps*^{MF} mice.

fps^{MF} mice were found to display a complex array of hemostatic defects, including reduced whole blood platelet aggregation (WBPA; data not shown) and a mild bleeding diathesis. The latter defects are consistent with the premature death of *fps*^{MF} mice from internal hemorrhaging (median = 7 mo)[4]. In the absence of a detectible purified platelet aggregation defect, we propose that the thrombocytopenic phenotype in these mice is likely to be a major

contributing factor to the WBPA defect and ultimately to the bleeding tendency in these mice. However, given that this thrombocytopenia is relatively mild, we cannot exclude the involvement of other cellular or plasma proteins. An interesting candidate is P-selectin, the expression of which was reduced in *fps*^{MF} platelets stimulated with collagen (Figure 3). It is unlikely that this reduction impacts on platelet-platelet interactions in whole blood, since our observations, and those in P-selectin knockout mice suggest that purified platelet aggregation is normal[50]. If however, this *fps*^{MF} platelet P-selectin expression defect is also present in the endothelium, then a bleeding defect (as seen in P-selectin knockout mice) could arise from failed interactions between endothelial P-selectin and its counter-receptors PSGL-1 or GPIb-IX-V on platelets[51-53]. The importance of these interactions was also stressed in VWF knockout mice which have a bleeding defect that is attributed to less weibel-palade (WB)-mediated P-selectin translocation to the endothelial surface[54,55]. This is intriguing since VWF secretion and WB formation are reported to be reduced in hemangioma-derived ECs[56,57]. Thus, reduced P-selectin or VWF expression in *fps*^{MF} ECs represents a potential dysfunctional property of the endothelium of these mice.

A major pathological feature of KMS is bleeding associated with secondary development of disseminated intravascular coagulation (DIC)[31,58]. Perturbations such as thrombocytopenia, hypofibrinogenemia, hyperfibrinolysis and bleeding in *fps*^{MF} mice were reminiscent of DIC-like conditions. The presence of a normal PT and an abnormally accelerated aPTT in these mice however, were not indicative of classically interpreted DIC[31,59-62]. The importance of these tests in DIC has been argued to depend on the stage of progression. In decompensated states, these times are prolonged whereas in compensated DIC, they are either unaffected or shortened[59]. According to this view, the PT and aPTT of *fps*^{MF} mice may reflect a potential compensated

DIC-like phase which may precede a more lethal decompensated phase. In this respect, *fps*^{MF} mice might vary with respect to the proximity of their hemostatic systems to full decompensation. This is supported by evidence of two distinct clusters of bleeding times in *fps*^{MF} mice, by the erratic onset and severity of their hemostasis defects (not shown); and correspondingly, by the highly varied life-span of these animals (1-14 mo). In accordance with the latter two points, the onset and severity of DIC in many underlying pathologies is similarly unpredictable, and is limited only to a subset of patients[5,58,63]. Thus, while it is unclear whether *fps*^{MF} mice develop a "true" DIC phenotype, they do display hemostatic perturbations that are reminiscent of a DIC-like state, and these are consistent with a hemostatically dysfunctional endothelium.

The complex array of hematological and hemostatic perturbations in *fps*^{MF} mice reported here correlate with their vascular disorders and with a dysfunctional endothelium and implicate Fps in regulating aspects of endothelial function related to hemostasis. It is important to mention here that since the Fps transgene in these mice is myristoylated, the phenotypes in this report may not reflect those expected from physiological Fps. However, several effects of MFps have been observed which suggest that its effects parallel that of catalytically-activated Fps[19,64] (and unpublished data). These include elevated whole-blood aggregation and increased red cell and platelet circulation in *fps* null mice[18,21]. The *fps*^{MF} line of mice then, constitutes an important model for the study of hemostasis and angiogenesis and the inter-relationship between these processes[65]. In addition, this line may also be suitable for studying how Fps regulates EC functions related to hemostasis and angiogenesis, including endothelial maturation and plasticity.

ACKNOWLEDGEMENTS

We would like Dr. Mike Nesheim (Dept. of Biochemistry, Queen's University) and Dr. David Lillicrap (Dept. of Pathology, Queen's University) for providing input on data interpretation and for providing helpful suggestions on the manuscript. Thanks also to Dr. Keyue Ding for help with statistical analysis and Dr Steve Watson (Dept. of Pharmacology, Oxford University) for kindly providing CRP. We also acknowledge John DeCosta for his assistance with EM analysis, Derek Schultz and Jeff Mewburn for flow cytometry, and the members of the Kingston General Hospital Core Lab for assistance with the peripheral blood analysis. W.S. was supported by a fellowship award from the US Department of Defense Breast Cancer Research Program (Grant ID: BCRP – DAMD17-0110382). This study was funded by a grant from National Cancer Institute of Canada (Grant # 012183), with funds from the Canadian Cancer Society.

Table 1. Hematological Parameters.

Hematological Parameter	*wild type* (*n*)	*fps*^{MF} (*n* / *p*-value)
White Blood Cells (10^{12}/l)	7.0 ± 0.4 (27)	7.5 ± 0.7 (21 / 0.5)
Platelets (10^{9}/l)	532.0 ± 15.0 (25)	**369.8 ± 29.2** (19 / $<10^{-4}$)
Mean Platelet Volume (MPV) (*fl*)	6.9 ± 0.04 (27)	**7.1 ± 0.1** (21 / 0.05)
Red Blood Cells (10^{12}/l)	9.1± 0.1 (28)	**7.8 ± 0.1** (22 / $<10^{-10}$)
Total Hemoglobin (THb) (g/l)	145.1 ± 1.6 (28)	**132.3 ± 1.9** (22 / $<10^{-5}$)
O_2 Content (ml/dl)	18.9 ± 0.5 (5)	**15.9 ± 0.6** (5 / 0.03)
O_2 Capacity (ml/dl)	19.4 ± 0.5 (5)	**16.3 ± 0.5** (5 / 0.03)
Oxyhemoglobin Percentage (%)	98.9 ± 0.9 (5)	98.0 ± 0.4 (5 / 0.38)
Methemoglobin Percentage (%)	0.6 ± 0.2 (5)	1.0 ± 0.4 (5 / 0.35)
Reduced Hemoglobin Percentage (%)	2.7 ± 0.2 (5)	2.7 ± 0.3 (5 / 0.831)
Hematocrit (ml/l)	461 ± 4 (28)	**438 ± 7** (22 / <0.01)
Mean Corpuscular Volume (MCV) (*fl*)	50.5 ± 0.4 (28)	**55.9 ± 0.4** (22 / $<10^{-11}$)
Mean Corpuscular Hemoglobin (MCH) (*pg*)	15.9 ± 0.1 (28)	**16.9 ± 0.1** (22 / $<10^{-5}$)
MCHC (g/l)	314.7 ± 1.4 (28)	**302.3 ± 1.2** (22 / $<10^{-7}$)
Total Bilirubin (μM) (†)	undetectable (6) *	**2.4 ± 0.9** (5 / 0.013) **
Serum Iron (μM) (†)	42.2 ± 1.8 (6)	40.2 ± 3.2 (5 / 0.61)
Total Iron Binding Capacity (TIBC) (μM) (†)	1507 ± 144 (6)	1618 ± 103 (5 / 0.55)
RDW-SD (*fl*)	26.1 ± 0.4 (28)	**30.5 ± 2.6** (22 / $<10^{-6}$)

Blood was acquired from *wt* (4.5 ± 0.2 mo) and *fps*^{MF} (4.3 ± 0.2 mo.) mice by cardiac puncture. Peripheral blood was analyzed using a SYSMEX XE-2100 Automated Hematological Analyzer. Data are presented as mean ± standard error of the mean (SEM) along with P-values (*p*) and the number of animals used in the analyses (*n*). Statistically significant parameters are bolded. (†)*wt*, *fps*^{MF} (4.1 ± 0.1 mo.). (*)5 out of 6 *wt* mice had undetectable bilirubin, while one *wt* mouse had a value of 2 μM. (**)P-value derived using a Wilcoxin rank sum test. O_2 Content is based on total hemoglobin (THb). O_2 capacity is based on hemoglobin fraction capable of binding O_2 and excludes methemoglobin and carboxyhemoglobin fractions. Oxyhemoglobin is expressed as a percent of THb. Oxygen saturation is based on hemoglobin available for binding O_2 and excludes methemoglobin and carboxyhemoglobin. Reduced hemoglobin is the fraction of hemoglobin which is O_2 free. MCHC, mean corpuscular hemoglobin concentration; RDW-SD, red cell distribution width – standard deviation.

Table 2: Hemostasis Parameters.

Parameter	*wild-type* (*n*)	*fps*^{MF} (*n* / *p*-value)
aPTT (s)	34.5 ± 1.5 (12)	**26.5 ± 0.8** (12 / < 10^{-3})
PT (s)	13.2 ± 0.7 (12)	13.3 ± 0.7 (12 / 0.89)
TCT (s)	286.4 ± 29.9 (12)	**393.9 ± 34.5** (12 / 0.028)
Fibrinolysis [t_{50} (min)]	43.8 ± 7.3 (8)	**24.7 ± 10.6** (8 / 0.04)
Relative Fibrinogen Percentage	100 ± 4.4 % (12)	**88 ± 5.1** (12 / 0.05)

aPTT, PT, TCT and relative fibrinogen percentages were determined on *wt* and *fps*^{MF} mice that were 3.11 ± 0.09 mo and 2.95 ± 0.08 mo of age, respectively. The fibrinolysis parameter (t_{50}) was determined on *wt* and *fps*^{MF} mice that were 3.2 ± 0.1 mo and 3.1 ± 0.1 mo of age, respectively. Data are presented as mean ± standard error of the mean (SEM) along with P-values (*p*) and the number of animals used in the analyses (*n*). Statistically significant parameters are bolded. aPTT, activated partial thromboplastin time; PT, prothrombin time; TCT, thrombin clot time.

Figure 1

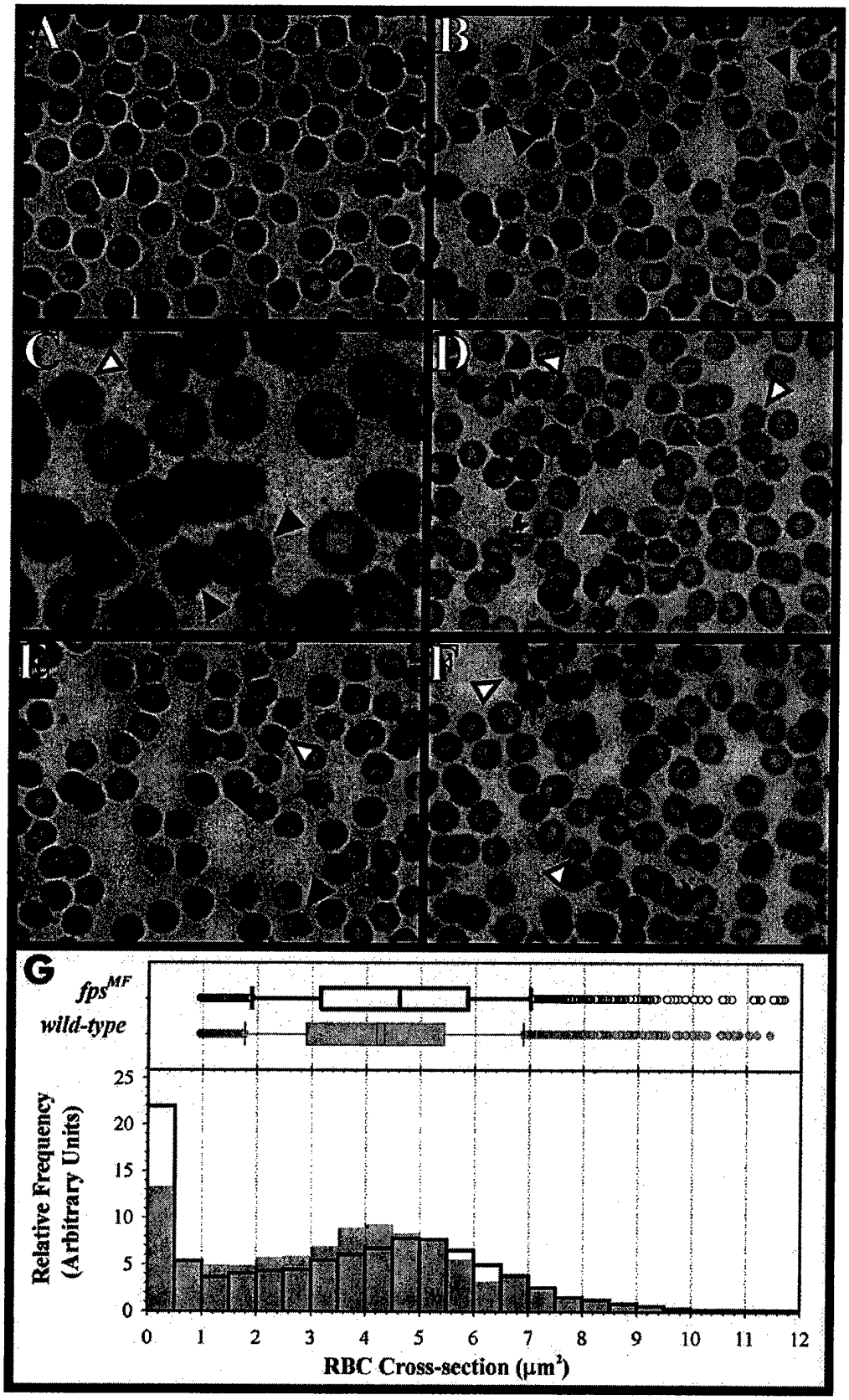
A
B
C
D
E
F
G
fps^MF
wild-type
Relative Frequency (Arbitrary Units)
0
5
10
15
20
25
0
1
2
3
4
5
6
7
8
9
10
11
12
RBC Cross-section (μm²)

Figure 2

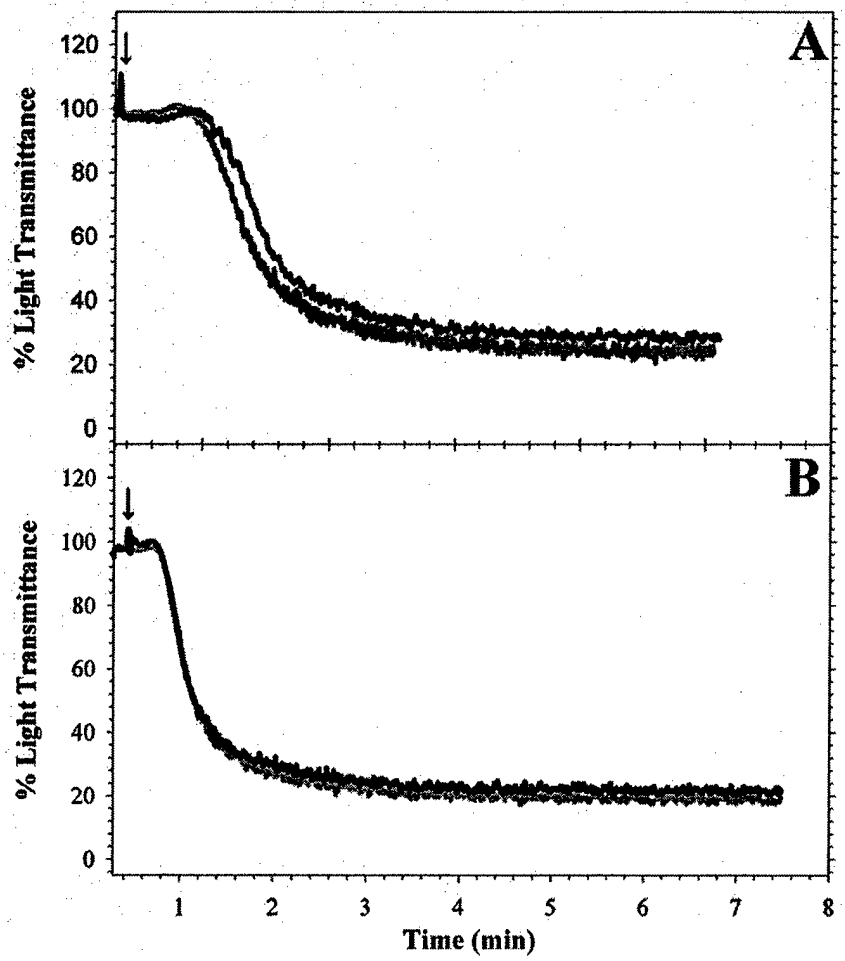
A
B
% Light Transmittance
% Light Transmittance
120
100
80
60
40
20
0
1
2
3
4
5
6
7
8
Time (min)

Figure 3

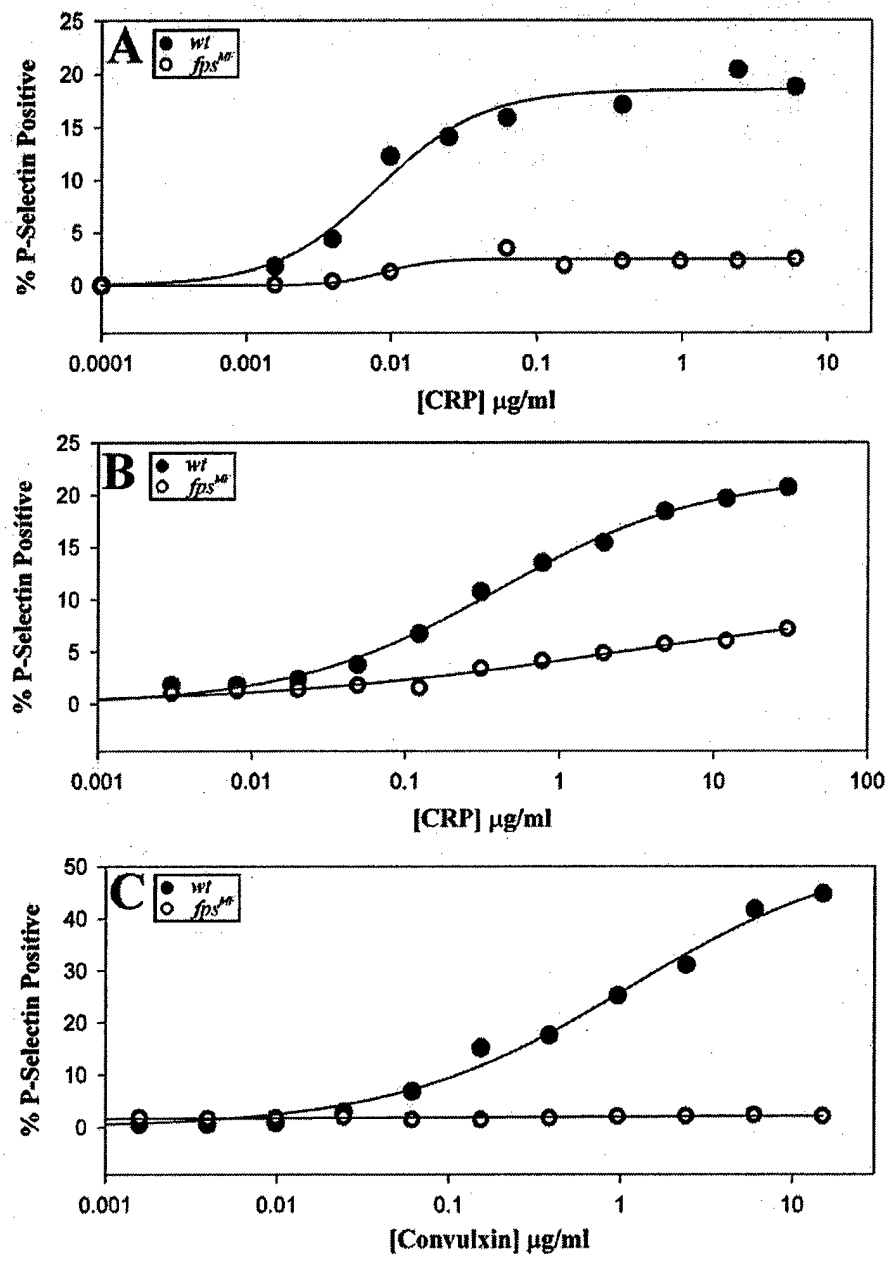
A
wt
fps^-/-
% P-Selectin Positive
25
20
15
10
5
0
0.0001
0.001
0.01
0.1
1
10
[CRP] µg/ml
B
wt
fps^-/-
% P-Selectin Positive
25
20
15
10
5
0
0.001
0.01
0.1
1
10
100
[CRP] µg/ml
C
wt
fps^-/-
% P-Selectin Positive
50
40
30
20
10
0
0.001
0.01
0.1
1
10
[Convulxin] µg/ml

Figure 4

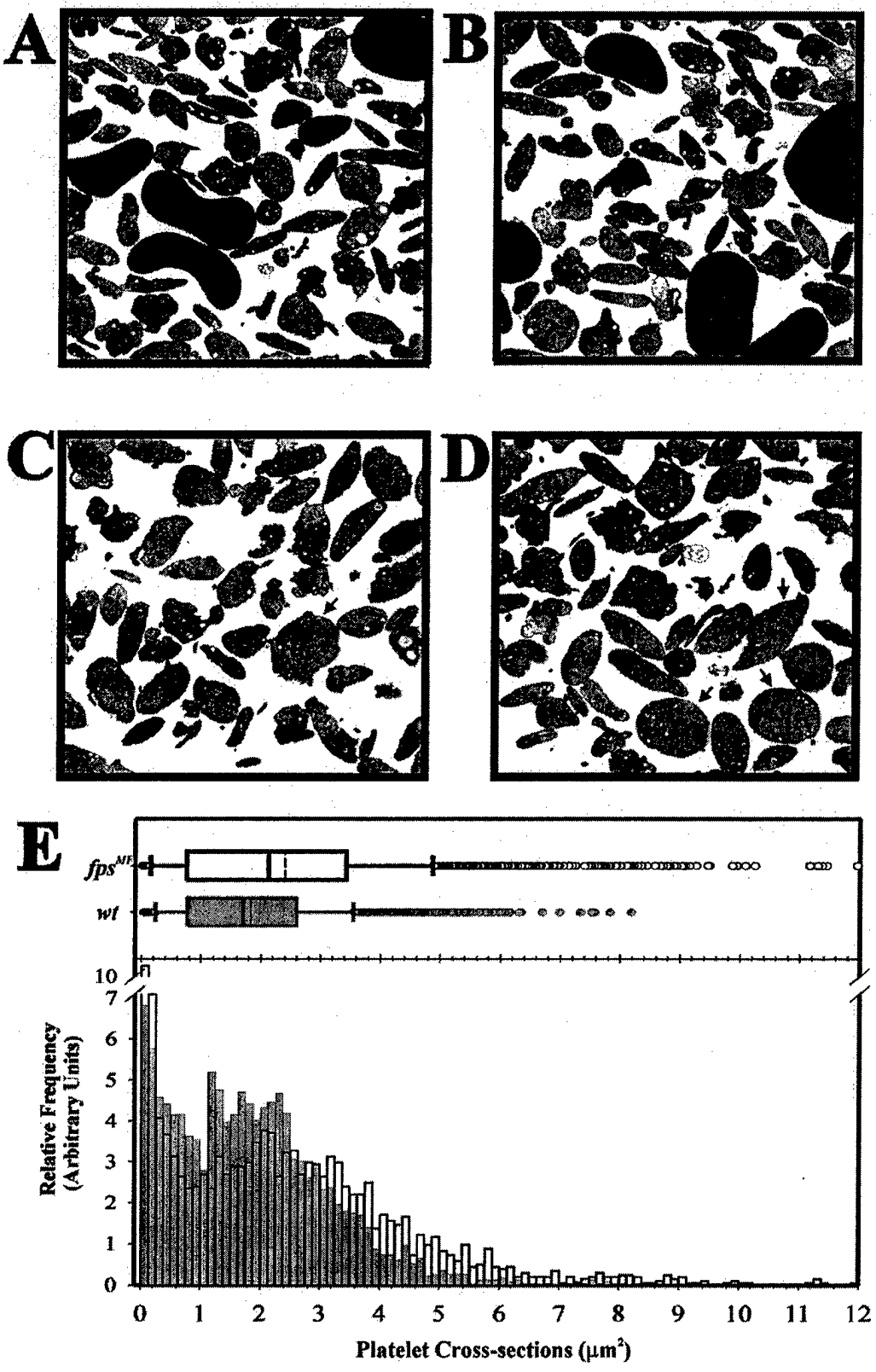
A
B
C
D
E
fps^NF
wt
10
7
6
5
4
3
2
1
0
Relative Frequency (Arbitrary Units)
0 1 2 3 4 5 6 7 8 9 10 11 12
Platelet Cross-sections (μm²)

Figure 5

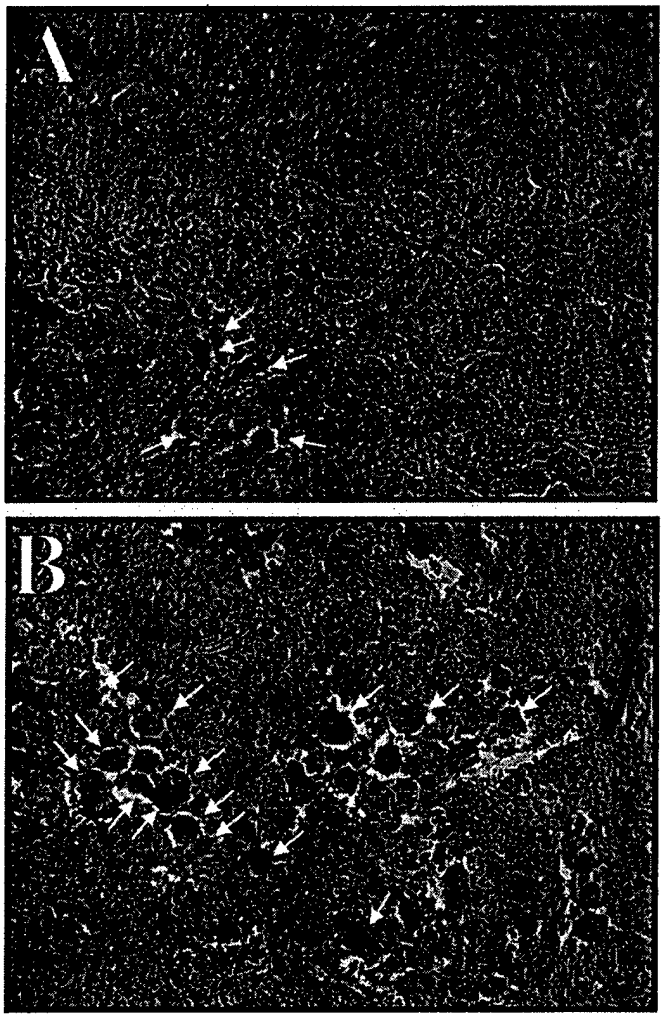

Figure 6

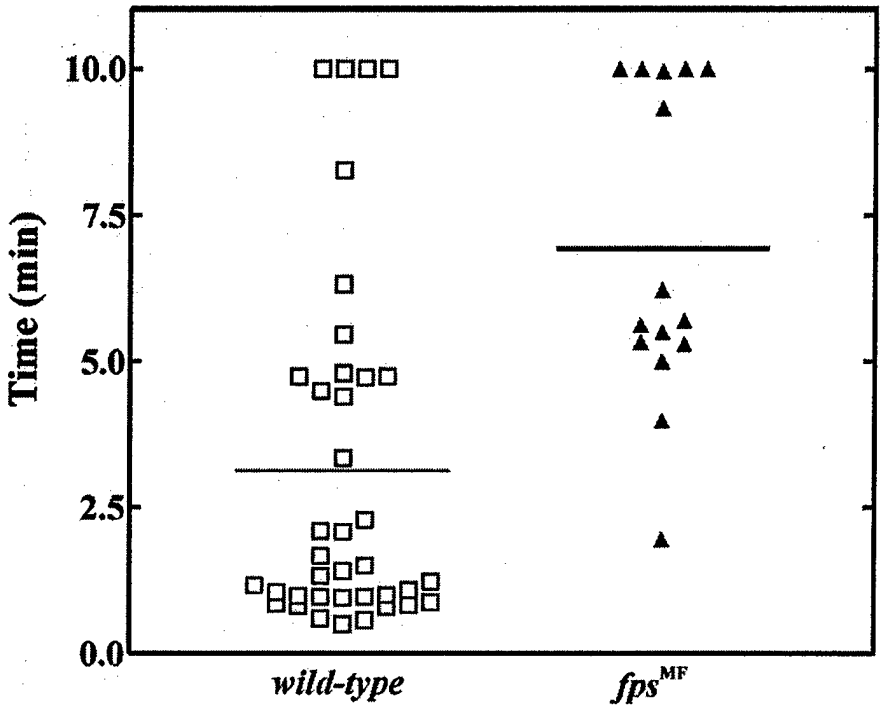

Figure 1. Peripheral blood smears. Whole blood smears were prepared and fixed in Wright stain. Large subpopulations of acanthocytes (examples indicated by "▲") and more minor populations of keratocytes/schistocytes (Δ) were visibly evident in *fps*^{MF} blood smears. (A) wt; 600X, $n = 6$, 4.0 ± 0.8 mo; (B, D-F) *fps*^{MF}; 600X, $n = 6$, 4.5 ± 0.6 mo.; (C) *fps*^{MF}; 1000X. (G) Blood cell sediments were fixed, sectioned and prepared for viewing on a Hitachi H500 transmission electron microscope. Areas of RBC cross-sections on transmission electron micrographs were quantified using ImagePro Plus morphometric analysis software. (G; upper panel) Box plot of individual RBC cross-sections for *fps*^{MF} (white bars) and *wt* (grey bars) mice; median (solid line), average (dashed lines), 5^{th} – 95^{th} percentiles (symbols), 10^{th} - 90^{th} percentile (whiskers) 10^{th} - 25^{th} percentile (boxes). (G; lower panel) Frequency distribution analysis of RBC cross-sectional areas of *fps*^{MF} (white bars) and *wt* (grey bars) mice. The distribution curve of RBC cross-sectional areas from *fps*^{MF} mice is wider, flatter and slightly shifted to the right suggesting increases in RBC volume and decreased size uniformity. In addition, the bin representing 0-0.5 μm^2 was elevated in *fps*^{MF} mice suggesting increased levels of RBC fragmentation. Median: *fps*^{MF}, 4.6 μm^2; *wt*, 4.2 μm^2. Mean ± S.E.M.: *fps*^{MF}, 4.59 ± 0.04 μm^2, n = 2878; *wt*, 4.32 ± 0.04 μm^2, $n = 2644$.

Figure 2. Platelet aggregation of washed platelets is normal in *fps*^{MF} mice. Washed platelets pooled from 2-3 *wt* [(black line); $n = 7$, 2.7 ± 0.2 mo] and 2-3 *fps*^{MF} mice [(grey line); $n = 10$, 2.5 ± 0.2 mo)] were stimulated with (A) collagen (4 μg/ml) or (B) convulxin (0.16 μg/ml). (A) Representative aggregation traces of experiments comparing two separate pools of *wt* and *fps*^{MF} mice stimulated with collagen (4 μg/ml). These data show that *fps*^{MF} platelets aggregate normally in response to collagen. (B) Aggregation traces are representative of experiments which

tested the aggregation capacity of three independent pools of *wt* mice and 4 independent pools of *fps*^{MF} mice to aggregate in response to convulxin (0.16 µg/ml). As observed with collagen, the aggregation response of *fps*^{MF} platelets to convulxin was normal.

Figure 3. Abnormal P-selectin expression in whole blood and washed platelets from *fps*^{MF} mice. Whole blood or washed platelets obtained from *wt* and *fps*^{MF} mice were incubated with a range of CRP and convulxin concentrations and P-selectin expression was assessed by flow cytometry using FITC-conjugated rat anti-mouse CD62P monoclonal antibodies. Representative P-selectin expression response profiles are shown in each of the three panels for *wt* (•) and *fps*^{MF} (○). (A) Impaired P-selectin expression in *fps*^{MF} platelets in diluted whole blood was observed to varying extents in response to CRP. (n = 5/genotype). (B) Variable hypo-expression of P-selectin in *fps*^{MF} washed platelets in response to CRP was observed 6 out of 7 times (n = 7/genotype). (C) Variable extents of reduction of P-selectin expression was also observed in *fps*^{MF} washed platelets in response to convulxin (n = 3/genotype).

Figure 4. Transmission electron microscopy and cross-sectional area analysis of platelets reveals increased platelet size and fragmentation in *fps*^{MF} mice. A subpopulation of larger platelets were seen in whole blood from *fps*^{MF} mice (C, D) relative to *wt* mice (A, B) as assessed by TEM (2500X). Arrows in panels C and D indicate *fps*^{MF} platelets of particularly large size. Areas of platelet cross-sections on TEM were quantified using Image Pro Plus morphometric analysis software (E). The upper panel in (E) depicts a box plot of individual platelet cross-sections for *fps*^{MF} (white bars) and *wt* (grey bars) mice; median (solid lines), average (dashed lines), outliers (symbols), 10^{th} - 25^{th} percentile (boxes), 10^{th} - 90^{th} percentile (whiskers). The

lower panel in (E) shows a frequency distribution analysis of platelets areas from *fps*^{MF} (white bars) and *wt* (grey bars) mice. Median: *wt*, 1.7 μm^2; *fps*^{MF}, 2.2 μm^2. Mean ± SEM: *wt*, 1.83 ± 0.03 μm^2, $n = 2782$; *fps*^{MF}, 2.40 ± 0.04 μm^2, $n = 2562$.

Figure 5. Increased megakaryocytes in spleens of *fps*^{MF} mice. Hematoxylin and eosin stained cross-sections of (A) *wt* and (B) *fps*^{MF} spleens (200X). Megakaryocytes were present in significantly increased numbers in *fps*^{MF} relative to *wt* spleens. Quantitative analysis revealed a 3.3-fold increase in the number of megakaryocytes per unit tissue-area (*wt*: 5.2 ± 1.1, $n = 9$; *fps*^{MF}: 17.3 ± 3.3, $n = 8$; $p = 0.002$).

Figure 6. Bleeding defect in *fps*^{MF} mice. Experiments in which tail-bleeding times exceeded 10 minutes were terminated by cauterization. All bleeding times exceeding 10 min are depicted as 10 min, and in such cases, 10 min was used for calculation of mean values. A dot-plot graph of individual bleeding times of *wt* (□) and *fps*^{MF} (▲) mice is shown. The horizontal lines intersecting the graph points denote the mean value of bleeding times. Tail bleeds from *fps*^{MF} mice were 2.2 times longer than *wt* mice (*wt*, 3.1 ± 0.5 min, $n = 38$; *fps*^{MF}, 6.9 ± 0.7 min, $n = 15$, $p < 10^{-3}$).

REFERENCES

1. Greer PA. Closing in on the biological functions of Fps/Fes and Fer. Nature Reviews Molecular Cell Biology 2002; 3:278-89.
2. Aspenstrom P. A Cdc42 target protein with homology to the non-kinase domain of FER has a potential role in regulating the actin cytoskeleton. Curr Biol 1997; 7:479-87.
3. Senis YA, Craig AWB, Greer PA. Fps/Fes and Fer protein-tyrosine kinases play redundant roles in regulating hematopoiesis. Experimental Hematology 2003; 31:673-81.
4. Greer P, Haigh J, Mbamalu G, Khoo W, Bernstein A, Pawson T. The Fps/Fes protein-tyrosine kinase promotes angiogenesis in transgenic mice. Mol Cell Biol 1994; 14:6755-63.
5. Szlachetka DM. Kasabach-Merritt syndrome: a case review. Neonatal Netw 1998; 17:7-15.
6. Mulliken JB, Glowacki J. Hemangiomas and vascular malformations in infants and children: a classification based on endothelial characteristics. Plast Reconstr Surg 1982; 69:412-22.
7. Verkarre V, Patey-Mariaud de Serre N, Vazeux R, Teillac-Hamel D, Chretien-Marquet B, Le Bihan C, Leborgne M, Fraitag S, Brousse N. ICAM-3 and E-selectin endothelial cell expression differentiate two phases of angiogenesis in infantile hemangiomas. J Cutan Pathol 1999; 26:17-24.
8. Dosanjh A, Chang J, Bresnick S, Zhou L, Reinisch J, Longaker M, Karasek M. In vitro characteristics of neonatal hemangioma endothelial cells: similarities and differences between normal neonatal and fetal endothelial cells. J Cutan Pathol 2000; 27:441-50.
9. Sangrar W, Mewburn J, Vincent S, Fisher J, Greer P. Vascular defects in gain-of-function fps/fes transgenic mice correlate with PDGF- and VEGF-induced activation of mutant Fps/Fes kinase in endothelial cells. Journal of Thrombosis and Haemostasis 2004; 2:820-32.
10. Mochizuki Y, Nakamura T, Kanetake H, Kanda S. Angiopoietin 2 stimulates migration and tube-like structure formation of murine brain capillary endothelial cells through c-Fes and c-Fyn. J Cell Sci 2002; 115:175-83.
11. Haigh J, McVeigh J, Greer P. The fps/fes tyrosine kinase is expressed in myeloid, vascular endothelial, epithelial, and neuronal cells and is localized in the trans-golgi network. Cell Growth Differ 1996; 7:931-44.
12. Wang SJ, Greer P, Auerbach R. Isolation and propagation of yolk-sac-derived endothelial cells from a hypervascular transgenic mouse expressing a gain-of-function fps/fes proto-oncogene. In Vitro Cell Dev Biol Anim 1996; 32:292-9.
13. Dubois NA, Kolpack LC, Wang R, Azizkhan RG, Bautch VL. Isolation and characterization of an established endothelial cell line from transgenic mouse hemangiomas. Exp Cell Res 1991; 196:302-13.
14. Kanda S, Lerner EC, Tsuda S, Shono T, Kanetake H, Smithgall TE. The nonreceptor protein-tyrosine kinase c-Fes is involved in fibroblast growth factor-2-induced chemotaxis of murine brain capillary endothelial cells. J Biol Chem 2000; 275:10105-11.
15. Kanda S, Mochizuki Y, Miyata Y, Kanetake H. The role of c-Fes in vascular endothelial growth factor-A-mediated signaling by endothelial cells. Biochem Biophys Res Commun 2003; 306:1056-63.
16. Haigh J, Ema M, Haigh K, Gertsenstein M, Greer P, Rossant J, Nagy A, Wagner EF. Activated Fps/Fes can functionally substitute for Flk1 deficiency in vascular development in vivo. Blood 2004; 103:912-20.
17. Hackenmiller R, Kim J, Feldman RA, Simon MC. Abnormal Stat activation, hematopoietic homeostasis, and innate immunity in c-fes-/- mice. Immunity 2000; 13:397-407.

18. Zirngibl RA, Senis Y, Greer PA. Enhanced endotoxin-sensitivity in Fps/Fes-null mice with minimal defects in hematopoietic homeostasis. Mol Cell Biol 2002; 22:2472-86.
19. Sangrar W, Gao Y, Zirngibl R, Scott M, Greer P. The fps/fes proto-oncogene regulates hematopoietic lineage output. Experimental Hematology 2003; 31:1259-67.
20. Keller P, Payne JL, Tremml G, Greer PA, Gaboli M, Pandolfi PP, Bessler M. FES-Cre targets phosphatidylinositol glycan class A (PIGA) inactivation to hematopoietic stem cells in the bone marrow. J Exp Med 2001; 194:581-9.
21. Senis YA, Sangrar W, Zirngibl RA, Craig AWB, Lee DH, Greer PA. Fps/Fes and Fer Nonreceptor Protein-Tyrosine Kinases Regulate Collagen- and ADP-Induced Platelet Aggregation. Journal of Thrombosis and Haemostasis. 2003; 1:1062-70.
22. Macart M, Koffi A, Henocque G, Mathieu JF, Guilbaud JC. Optimized microturbidimetric assay for fibrinogen. Clin Chem 1989; 35:211-4.
23. Nagashima M, Yin ZF, Zhao L, White K, Zhu Y, Lasky N, Halks-Miller M, Broze GJ, Jr., Fay WP, Morser J. Thrombin-activatable fibrinolysis inhibitor (TAFI) deficiency is compatible with murine life. J Clin Invest 2002; 109:101-10.
24. Ware J, Russell S, Ruggeri ZM. Generation and rescue of a murine model of platelet dysfunction: the Bernard-Soulier syndrome. Proc Natl Acad Sci U S A 2000; 97:2803-8.
25. Dubois-Stringfellow N, Kolpack-Martindale L, Bautch VL, Azizkhan RG. Mice with hemangiomas induced by transgenic endothelial cells. A model for the Kasabach-Merritt syndrome. Am J Pathol 1994; 144:796-806.
26. Good TA, Carnazzo SF, Good R. Thrombocytopenia and giant hemangioma in infants. Am J Dis Child 1955; 90:260-74.
27. Shim WK. Hemangiomas of infancy complicated by thrombocytopenia. Am J Surg 1968; 116:896-906.
28. Drolet BA, Esterly NB, Frieden IJ. Hemangiomas in children. N Engl J Med 1999; 341:173-81.
29. Kasabach H, Merritt K. Capillary hemangioma with extensive purpura: report of a case. Am J Dis Child 1940; 59:1063-70.
30. Layendecker SJ, McDonald TP. The relative roles of the spleen and bone marrow in platelet production in mice. Exp Hematol 1982; 10:332-42.
31. Larsen EC, Zinkham WH, Eggleston JC, Zitelli BJ. Kasabach-Merritt syndrome: therapeutic considerations. Pediatrics 1987; 79:971-80.
32. Miller JG, Orton CI. Long term follow-up of a case of Kasabach-Merritt syndrome successfully treated with radiotherapy and corticosteroids. Br J Plast Surg 1992; 45:559-61.
33. Esterly NB. Kasabach-Merritt syndrome in infants. J Am Acad Dermatol 1983; 8:504-13.
34. Schulz AS, Urban J, Gessler P, Behnisch W, Kohne E, Heymer B. Anaemia, thrombocytopenia and coagulopathy due to occult diffuse infantile haemangiomatosis of spleen and pancreas. Eur J Pediatr 1999; 158:379-83.
35. Pierce RN, Dunn L, Knisely AS. Consumptive coagulopathy in utero associated with multiple vascular malformations. Pediatr Pathol 1992; 12:67-71.
36. Tanaka K, Shimao S, Okada T, Tanaka A. Kasabach-Merritt syndrome with disseminated intravascular coagulopathy treated by exchange transfusion and surgical excision. Dermatologica 1986; 173:90-4.
37. Lang PG, Dubin HV. Hemangioma-thrombocytopenia syndrome; a disseminated intravascular coagulopathy. Arch Dermatol 1975; 111:105-7.

38. Enjolras O, Wassef M, Mazoyer E, Frieden IJ, Rieu PN, Drouet L, Taieb A, Stalder JF, Escande JP. Infants with Kasabach-Merritt syndrome do not have "true" hemangiomas. J Pediatr 1997; 130:631-40.
39. Sutherland D, Clark H. Hemangioma associated with thrombocytopenia. Am J Med 1962; 33:150-7.
40. Seo SK, Suh JC, Na GY, Kim IS, Sohn KR. Kasabach-Merritt syndrome: identification of platelet trapping in a tufted angioma by immunohistochemistry technique using monoclonal antibody to CD61. Pediatr Dermatol 1999; 16:392-4.
41. Brizel HE, Raccuglia G. Giant hemangioma with thrombocytopenia. Radioisotopic demonstration of platelet sequestration. Blood 1965; 26:751-64.
42. Warrell RP, Jr., Kempin SJ, Benua RS, Reiman RE, Young CW. Intratumoral consumption of indium-111 labeled platelets in a patient with hemangiomatosis and intravascular coagulation (Kasabach-Merritt syndrome). Cancer 1983; 52:2256-60.
43. Hillman RS, Phillips LL. Clotting-fibrinolysis in a cavernous hemangioma. Am J Dis Child 1967; 113:649-53.
44. Castoldi G. Erythrocytes. In: Zucker-Franklin D, Greaves MF, Grossi CE, Marmont AM, editors. Atlas of Blood Cells - function and pathology. Philadelphia: Lea & Febiger; 1981. p. 347-660.
45. Mohandas N, Phillips WM, Bessis M. Red blood cell deformability and hemolytic anemias. Semin Hematol 1979; 16:95-114.
46. Ways P, Simon E. The role of serum in acanthocyte autohemolysis and membrane lipid composition. J. Clin. Invest 1964; 43:1322-8.
47. Biemer JJ. Acanthocytosis--biochemical and physiological considerations. Ann Clin Lab Sci 1980; 10:238-49.
48. Akashi K, Traver D, Miyamoto T, Weissman IL. A clonogenic common myeloid progenitor that gives rise to all myeloid lineages. Nature 2000; 404:193-7.
49. Li J, Kuter DJ. The end is just the beginning: megakaryocyte apoptosis and platelet release. Int J Hematol 2001; 74:365-74.
50. Subramaniam M, Frenette PS, Saffaripour S, Johnson RC, Hynes RO, Wagner DD. Defects in hemostasis in P-selectin-deficient mice. Blood 1996; 87:1238-42.
51. Romo GM, Dong JF, Schade AJ, Gardiner EE, Kansas GS, Li CQ, McIntire LV, Berndt MC, Lopez JA. The glycoprotein Ib-IX-V complex is a platelet counterreceptor for P-selectin. J Exp Med 1999; 190:803-14.
52. Frenette PS, Johnson RC, Hynes RO, Wagner DD. Platelets roll on stimulated endothelium in vivo: an interaction mediated by endothelial P-selectin. Proc Natl Acad Sci U S A 1995; 92:7450-4.
53. Frenette PS, Denis CV, Weiss L, Jurk K, Subbarao S, Kehrel B, Hartwig JH, Vestweber D, Wagner DD. P-Selectin glycoprotein ligand 1 (PSGL-1) is expressed on platelets and can mediate platelet-endothelial interactions in vivo. J Exp Med 2000; 191:1413-22.
54. Denis CV, Andre P, Saffaripour S, Wagner DD. Defect in regulated secretion of P-selectin affects leukocyte recruitment in von Willebrand factor-deficient mice. Proc Natl Acad Sci U S A 2001; 98:4072-7.
55. Denis C, Methia N, Frenette PS, Rayburn H, Ullman-Cullere M, Hynes RO, Wagner DD. A mouse model of severe von Willebrand disease: defects in hemostasis and thrombosis. Proc Natl Acad Sci U S A 1998; 95:9524-9.

56. Pasyk KA, Grabb WC, Cherry GW. Cellular haemangioma. Light and electron microscopic studies of two cases. Virchows Arch A Pathol Anat Histol 1982; 396:103-26.
57. Yasunaga C, Sueishi K, Ohgami H, Suita S, Kawanami T. Heterogenous expression of endothelial cell markers in infantile hemangioendothelioma. Immunohistochemical study of two solitary cases and one multiple one. Am J Clin Pathol 1989; 91:673-81.
58. Levi M, Ten Cate H. Disseminated intravascular coagulation. N Engl J Med 1999; 341:586-92.
59. Mammen EF. Disseminated intravascular coagulation (DIC). Clin Lab Sci 2000; 13:239-45.
60. Taylor FB, Jr., Toh CH, Hoots WK, Wada H, Levi M. Towards definition, clinical and laboratory criteria, and a scoring system for disseminated intravascular coagulation. Thromb Haemost 2001; 86:1327-30.
61. Gando S, Kameue T, Nanzaki S, Nakanishi Y. Disseminated intravascular coagulation is a frequent complication of systemic inflammatory response syndrome. Thromb Haemost 1996; 75:224-8.
62. Horan JT, Francis CW. Fibrin degradation products, fibrin monomer and soluble fibrin in disseminated intravascular coagulation. Semin Thromb Hemost 2001; 27:657-66.
63. Okajima K, Sakamoto Y, Uchiba M. Heterogeneity in the incidence and clinical manifestations of disseminated intravascular coagulation: a study of 204 cases. Am J Hematol 2000; 65:215-22.
64. Senis Y, Zirngibl R, McVeigh J, Haman A, Hoang T, Greer PA. Targeted disruption of the murine fps/fes proto-oncogene reveals that Fps/Fes kinase activity is dispensable for hematopoiesis. Mol Cell Biol 1999; 19:7436-46.
65. Browder T, Folkman J, Pirie-Shepherd S. The hemostatic system as a regulator of angiogenesis. J Biol Chem 2000; 275:1521-4.

Journal of Thrombosis and Haemostasis, 2: 820–832

APPENDIX 4

ORIGINAL ARTICLE

Vascular defects in gain-of-function *fps/fes* transgenic mice correlate with PDGF- and VEGF-induced activation of mutant Fps/Fes kinase in endothelial cells

W. SANGRAR,*† J. D. MEWBURN,* S. G. VINCENT,‡ J. T. FISHER‡ and P. A. GREER*†

*Division of Cancer Biology and Genetics, Queen's University Cancer Research Institute, †Department of Pathology and Molecular Medicine and ‡Department of Physiology and Medicine, Queen's University, Kingston, Ontario, Canada

To cite this article: Sangrar W, Mewburn JD, Vincent SG, Fisher JT, Greer PA. Vascular defects in gain-of-function *fps/fes* transgenic mice correlate with PDGF- and VEGF-induced activation of mutant Fps/Fes kinase in endothelial cells. *J Thromb Haemost* 2004; **2**: 820–32.

Summary. *Background*: Fps/Fes is a cytoplasmic tyrosine kinase that is abundantly expressed in the myeloid, endothelial, epithelial, neuronal and platelet lineages. Genetic manipulation in mice has uncovered potential roles for this kinase in hematopoiesis, innate immunity, inflammation and angiogenesis. *Objective*: We have utilized a genetic approach to explore the role of Fps/Fes in angiogenesis. *Methods*: A hypervascular line of mice generated by expression of a 'gain-of-function' human *fps/fes* transgene (fps^{MF}) encoding a myristoylated variant of Fps (MFps) was used in these studies. The hypervascular phenotype of this line was extensively characterized by intravital microscopy and biochemical approaches. *Results*: fps^{MF} mice exhibited 1.6–1.7-fold increases in vascularity which was attributable to increases in the number of secondary vessels. Vessels were larger, exhibited varicosities and disorganized patterning, and were found to have defects in histamine-induced permeability. Biochemical characterization of endothelial cell (EC) lines derived from fps^{MF} mice revealed that MFps was hypersensitive to activation by vascular endothelial growth factor (VEGF) and platelet-derived growth factor (PDGF). *Conclusions*: MFps mediates enhanced sensitization to VEGF and PDGF signaling in ECs. We propose that this hypersensitization contributes to excessive angiogenic signaling and that this underlies the observed hypervascular phenotype of fps^{MF} mice. These phenotypes recapitulate important aspects of the vascular defects observed in both VEGF and angiopoietin-1 transgenic mice. The *fps/fes* proto-oncogene product therefore represents a novel player in the regulation of angiogenesis, and the fps^{MF} line of mice constitutes a unique new murine model for the study of this process.

Correspondence: Peter A. Greer, Division of Cancer Biology and Genetics, Queen's University Cancer Research Institute, Botterell Hall, Room A309, Kingston, Ontario K7L 3 N6, Canada.
Tel.: +1 613 533 2813; fax: +1 613 533 6830; e-mail: greerp@post.queensu.ca

Received 6 November 2003, accepted 17 December 2003

Keywords: angiogenesis, *fps/fes*, platelet-derived growth factor, vascular endothelial growth factor.

Introduction

Vasculogenesis involves the development of a primary vascular plexus, a process regulated primarily by vascular endothelial growth factor (VEGF) and basic fibroblast growth factor (bFGF) (reviewed in [1–4]). The primary plexus then undergoes angiogenesis, a process of vascular expansion and remodeling. The VEGFs and angiopoietins are critical for vascular development and are thought to play coordinated and complementary roles. VEGF induces endothelial sprouting, while angiopoietin-1 (Ang1) and angiopoietin-2 (Ang2) play antagonistic roles in vessel stabilization and destabilization, respectively. Final maturation of the vascular network, or arteriogenesis, involves pericyte recruitment, proliferation and migration and results in the generation of a smooth muscle coating around endothelial tubes (reviewed in [1]). Mural cell coatings provide stabilization to newly emergent vessels by providing viscoelastic and vasomotor properties and hemostatic control.

Platelet-derived growth factor (PDGF)-B has been associated with regulating smooth muscle proliferation and migration during arteriogenesis. PDGF mediates a diversity of biological effects including wound healing [5], angiogenesis [6], and atherosclerosis [7]. PDGF is also oncogenic, although its cellular transforming ability has been shown to be dependent on the particular genetic background of the cell [8]. Genetic analysis of PDGF and its cognate receptors has revealed critical requirements for this ligand/receptor pair in embryonic development. Genetic disruption of PDGF-B and PDGF receptor-β (PDGFRβ) resulted in lethality, induced by sudden onsets of microvascular hemorrhaging [9–13]. A large subset of defects were associated with failed recruitment of pericytes; these included abnormal vascular morphogenesis, dilatation of large and small caliper

blood vessels, endothelial cell (EC) hyperplasia, abnormal EC ultrastructure and increased transendothelial permeability [9,11–14].

Fps/Fes (here after called Fps) and its closely related homolog Fer comprise a unique family of non-receptor cytoplasmic tyrosine kinases [15]. Structurally, these kinases are defined by an N-terminal Cdc42 interacting Fer-CIP4 (FCH) homology domain, central coiled-coil and SH2 domains and a C-terminal tyrosine kinase domain [15,16]. Fps expression has been described in myeloid, endothelial, epithelial, neuronal and platelet lineages [17,18]. Genetic analyses of gene-targeted mice have revealed roles in hematopoietic homeostasis, innate immunity and inflammation [19–23]. Genetic analysis has also been employed using two transgenic *fps* lines. Remarkably, 20-fold tissue-specific overexpression of wild-type Fps from a transgene consisting of the complete human *fps* did not produce any observable phenotype [24]. This transgene appeared to contain the complete human *fps* locus, including a locus control element, because it was found to drive the same tissue-specific expression pattern in seven independent lines [24]. Another group has since mapped a locus control element within this same sequence [25]. A derivative of this transgene differing only by the presence of an additional activating N-terminal Src-like myristoylation consensus sequence (fps^{MF}) was also engineered. This derivative encoded a myristoylated, and consequently activated form of Fps (MFps) which gave rise to pronounced vascular hyperplasia when tissue-specifically overexpressed (5-fold) in mice [26]. Based on the expression pattern of Fps, MFps was expectedly detected in myeloid, epithelial, neuronal and endothelial cells, and also in platelets. Its expression in the endothelium and its apparent effect on vascular density led us to propose that Fps might regulate vasculogenic and/or angiogenic processes [26]. Since then, several *in vitro* studies utilizing immortalized EC lines have supported this hypothesis by demonstrating that Fps regulates endothelial tube formation, chemotaxis and migration, and that it may function in FGF-2, Ang2 and VEGF signaling [27–30]. Most recently, expression of MFps in VEGFR-2 null embryonic stem cells was shown to rescue their ability to contribute to vasculogenesis in chimeric embryos; this suggested a 'gain-of-function' activity of MFps acting downstream of the principle VEGF receptor [31].

In this study, we have quantified the extent of hypervascularity in these mice. In addition, we have observed unexpected and striking defects in the morphological characteristics of the vasculature, including highly disorganized and tortuous patterning. Permeability defects in response to the inflammatory mediator histamine were also observed, consistent with a possible role for Fps in the regulation of cell–cell adhesion. Lastly, we report that VEGF and PDGF induced phosphorylation of MFps in ECs derived from fps^{MF} mice. Fps phosphorylation, however, was undetectable, suggesting that myristoylation of Fps confers an enhanced sensitization of ECs to these growth factors.

Materials and methods

Mice

Transgenic mice (fps^{MF}) tissue-specifically overexpressing a myristoylated form of Fps (MFps) were generated in a CD-1 background. Continuous brother–sister inbreeding over more than 20 generations is expected to have resulted in a homozygous inbred status of this line. Mice were housed at the Animal Care Facility at Queen's University, Kingston, Ontario [26]. All experimental procedures were approved by the Queen's University Animal Care Committee.

Quantification of cremaster vascular networks and vessel permeability

Fluorescence intravital video microscopy (FIVM) was used to quantify cremaster vascular networks [32]. FITC–albumin was injected intravenously (25 mg kg^{-1}) enabling fluorescence-based visualization of the vascular network. Microscope images of cremaster muscle preparations were collected sequentially for the entire exteriorized muscle. Image composites were then assembled for the entire area studied (approximately 6.5 mm^2). Vascular lengths were obtained by manual traces of individually captured images and total length of the traced vessels were calculated per unit tissue area using Image-Pro Plus 4.0 software (Media Cybernetics, Silver Spring, MD, USA). Vascular areas were determined using bitmap intensity analysis. This was based on the selection of pixels that fell within threshold intensity ranges corresponding to vascular areas in which FITC-labeled albumin was present. Identical threshold intensity ranges were employed for all images. From this data, 3-D histograms were charted for each genotype and ratios of vascular to tissue area were calculated. Microvascular permeability of postcapillary venules from cremaster muscle preparations was assessed by the quantification of FITC–albumin extravasation in response to histamine suffusion as previously described [33].

Brain, heart and hepatic vascular network imaging

FITC–albumin (25 mg kg^{-1}) was administered by venous cannulation into anesthetized mice. Approximately 3 min postinjection, identical regions of the brain, heart and liver tissue were surgically removed and visualized using a Leica TCS SP2 multiphoton microscope. Images were captured at steps of 1.5 μm to a total tissue depth of 75–105 μm. Captured images were stacked and rendered using ImageJ 1.26 image processing software.

Heart rate and blood pressure determination

Mice were anesthetized with an intraperitoneal injection of sodium pentobarbital (60 mg kg^{-1} diluted 50% with saline) and mechanically ventilated (Harvard Apparatus, Saint-Laurent, PQ, Canada) with 40% oxygen at a constant

volume of 8–10 mL kg^{-1} and a frequency of 115 breaths min^{-1}. These ventilator settings result in a peak airway pressure of 6–8 cmH_2O, and have been shown previously to provide normal arterial blood gases [34]. A low-volume catheter line (< 10 μL) was placed in the abdominal vena cava for intravenous administration of anesthetic and other drugs (injection volumes of 1 mL kg^{-1}). Electrocardiogram electrodes were placed subcutaneously for the measurement of heart rate (HR) and a blood pressure transducer (Mikro-Tip® Catheter 1.4F; Millar Instruments, Houston, TX, USA) was inserted into the left branch of the carotid artery for measurement of arterial blood pressure. Mice were paralyzed with doxacurium chloride (0.25 mg kg^{-1}) (Abbott Labs, Saint-Laurent, PQ, Canada) to prevent respiratory efforts. Arterial blood pressure and electrocardiogram signals were acquired by a computer data acquisition package (CODAS DATAQ; Akron, OH, USA) at a sampling frequency of 1000 samples s^{-1} $channel^{-1}$. Acquired data were analyzed using peak detection software and data were imported to a spreadsheet for calculation of HR and mean arterial blood pressure (MAP).

Methylcholine stimulation of heart rate and blood pressure

Increasing doses of methylcholine (MCh) (5, 25, 50, and 100 μg kg^{-1}) were injected intravenously into anesthetized, paralyzed, and ventilated mice 2 min post volume history maneuvers to total lung capacity. Average values for HR, diastolic and systolic blood pressures were calculated for 30 s of data acquired prior to injection of MCh (control) and in 10 s bins for 140 s after MCh injection. Peak responses to MCh were measured at 30 s post injection.

VEGF and PDGF stimulation of C166 endothelial cell lines

C166 ECs isolated from day-12 yolk sacs of fps^{MF} mice were cultured as previously described [35]. VEGF and PDGF stimulation experiments were performed on native C166 lines and on C166 cell lines ectopically expressing C-terminal-Myc-epitope-tagged variants of Fps that were generated by retroviral transduction [36]. The following pMSCV (murine stem cell virus) constructs encoding variants of Fps were utilized: (i) *pMSCV-fps-myc*, myc-epitope-tagged wild type Fps (C166-Fps-Myc cell line); and (ii) *pMSCV-fps^{MF}-myc*, myc-epitope-tagged variant of Fps containing an N-terminal Src-like myristoylation target sequence [26] (C166-MFps-Myc cell line). Cells were serum starved overnight, stimulated with PDGF (0–3.3 nM) or VEGF (0–2.4 nM) (R&D Systems Inc., Minneapolis, MN, USA) for 2.5–5 min and lyzed in phospholipase C lysis buffer containing a cocktail of protease inhibitors [37]. Cell lysates were either immunoprecipitated (IP) with FpsQE antisera specific for Fps and Fer (anti-Fps/Fer), with FerLA antisera specific for Fer (anti-Fer) [17], or with anti-Myc ascites (anti-Myc) (MYC 1-9E10.2; ATCC, Rockville, MD, USA). In some cases, soluble cell lysates (SCLs) were analyzed directly by immunoblotting (IB). IPs and SCLs were subsequently probed with the following antibodies according to manufacturer instructions or as described previously [17]: anti-Fps/Fer, anti-Fer, anti-Myc, and antiphosphotyrosine (Santa Cruz Biotechnology, Santa Cruz, CA, USA).

Results

Reduced embryonic viability of fps^{MF} mice

Knockouts of VEGF, Ang1, PDGF-B and their respective receptors have displayed moderate to severe embryonic lethality due to defects associated with compromised vasculogenesis and/or angiogenesis. Initial attempts to generate fps^{MF} transgenic mice suggested that moderate levels of MFps expression were tolerated, but higher levels caused embryonic or perinatal lethality [26]. This observation, coupled with reported associations between failed embryogenesis and abnormal vascular development, led us to speculate that some fps^{MF} mice might be dying *in utero*. In order to test this, we performed genotypic analysis of offspring derived from hemizygous fps^{MF} (♂) × *wt* (♀) breeding pairs. A statistically significant increase in the expected number of *wt* vs. hemizygous fps^{MF} progeny [57 : 43 vs. expected 50 : 50 ratio (*wt* : fps^{MF}) ($\chi^2 = 3 \times 10^{-6}$)], was found. This suggested that some fps^{MF} mice might be dying *in utero*, possibly due to complications associated with MFps-induced vascular hyperplasia [26].

Phenotypic similarities of fps^{MF} mice with VEGF and Ang1 transgenic mice

Overexpression of either Ang1 or VEGF from the keratin 14 promoter in mice (K14-Ang1 and K14-VEGF) gave rise to tortuous vessel morphology, aberrant patterning and increased vessel density in the skin [38–40]. Ang1 transgenic mice also displayed excessive dilatation of blood vessels [39,40]. The phenotypes exhibited by these transgenic lines were characterized by redness of the skin on the ears and on the underside of the nose and feet [38–40]. Although transgenic targeting was not skin specific in fps^{MF} mice, a remarkably similar redness of skin was also observed, pointing to the existence of similar defects in vascular morphology (data not shown). Moreover, this redness was also strongly observed in fps^{MF} neonates (data not shown), suggesting that defects in vascularity arise during embryogenesis. The similarities in phenotypes between fps^{MF} and the above-described Ang1 or VEGF transgenic mice argued that the Fps kinase might play a role in regulating signaling pathways triggered by these growth factors.

Hypervascularity and aberrant vascular patterning in fps^{MF} mice

The initial hypervascular characterization of the fps^{MF} mouse line was based solely on immunohistochemical analysis of vessel density in the brown adipose tissue of neonatal animals [26]. Here we have extended this analysis, showing abnormal vascular patterning, excessive tortuosity, and vascular varicosities in the blood vessels of fps^{MF} mice (Fig. 1).

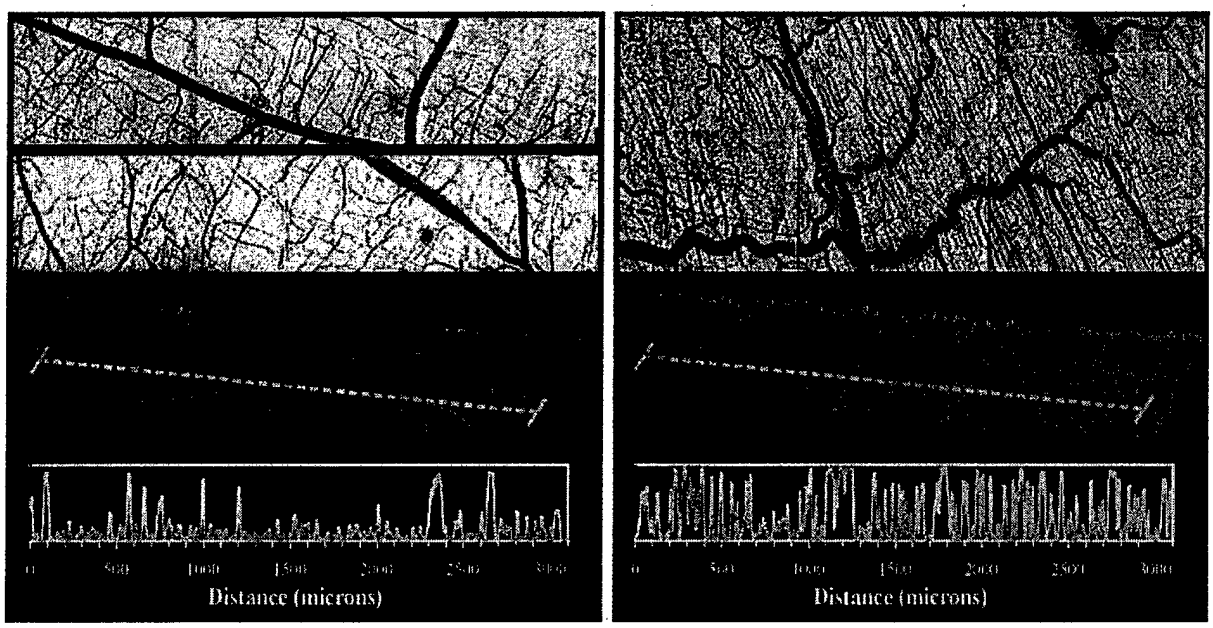

Fig. 1. Comparison of vascular patterning and morphology in cremaster muscle using fluorescence intravital microscopy. The upper section of each panel represents two-dimensional composite images of vessel networks visualized by fluorescence microscopy (× 100 magnification). The middle section of each panel is the corresponding three-dimensional fluorescence intensity plot of vessel networks in cremaster muscle. The bottom section of each panel represents a linear intensity plot of the region traversed by the dotted line shown in the middle section of each panel. These images clearly show that fps^{MF} mice exhibit pronounced hypervascularity, aberrant patterning, excessive tortuosity and vascular varicosities (A, *wt*; B, fps^{MF}). Also apparent were increases in the vascular density of vessels emanating from primary branches.

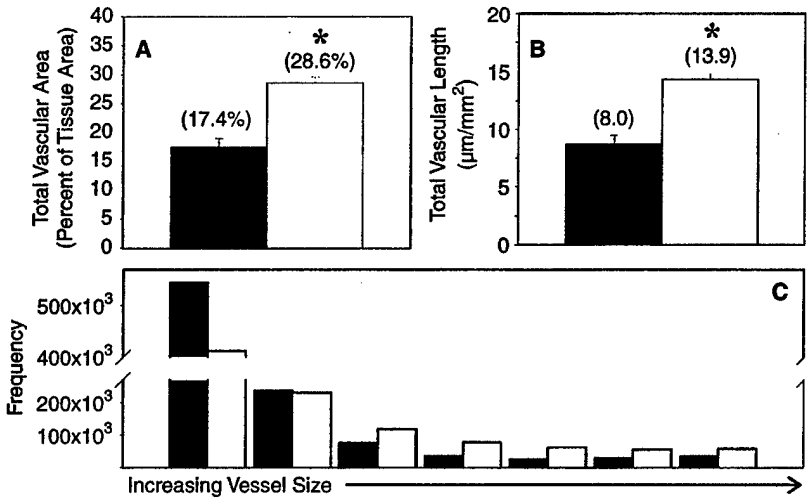

Fig. 2. Vessel density and size in cremaster muscle. Morphometric analysis of composite images of cremaster muscle digitally captured at × 100 magnification were utilized to yield estimates of vascularity. fps^{MF} mice were found to have a 1.6-fold increase in total vascular area [A, *wt* (■) 17.4 ± 0.9%; fps^{MF} (□) 28.6 ± 0.6%; $n = 3$, $P = 0.0005$*] and a 1.7-fold increase in total vascular length per unit tissue area [B, *wt* (■) 8.0 ± 1.5 μm mm^{-2}; fps^{MF} (□) 13.9 ± 0.8 μm mm^{-2}; $n = 3$, $P = 0.05$*]. Frequency distribution analysis of intensity data captured by fluorescence intravital video microscopy was performed. This analysis suggested that larger vessels occur with increasing frequency in fps^{MF} mice [C, *wt* (■); fps^{MF} (□)].

Morphometric analyses of the vascular network in cremaster muscle preparations visualized by intravascular perfusion of FITC–albumin suggested a 1.6-fold ($P = 0.0005$) increase in total vascular area in fps^{MF} mice (Fig. 2A), and a corresponding 1.7-fold ($P = 0.05$) increase in total vascular length per unit tissue area (Fig. 2B). Visual inspection of these images indicated that hypervascularity was primarily attributable to increased branching of vessels of secondary order (arterioles and venules) emanating from primary vessels (Fig. 1). This is quantitatively depicted in the volumetric (red) and linear (yellow) intensity profiles of each image, which show increased signals of intermediate FITC–albumin intensity in regions between primary vessels in fps^{MF} mice (Fig. 1). Visual inspection of capillary density was partially

limited by resolution; however, comparable or very modest decreases in capillary density were discernable (data not shown). Since intensity values correlate with vessel size in these plots, a frequency distribution profile of vessel size can be generated in the absence of spatial information. This type of analysis revealed that vessels of increased size occurred with greater frequency in fps^{MF} mice (Fig. 2C). Interestingly, this morphometric analysis also predicted fewer of the smallest sized vessels in fps^{MF} mice, confirming our subjective observations of modest decreases in capillary density. Overall, these abnormalities are reminiscent of the phenotypes in K14-VEGF and K14-Angl mice, in that they display defects in patterning, vessel density, branching and size.

Vascular hyperplasia and malformations in brain and heart of fps^{MF} mice

We next wanted to examine the extent of vascular hyperplasia and malformations in other tissues of fps^{MF} mice. We employed two-photon laser confocal microscopy for this purpose and focused on brain, heart and hepatic tissue obtained from FITC–albumin-injected mice. Images of brain and heart tissue of equivalent thickness showed gross vascular aberrations reminiscent of that seen in highly vascularized tumors. Vessels in these tissues displayed dramatically aberrant patterning, tortuosity and varicosities (Fig. 3; compare Fig. 3A,C,E with Fig. 3B,D,F). As in the cremaster muscle,

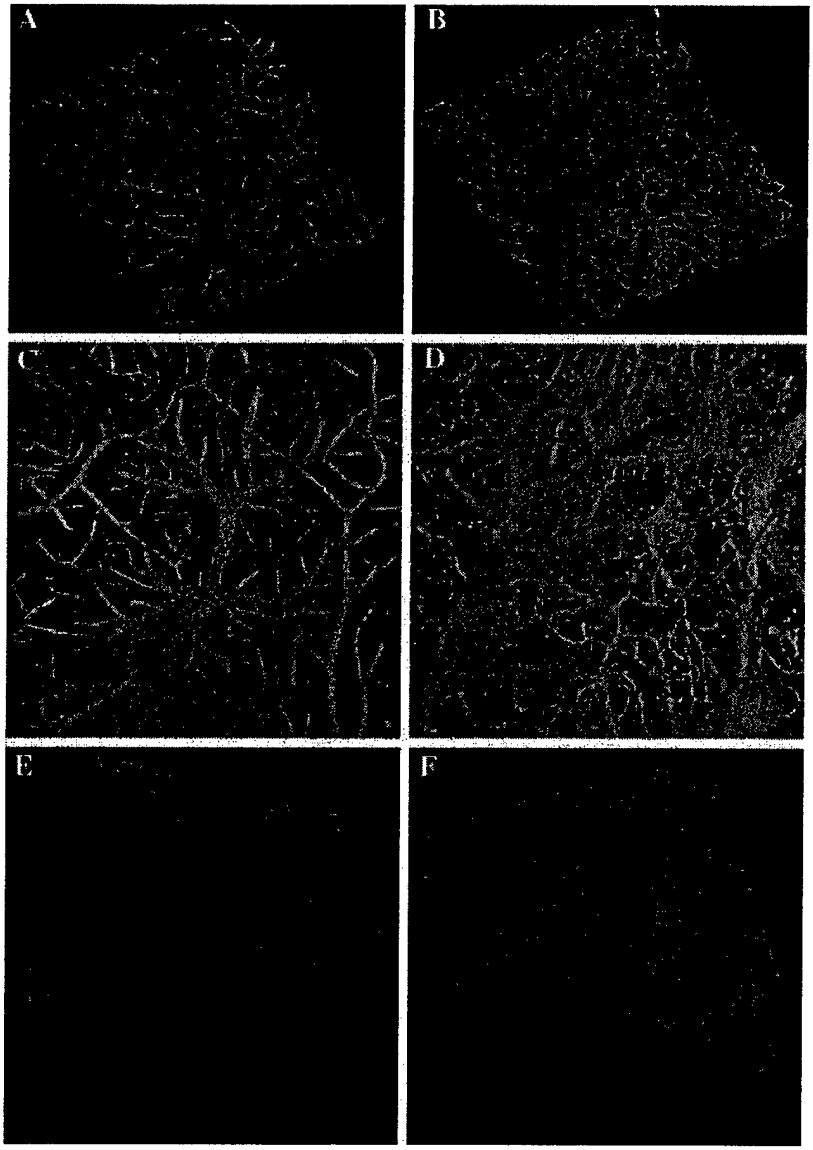

Fig. 3. Comparison of vascular networks in brain and heart using two-photon confocal microscopy. Images were obtained using two-photon confocal microscopy of whole tissue. Hypervascularity and tortuous vascular patterning were also found in the brain (B, D, fps^{MF}; A, C , *wt*; ×100; 75 μm) and heart (F, fps^{MF}; E, *wt*; ×100; 105 μm) of fps^{MF} mice. Also evident in these images were increases in the number of second-order vessels in both the brain and heart of fps^{MF} mice (compare D and F with C and E, respectively).

increased vascularity and branching appeared to be associated with second-order vessels. This was more apparent when images of the brain were rendered at different angles (Fig. 3C,D). In addition, primary vessels were larger, which was in agreement with the frequency distribution analysis in Fig. 2C. In order to assess vessel density and morphology at the capillary level, we examined the sinusoidal hepatic capillaries under higher magnification. The patterning and degree of branching of fps^{MF} hepatic capillary networks appeared to be similar to that in *wt* hepatic networks (data not shown). This further argued that increases in vessel density are associated with second-order vessels, and that alterations in capillary density, morphology, and patterning are negligible or modest at best. Collectively, these data confirmed earlier predictions of tissue-wide hypervascularity [26] and moreover, demonstrated that MFps overexpression resulted in comparable vascular aberrations in a number of different tissues.

Enhanced vessel permeability in response to histamine

K14-VEGF mice and knockouts of Angl and Tie2 gave rise to leaky-vessel phenotypes, while K14-Angl mice gave rise to leakage-resistant vessels, suggesting an association between hyperplasia and defects in vessel permeability [40–43]. These associations prompted us to examine whether the vascular hyperplasia in fps^{MF} mice was also accompanied by permeability defects. We employed the permeability-inducing agent histamine, which induces cell contractility and has been shown to induce phosphorylation of endothelial adherens junctions proteins [44]. Histamine was directly suffused over cremaster preparations at a constant rate and plasma extravasation as a function of FITC–albumin intensity was measured. Upon suffusion, leakage began by approximately 150 s and progressed linearly until saturation levels were reached due to upstream vasoconstriction or localized coagulation (*wt*, $n = 4$;

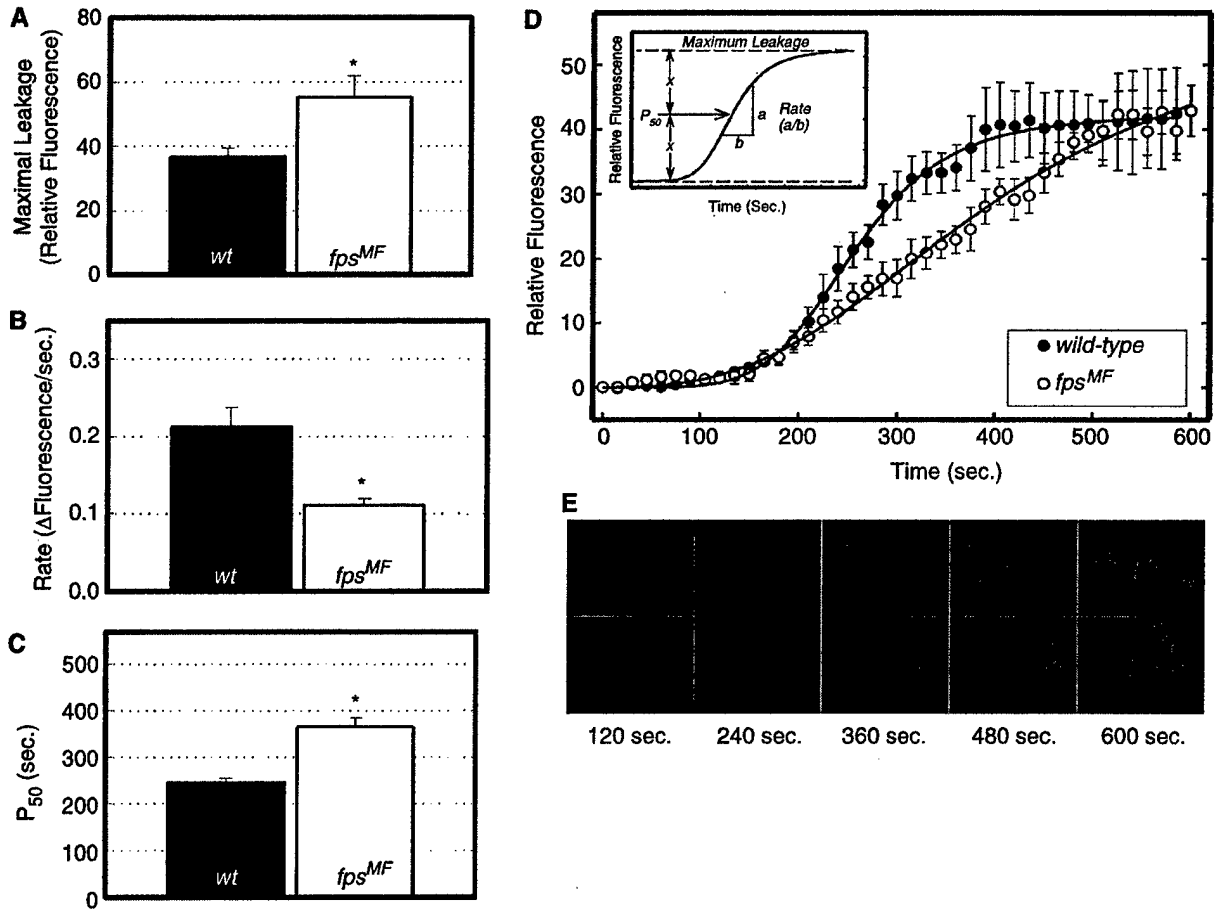

Fig. 4. Reduced vascular permeability in response to histamine in fps^{MF} mice. Intravital microscopy was employed to monitor histamine-induced extravasation of FITC–albumin. Extravasation was measured as a function of total fluorescence intensity within a defined rectangular area encompassing both the vessel lumen and adjacent extravascular regions. Rate of FITC–albumin extravasation was readily visualized over time and showed that histamine-induced vascular permeability is compromised (E, upper row, *wt*; lower row, fps^{MF}). This is quantitatively represented by temporal fluorescence profiles post-histamine suffusion [D (average ± SEM): fps^{MF} (○), $n = 5$; *wt* (●), $n = 4$]. Three parameters of the average fluorescence intensity profiles were assessed (D, inset). The maximal leakage parameter was increased in fps^{MF} mice [A, fps^{MF} (□), 55.2 ± 6.7; *wt* (■), 36.7 ± 2.7; $P = 0.048$*]. The rate parameter, however, was decreased [B, fps^{MF} (□), 0.11 ± 0.01 Δ intensity s^{-1}; *wt* (■), 0.21 ± 0.03 Δ intensity s^{-1}; $P = 0.003$*]. Changes in the latter two parameters were reflected by increases in the half-maximal time of leakage (P_{50}) in fps^{MF} mice [C, fps^{MF} (□), 364 ± 20 s; *wt* (■), 245 ± 9 s; $P = 0.005$*].

fps^{MF}, $n = 5$; Fig. 4D,E). We estimated the maximal extent of leakage, rate, and half-maximal time (P_{50}) of plasma extravasation for each mouse; these parameters are graphically depicted in the inset of Fig. 4D. Using linear regression analyses, a mean 48% decrease in the rate parameter ($P = 0.003$) was calculated, consistent with the existence of a retarded rate of leakage in the blood vessels of fps^{MF} mice (Fig. 4B). Non-linear regression analyses using a Hill 3-parameter sigmoidal function provided estimates of P_{50} and maximal levels of leakage. Interestingly, mean levels of these parameters were both elevated 1.5-fold in fps^{MF} mice ($P = 0.005$ and $P = 0.048$, respectively; Fig. 4A,C). The latter results suggested that although permeability rate was decreased, restoration of the vessel to resting permeability states could be delayed, resulting in overall increases in the levels of extravasated plasma.

Cardiac abnormalities in fps^{MF} mice

Transgenic mice expressing an activated *fps* allele from a β-globin promoter gave rise to enlarged subcutaneous blood vessels and to cardiac abnormalities including cardiomegaly [45]. Cardiac abnormalities have also been observed in PDGF-B [12], Ang1 [43] and Tie2 [42] knockouts. Examination of lateral and longitudinal cross-sections of the hearts of fps^{MF} mice revealed no overt differences in morphology suggesting normal heart function (data not shown). However, their mean heart size (percent of body weight) was increased [*wt* (4.9 ± 0.8 months), 0.45 ± 0.01%, $n = 28$; fps^{MF} (4.8 ± 0.9 months), 0.50 ± 0.01%, $n = 21$; $P = 0.02$] and systemic MAP was reduced in fps^{MF} mice (*wt*, 55.4 ± 1.2 mmHg, $n = 4$; fps^{MF}, 39.2 ± 1.6 mmHg, $n = 4$; $P = 1.4 \times 10^{-7}$). This result indicated that there might be vascular-associated perturbations of cardiac function in fps^{MF} mice.

We further explored potential defects in cardiac function by examining heart rate and MAP responses to the muscurinic agonist MCh. MCh induces nitric oxide secretion to cause vasodilatation peripherally and engages the M2 muscurinic receptor expressed on myocytes in the atria and ventricle to induce bradychardia (reviewed in [46–48]). Heart rates under unchallenged conditions were normal, but increased sensitivity to MCh-induced bradychardia was observed in fps^{MF} mice (Fig. 5A). MCh induced similar dose-dependent decreases in MAP in both *wt* and fps^{MF} mice, suggesting that dilatation capacity of blood vessels is intact in fps^{MF} mice (Fig. 5B). When the vasoconstrictor phenylephrine was administered, increases in MAP were also comparable, indicating that vessel constriction capacity is also normal in fps^{MF} mice (data not shown).

Fps is activated downstream of PDGF in C166 endothelial cells

Preliminary attempts to delineate the molecular basis of defective angiogenesis involved the testing of key angiogenic factors on C166 ECs, which were derived from the yolk sac of fps^{MF} mice [35]. Stimulation of C166 cells with recombinant FGF-2 or with Ang1-conditioned media did not elicit detectable Fps or MFps activation (data not shown). When C166 cells were stimulated with PDGF-B, we observed a striking response in the global tyrosine phosphorylation profile (Fig. 6A). An identically potent response was observed in a hemangioendothelioma cell line (EOMA) (Fig. 6B), suggesting that the PDGFR is expressed in both lines of ECs. Subsequent IP and IB analyses revealed a dose-dependent increase in tyrosine phosphorylated Fps/MFps [(M)Fps] species in response to PDGF in C166 cells (Fig. 6C). Quantification of the (M)Fps phosphotyrosine signal revealed a sigmoidal activation profile indicative of an ultrasensitive response to PDGF [49,50] (Fig. 6F). In EOMA cells, basal levels of activation of Fps (and Fer) were elevated and remain unchanged with increases in PDGF-B doses (data not shown).

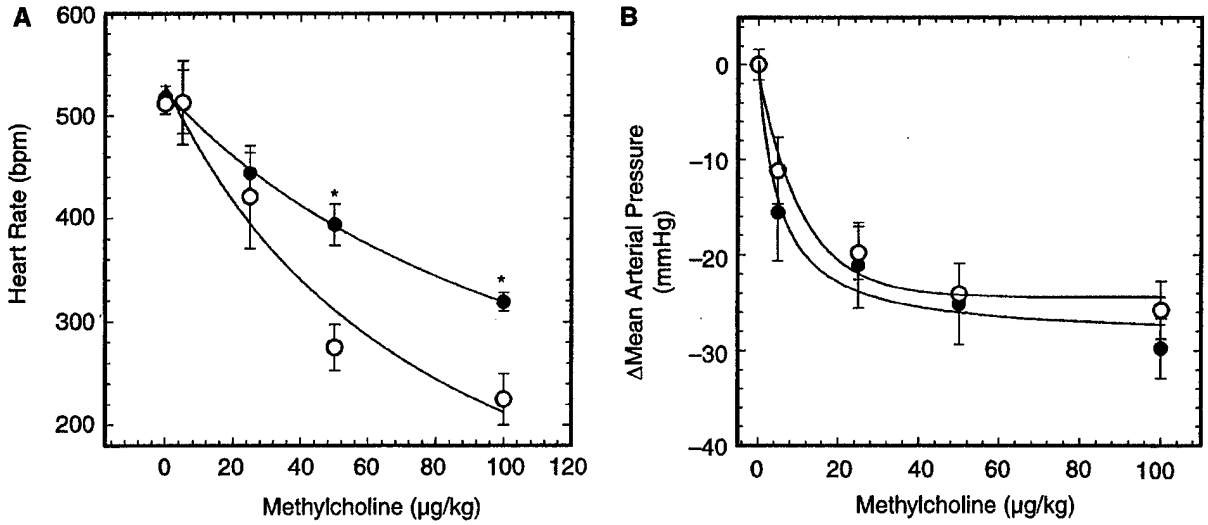

Fig. 5. Response of heart rate and blood pressure to methylcholine. fps^{MF} mice were more sensitive to methylcholine-induced decreases in heart rate [A, *wt* (●), fps^{MF} (○); $n = 3$; $P < 0.05$*]. Decreases in mean arterial pressure were comparable between genotypes. [B, *wt* (●); fps^{MF} (○); $n = 3$].

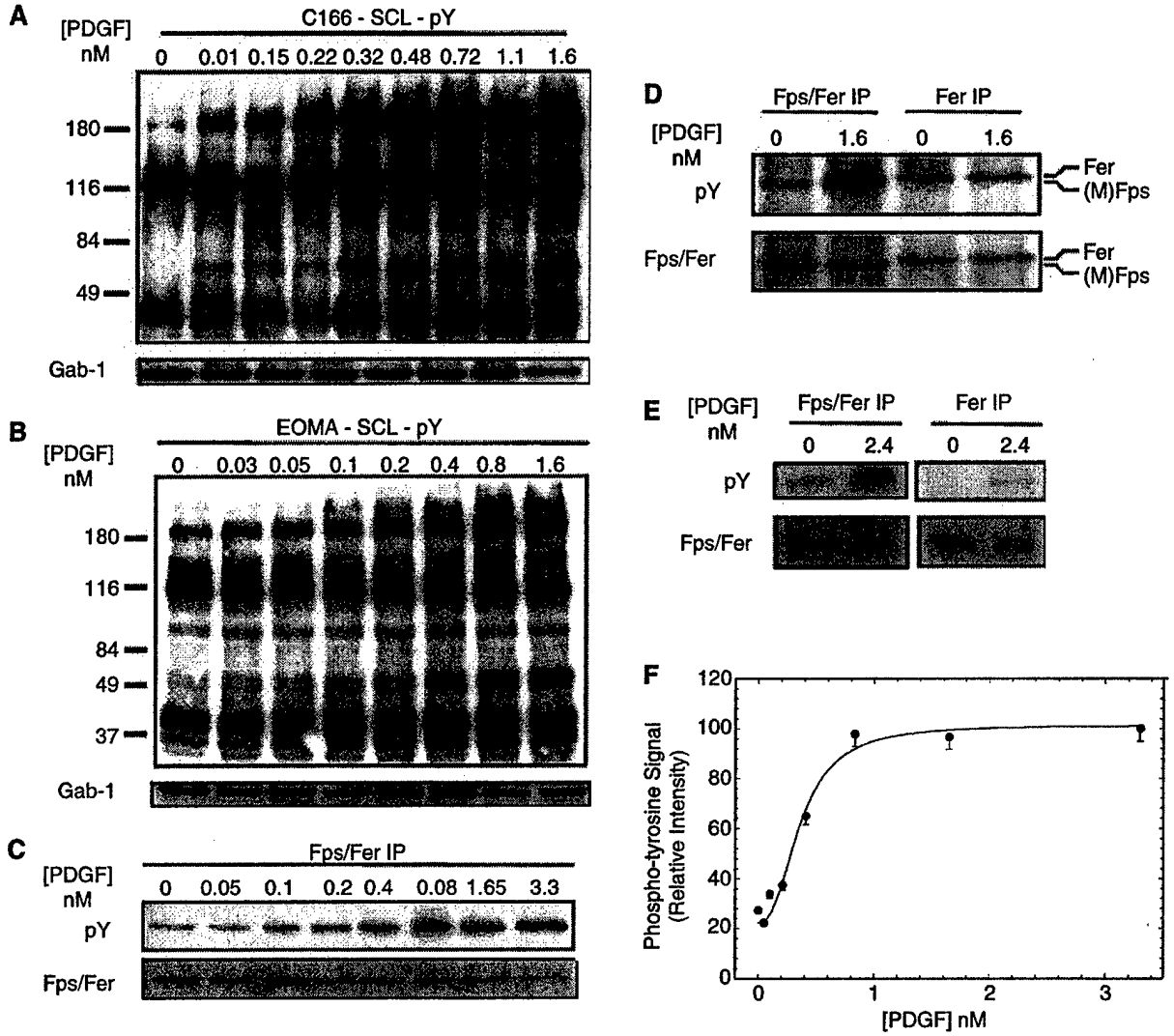

Fig. 6. Platelet-derived growth factor (PDGF)-induced tyrosine phosphorylation of Fps in C166 cells. Global tyrosine phosphorylation (pY) responses to increasing concentrations of PDGF in C166 cells and hemangioendothelioma (EOMA) cells were assessed by anti-pY immunoblotting (A and B, respectively). The blots were stripped and reprobed with an anti-Gab1 polyclonal antibody (Upstate Biotechnologies, Lake Placid, NY, USA) in order to confirm equal protein loading of samples (A,B). Migration of MFps and Fps were indistinguishable due to significant overexpression of MFps relative to Fps. A band corresponding to both MFps and Fps [(M)Fps] was phosphorylated in a dose-dependent manner by PDGF (C, anti-pY blot). The response was ultrasensitive as indicated by a Hill coefficient parameter (n_H) of 2.43, obtained by non-linear regression using a Hill 3-parameter function. n_H has been utilized to differentiate between the sensitivity of responses in biological systems where values of 1 represent Michaelis–Menton-like (hyperbolic) sensitivity whereas values below and above 1 represent sub- and ultrasensitivity thresholds, respectively [50]. Probing the same blots with anti-Fps/Fer confirmed equal loading (C, anti-Fps/Fer blot). (M)Fps pY levels, which reflect the kinase activation status [75], are quantified in F. Fer activation was not readily apparent at 1.6 nM PDGF (D), but was slightly visible at 2.4 nM PDGF (E), while (M)Fps was strongly tyrosine phosphorylated at both concentrations of PDGF (C,D,E), suggesting that pY signals were predominantly attributable to Fps.

Fer (94 kDa) migrates closely with Fps and MFps (both approximately 92 kDa) and these kinases are routinely visualized as doublets on SDS–PAGE [17,18]. The ratio of Fps plus MFps to Fer expression in C166 cells is apparently extremely large because only a single band corresponding to Fps plus MFps was apparent when an antibody known to be cross-reactive to Fps and Fer (anti-Fps/Fer) [17] was used in sequential IP and IB analysis (Fig. 6C, lower panel). Furthermore, when IPs were performed with a Fer-specific antibody in parallel with this Fps/Fer cross-reactive antibody, subsequent IB analysis with the cross-reactive anti-Fps/Fer antibody revealed a band corresponding to p94 Fer which was readily distinguished from the faster migrating (M)Fps species (Fig. 6D, compare Fps/Fer IP lanes to Fer IP lanes). Based upon this analysis, it is unlikely that there is any substantial amount of Fer in the anti-Fps/Fer IPs, and the phosphotyrosine signals must therefore originate from either Fps or MFps. However, since Fer has been shown to be activated by PDGF [51], we took additional precautionary measures and examined the degree to which Fer activation might contribute to the

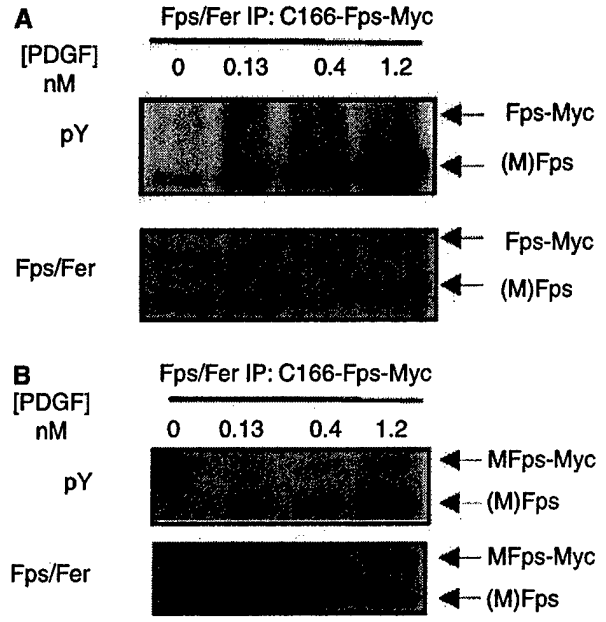

Fig. 7. MFps, but not Fps, was specifically activated by platelet-derived growth factor (PDGF). C166 cell lines expressing Myc-epitope-tagged wild-type Fps (Fps-Myc) and Myc-epitope-tagged myristoylated Fps (MFps-Myc) were stimulated with PDGF. Myc-tagged variants have higher molecular weights (approximately 120 kDa) and migrate slower than endogenous Fps (92 kDa) on SDS–PAGE (A,B). Upper blots in each panel represent anti-pY blots, while lower blots represent the same blots after stripping and reprobing with anti-Fps/Fer to assess loading of either endogenous Fps or Fps-Myc species. The positions of endogenous Fps or MFps, and exogenous Fps-Myc or MFps-Myc are indicated by arrows. PDGF stimulation of C166-Fps-Myc did not show activation of the Fps-Myc variant (A). This observation was confirmed with anti-Myc immunoprecipitations (data not shown). As expected, endogenous MFps present in these lines was dose-dependently activated by PGDF (A,B; pY blot; lower arrows). Activation of both endogenous MFps and Myc-tagged MFps species was observed when C166-MFps-Myc cells were stimulated with PDGF (B), suggesting that MFps, but not Fps is sensitized to activation downstream of PDGF.

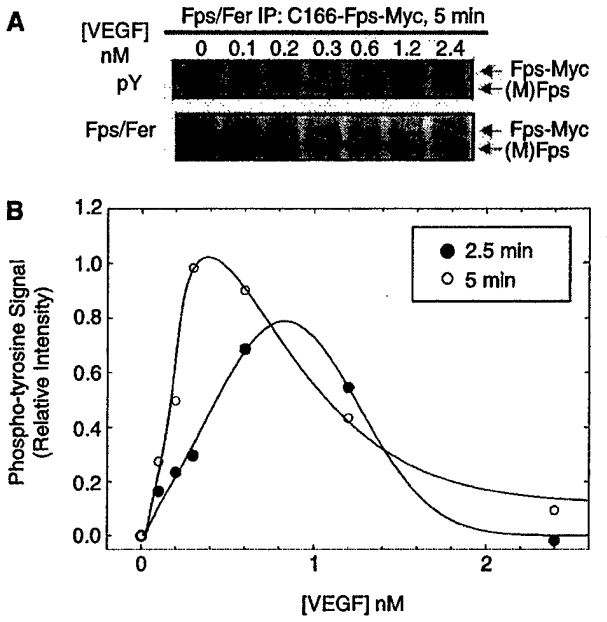

Fig. 8. MFps, but not Fps, is specifically activated by vascular endothelial growth factor (VEGF). C166 cell lines expressing Myc-epitope-tagged wild-type Fps were stimulated with 0–2.4 nM VEGF for 5 min. Dose-dependent tyrosine phosphorylation of (M)Fps, but not Fps-Myc was observed (A, pY blot). Blots were stripped and reprobed with anti-Fps/Fer to confirm loading (A, Fps/Fer blot). Quantification of the level of activation of MFps with 0–2.4 nM VEGF at 2.5 and 5 min time points is displayed (B). The chart displays transient activation of MFps in response to PDGF. The amplitude of activation appears to increase with time.

phosphotyrosine signal generated in the Fps/Fer IPs shown in Fig. 6C. When Fer was selectively immunoprecipitated using the Fer-specific antibody (anti-Fer), and immunoblotted with anti-pY, inducible activation of Fer was barely observable at concentrations of PDGF as high as 1.6 nM and 2.4 nM (Fig. 6D,E). This confirmed that the PDGF-induced phosphotyrosine signal in Fps/Fer IPs is predominantly due to Fps and/or MFps activation.

MFps sensitizes C166 endothelial cells to PDGF signaling

In order to delineate the relative proportions of activation of endogenous MFps and Fps by PDGF we utilized C166 cell lines that had been transduced with retroviruses encoding myc-epitope-tagged Fps (Fps-Myc) and MFps (MFps-Myc). These epitope-tagged variants migrate at approximately 120 kDa and could be easily distinguished from endogenous Fps and MFps signals at 92 kDa. Dose-dependent increases in tyrosine phosphorylation were seen in a 92-kDa band in both C166 lines (Fig. 7A,B). However, it was not possible to determine if this corresponded to endogenous Fps, the transgene encoded MFps, or a combination of both. Interestingly, while we did not detect tyrosine phosphorylation of Fps-Myc in the cell line transfected with this variant (Fig. 7A), we clearly observed dose-dependent tyrosine phosphorylation of transfected MFps-Myc (Fig. 7B). This suggested that compared with native Fps, the myristoylated (activated) MFps variant is highly sensitive to PDGF. The latter results were consistently observed regardless of whether anti-Myc (not shown) or anti-Fps/Fer was used for IPs. These data suggest that MFps mediates a strong response to PDGF in ECs from *fps*^{MF} mice.

Activation of MFps in response to VEGF in C166 cells

C166-Fps-Myc cells were treated with 0–2.4 nM VEGF and phosphorylation states of (M)Fps and exogenously expressed Fps-Myc were assessed using antiphosphotyrosine antibodies. A modest activation of (M)Fps was reproducibly detectable at 2.5 (data not shown) and 5 min (Fig. 8A). Quantification of the activation profiles suggested that the response to VEGF was transient (Fig. 8B). As was the case in PDGF-treated cells, Fps-Myc was not detectably phosphorylated in VEGF-treated cells (Fig. 8A). Thus, MFps also appears to hypersensitize C166 cells to VEGF signaling.

Discussion

Cardiovascular defects are frequently associated with defective vasculogenesis [12,43,52–54]. fps^{MF} mice exhibited mild cardiomegaly, and enhanced MCh-induced bradychardia, but tissue architecture was essentially normal. Although the former observations suggest that there may be some heart defects at the functional level, normal tissue architecture suggests that vascular defects in fps^{MF} mice do not occur during vasculogenesis, since this process is spatially and temporally linked to heart development. We propose therefore that their vascular defects arise during the subsequent phase of angiogenic remodeling consistent with branching and patterning defects of vessels of secondary order and with an apparent lack of vascular defects in the yolk sacs of fps^{MF} mice (data not shown). Thus, cardiac failure is unlikely to underlie either pre- or postnatal death (1–14 months; median 7 months) [26]. Rather, death may be attributed to hemorrhaging associated with vascular hyperplasia [26]. This has recently been supported by unpublished data showing a bleeding defect arising from secondary complications of hemangiomas.

Both VEGF and Angl, when overexpressed in the skin, gave rise to increased vascularity; however, each was associated with unique physiological and morphological aberrations of the vasculature [39,40]. The hypervascularity and leakiness observed in fps^{MF} mice exhibit strong parallels to the increased vascularity and leaky vessels in K14-VEGF mice. fps^{MF} mice also exhibited a minor degree of vessel enlargement. This is similar to, but does not approach the magnitude of vessel enlargement observed in K14-Angl mice [41]. Moreover, unlike fps^{MF} mice, K14-mice exhibited leakage resistance. These observations argue that MFps participates in signaling pathways downstream of VEGF. This is consistent with the leaky phenotype in these mice and with observations of MFps activation downstream of VEGF, but not Angl (data not shown).

PDGF is expressed on nascent ECs during angiogenesis and acts in a paracrine fashion to potentiate vascular smooth muscle cell (vSMC) recruitment, migration and proliferation along nascent endothelial tubes [9–11,55,56]. As demonstrated in PDGF-B and PDGFR-β knockouts, failure to recruit vSMC led to impaired arteriogenesis, compromised vessel integrity, and an edematous phenotype [9,12,13,57]. The increased plasma extravasation in fps^{MF} mice (Fig. 4) conforms with a possibility that MFps-mediated PDGF signaling might have contributed to defects in arteriogenesis associated with abnormal vSMC/pericyte recruitment and coating of vessels [9,58]. Such a possibility is supported by occasional observations of edema in some aged fps^{MF} mice (unpublished observations). However, whether this edema is a result of abnormal mural coating is unclear, since normal vasodilatation and vasoconstriction responses suggest that this coating is intact and functioning normally. Additional studies will be required to assess mural coating morphology in blood vessels from these mice.

Alternatively, increased plasma extravasation in fps^{MF} ECs may be related to defects in cellular mechanisms that control endothelial cell–cell adhesion. Interestingly, both histamine and VEGF have been shown to augment vascular permeability by regulating tyrosine phosphorylation of endothelial adherens junctions (AJ) components, resulting in dissociation of VE-cadherin from the actin cytoskeleton [44,59]. Precedence for a possible involvement of (M)Fps in AJ function stems from evidence implicating its closely related homolog Fer in regulating the tyrosine phosphorylation status of AJ components in neuronal [60], intestinal epithelial [61] and embryonic fibroblasts [Xu et al., unpublished]. Thus, the observed reduction in rate of leakage and elevated levels of plasma extravasation in response to histamine could reflect MFps-mediated slowing of the kinetics of AJ disassembly and reassembly.

Heterozygous VEGF-deficient embryos ($VEGF^{+/-}$) generated by aggregation of $VEGF^{+/-}$ embryonic stem cells with tetraploid supporting embryos exhibited intermediate severity of blood vessel formation compared with $VEGF^{-/-}$ embryos, suggesting that VEGF dose-dependently regulated vessel development [62]. Another study showed that 3′ UTR deletion of the *VEGF* gene gave rise to increased stability of VEGF transcript and to modest increases in VEGF expression resulting in embryonic lethality due to abnormal heart development [53]. These studies imply that tight dosage regulation of VEGF is critical for vascular development. Thus, it is conceivable that MFps-mediated sensitization to VEGF, even though subtle and transient, might result in sufficient modulation of VEGF signaling to cause the defects in vascular development observed in fps^{MF} mice.

It has been difficult to establish what natural ligands are responsible for Fps activation, and many early reports focused on hematopoietic cytokines (reviewed in [15]). To our knowledge, there have been no previous reports of PDGF-induced activation of Fps in any cell system, although we and others have shown the related Fer protein is activated downstream of PDGF in fibroblasts [51,63]. Since we first described Fps expression in ECs [17,26] there have been a number of reports demonstrating activation of Fps by angiogenic growth factors, including FGF-2, stromal cell-derived growth factor-1α and VEGF [27,29,30]. In several of these cases, Fps expression correlated with enhanced growth factor-induced migration or tubule formation in ECs, and this effect appeared to require phosphatidyinositol 3 (PI3) kinase, but not MAP kinase activation. In similar studies with the pheochromocytoma cell line PC12, nerve growth factor-induced neurite outgrowth was enhanced by myristoylated Fps, and pharmacological inhibition experiments showed that this Fps effect was dependent upon PI3 kinase, but not MEK [64]. These observations suggest that Fps is acting upstream of PI3 kinase in ECs, and that activation of this enzyme is required for some downstream effects.

While we were unable to observe VEGF-induced activation of native Fps, we cannot rule out the possibility that Fps is also activated, albeit it with much less magnitude, compared with MFps. Indeed, others have provided some evidence that Fps can be activated by VEGF [30], and more recently compelling *in vivo* evidence was provided by experiments showing that MFps can partially substitute for VEGFR-2 deficiency during vascular development [31]. Coupled with the observations of

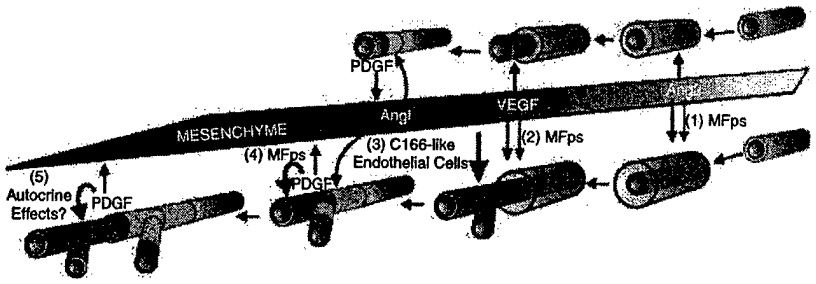

Fig. 9. Model of angiogenesis in *fps*^{MF} mice. MFps is proposed to alter angiogenesis at five points. For details refer to the main text. (Gray, endothelial tubes; textured gray, transformed endothelial tubes; light gray/white, mural coating). STEP 1, MFps promotes Ang2-mediated vessel destabilization in the genesis stages of angiogenesis. STEP 2, MFps promotes vascular endothelial growth factor-induced vessel sprouting and branching. STEP 3, Hyper-vessel sprouting and branching as a result of effects intrinsic to the properties of transformed-like endothelial cells in *fps*^{MF} mice. STEP 4, Hypersensitization of MFps to platelet-derived growth factor (PDGF) signaling alters normal output from this pathway resulting in pro-angiogenic effects. STEP 5, Abnormal PDGF autocrine signaling as a result of upregulation of PDGFR expression contributes to increased vessel sprouting and branching.

others, our data provide important new evidence which suggests that enhanced Fps activity might promote hypervascularity and irregular patterning through a mechanism involving amplification of VEGF signaling. This amplification may occur by increasing the local concentration of MFps near the plasma membrane, where receptor tyrosine kinase signal complexes are known to accumulate.

The physiological and molecular mechanisms underlying vasculogenesis and angiogenesis have been a subject of active interest given their therapeutic promise in heart disease and cancer. Recent genetic approaches have aided in the functional identification of numerous vasculogenic and angiogenic factors; however, the molecular mechanisms underlying these processes remain unclear. We provide here important new and supporting evidence to earlier studies [26–30] which suggested that the cytoplasmic tyrosine kinase Fps plays a significant role in vasculogenesis/angiogenesis. We further propose that enhanced activity of this kinase promotes vascular dysmorphogenesis through signaling networks regulated by VEGF and PDGF, and, as suggested by other studies, through Ang2 [1,2,28,65]. These experimental data are collectively represented in a working model of the effect of Fps on angiogenesis (Fig. 9). Current models of angiogenic remodeling propose that Ang2 mediates vessel destabilization which primes subsequent neoangiogenesis in the presence of VEGF (Fig. 9) [2]. Based on this observation, MFps might potentiate neoangiogenesis by promoting Ang2 destabilization of blood vessels (STEP 1, Fig. 9). In the presence of Ang2, VEGF promotes endothelial sprouting and branching [2]. MFps-mediated hypersensitization to VEGF signaling might result in modulation of this pathway, leading to increased kinetics and magnitude of vessel sprouting and branching (STEP 2, Fig. 9). This process might be exacerbated by the presence of transformed-like properties of ECs, as suggested by the ease of isolation of immortalized EC clones from *fps*^{MF} yolk sacs [35] (STEP 3, Fig. 9). Mouse models of Ang1/Tie2 and PDGF-B/PDGFRβ display defects in arteriogenesis associated with impaired pericyte recruitment [4,9–11,43]. It is thought that Ang1, secreted by surrounding mesenchymal cells, acts on ECs and induces PDGF secretion (Fig. 9) [4,66]. PDGF has been proposed to bind to PDGFRβ on undifferentiated perivascular mesenchymal cells and/or on pericytes/SMCs to induce pericyte generation and subsequent migration and proliferation of pericytes along nascent endothelial tubes (Fig. 9) [10]. In this context, an initial phase of endothelial PDGF autocrine signaling, followed by a switch to paracrine signaling, has also been previously proposed [6,67,68]. Our data are consistent with the existence of an initial phase of PDGF autocrine signaling and further suggest that an ultrasensitive response mediated by MFps could ensue during this phase. This activation might abnormally affect this phase of PDGF signaling since the activation of native Fps in response to this growth factor does not occur or is comparatively much lower. Hence, potentiation of PDGF autocrine signaling by MFps could act synergistically with effects on VEGF signaling to elevate endothelial proliferative and survival indices, resulting in increased kinetics of branching and sprouting (STEP 4; Fig. 9). Alternatively, it is possible that constitutive PDGFRβ activation or PDGF overexpression might be a property of the transformed endothelium in *fps*^{MF} mice. In this regard both PDGF and PDGFRβ overexpression have been shown to induce cell transformation [68–71]. Moreover, PDGFRβ has been shown to be highly expressed in the vasculature of gliomas but not normal brain, and it has been implicated in neovascularization of these tumors through autocrine mechanisms [70–73]. Thus, elevated PDGF autocrine signals might also promote endothelial hyperplasia, an effect that would be exacerbated by MFps-mediated ultrasensitivity to this growth factor (STEP 5; Fig. 9).

Lastly, we propose that *fps*^{MF} mice constitute a unique new model for angiogenesis, one that will enable elucidation of the VEGF- and PDGF-signaling events that regulate vascular remodeling. The uniqueness of this model is underscored by the lack of availability of appropriate animal models suitable for the study of VEGF and PDGF angiogenic mechanisms. In this regard, knockouts of VEGF, PDGF and their respective receptors are embryonic lethal, and VEGF transgenic mice have transgene-directed skin-specific vascular phenotypes. *fps*^{MF} mice, however, are relatively viable and are suitable for the study of both primitive and definitive vasculogenesis and angiogenesis in all tissues where Fps is expressed. In addition,

the process of arteriogenesis is an important aspect of angiogenic development and function; and in this respect, fps^{MF} mice might also constitute an important model for the study of this process. Therefore the fps^{MF} mouse model will be important for further exploring and delineating the biochemical and physiological pathways that regulate both angiogenesis and arteriogenesis, with respect to not only the role of Fps, but also key angiogenic and arteriogenic factors such as VEGF, PDGF, Angl and Ang2.

Acknowledgements

W.S. was supported by a fellowship award from the US Department of Defense Breast Cancer Research Program (Grant ID: BCRP–DAMD17-0110382). Recombinant FGF-2 was generously provided by the National Cancer Institute (Rockville, MD, USA). This study was funded by a grant from National Cancer Institute of Canada (Grant no. 012183), with funds from the Canadian Cancer Society.

References

1 Carmeliet P. Mechanisms of angiogenesis and arteriogenesis. *Nat Med* 2000; **6**: 389–95.
2 Yancopoulos GD, Davis S, Gale NW, Rudge JS, Wiegand SJ, Holash J. Vascular-specific growth factors and blood vessel formation. *Nature* 2000; **407**: 242–8.
3 Betsholtz C, Karlsson L, Lindahl P. Developmental roles of platelet-derived growth factors. *Bioessays* 2001; **23**: 494–507.
4 Folkman J, D'Amore PA. Blood vessel formation: what is its molecular basis? *Cell* 1996; **87**: 1153–5.
5 Davidson JM, Aquino AM, Woodward SC, Wilfinger WW. Sustained microgravity reduces intrinsic wound healing and growth factor responses in the rat. *FASEB J* 1999; **13**: 325–9.
6 Risau W, Drexler H, Mironov V, Smits A, Siegbahn A, Funa K, Heldin CH. Platelet-derived growth factor is angiogenic *in vivo*. *Growth Factors* 1992; **7**: 261–6.
7 Sano H, Sudo T, Yokode M, Murayama T, Kataoka H, Takakura N, Nishikawa S, Nishikawa SI, Kita T. Functional blockade of platelet-derived growth factor receptor-beta but not of receptor-alpha prevents vascular smooth muscle cell accumulation in fibrous cap lesions in apolipoprotein E-deficient mice. *Circulation* 2001; **103**: 2955–60.
8 Kim HR, Upadhyay S, Korsmeyer S, Deuel TF. Platelet-derived growth factor (PDGF) B and A homodimers transform murine fibroblasts depending on the genetic background of the cell. *J Biol Chem* 1994; **269**: 30604–8.
9 Hellstrom M, Gerhardt H, Kalen M, Li X, Eriksson U, Wolburg H, Betsholtz C. Lack of pericytes leads to endothelial hyperplasia and abnormal vascular morphogenesis. *J Cell Biol* 2001; **153**: 543–53.
10 Hellstrom M, Kalen M, Lindahl P, Abramsson A, Betsholtz C. Role of PDGF-B and PDGFR-beta in recruitment of vascular smooth muscle cells and pericytes during embryonic blood vessel formation in the mouse. *Development* 1999; **126**: 3047–55.
11 Lindahl P, Johansson BR, Leveen P, Betsholtz C. Pericyte loss and microaneurysm formation in PDGF-B-deficient mice. *Science* 1997; **277**: 242–5.
12 Leveen P, Pekny M, Gebre-Medhin S, Swolin B, Larsson E, Betsholtz C. Mice deficient for PDGF B show renal, cardiovascular, and hematological abnormalities. *Genes Dev* 1994; **8**: 1875–87.
13 Soriano P. Abnormal kidney development and hematological disorders in PDGF beta-receptor mutant mice. *Genes Dev* 1994; **8**: 1888–96.
14 Lindahl P, Hellstrom M, Kalen M, Karlsson L, Pekny M, Pekna M, Soriano P, Betsholtz C. Paracrine PDGF-B/PDGF-Rbeta signaling controls mesangial cell development in kidney glomeruli. *Development* 1998; **125**: 3313–22.
15 Greer PA. Closing in on the biological functions of Fps/Fes and Fer. *Nature Rev Mol Cell Biol* 2002; **3**: 278–89.
16 Aspenstrom P. A Cdc42 target protein with homology to the non-kinase domain of FER has a potential role in regulating the actin cytoskeleton. *Curr Biol* 1997; **7**: 479–87.
17 Haigh J, McVeigh J, Greer P. The fps/fes tyrosine kinase is expressed in myeloid, vascular endothelial, epithelial, and neuronal cells and is localized in the trans-golgi network. *Cell Growth Differ* 1996; **7**: 931–44.
18 Senis YA, Sangrar W, Zirngibl RA, Craig AWB, Lee DH, Greer PA. Fps/Fes and Fer nonreceptor protein-tyrosine kinases regulate collagen- and ADP-induced platelet aggregation. *J Thromb Haemost* 2003; **1**: 1062–70.
19 Hackenmiller R, Simon MC. Truncation of c-fes via gene targeting results in embryonic lethality and hyperproliferation of hematopoietic cells. *Dev Biol* 2002; **245**: 255–69.
20 Hackenmiller R, Kim J, Feldman RA, Simon MC. Abnormal Stat activation, hematopoietic homeostasis, and innate immunity in c-fes–/– mice. *Immunity* 2000; **13**: 397–407.
21 Senis Y, Zirngibl R, McVeigh J, Haman A, Hoang T, Greer PA. Targeted disruption of the murine fps/fes proto-oncogene reveals that Fps/Fes kinase activity is dispensable for hematopoiesis. *Mol Cell Biol* 1999; **19**: 7436–46.
22 Zirngibl RA, Senis Y, Greer PA. Enhanced endotoxin-sensitivity in Fps/Fes-null mice with minimal defects in hematopoietic homeostasis. *Mol Cell Biol* 2002; **22**: 2472–86.
23 Senis YA, Craig AWB, Greer PA. Fps/Fes and Fer protein-tyrosine kinases play redundant roles in regulating hematopoiesis. *Exp Hematol* 2003; **31**: 673–81.
24 Greer P, Maltby V, Rossant J, Bernstein A, Pawson T. Myeloid expression of the human c-fps/fes proto-oncogene in transgenic mice. *Mol Cell Biol* 1990; **10**: 2521–7.
25 Heydemann A, Warming S, Clendenin C, Sigrist K, Hjorth JP, Simon MC. A minimal c-fes cassette directs myeloid-specific expression in transgenic mice. *Blood* 2000; **96**: 3040–8.
26 Greer P, Haigh J, Mbamalu G, Khoo W, Bernstein A, Pawson T. The Fps/Fes protein-tyrosine kinase promotes angiogenesis in transgenic mice. *Mol Cell Biol* 1994; **14**: 6755–63.
27 Kanda S, Lerner EC, Tsuda S, Shono T, Kanetake H, Smithgall TE. The nonreceptor protein-tyrosine kinase c-Fes is involved in fibroblast growth factor-2-induced chemotaxis of murine brain capillary endothelial cells. *J Biol Chem* 2000; **275**: 10105–11.
28 Mochizuki Y, Nakamura T, Kanetake H, Kanda S. Angiopoietin 2 stimulates migration and tube-like structure formation of murine brain capillary endothelial cells through c-Fes and c-Fyn. *J Cell Sci* 2002; **115**: 175–83.
29 Kanda S, Mochizuki Y, Kanetake H. Stromal cell-derived factor-1alpha induces tube-like structure formation of endothelial cells through phosphoinositide 3-kinase. *J Biol Chem* 2003; **278**: 257–62.
30 Kanda S, Mochizuki Y, Miyata Y, Kanetake H. The role of c-Fes in vascular endothelial growth factor-A-mediated signaling by endothelial cells. *Biochem Biophys Res Commun* 2003; **306**: 1056–63.
31 Haigh J, Ema M, Haigh K, Gertsenstein M, Greer P, Rossant J, Nagy A, Wagner EF. Activated Fps/Fes can functionally substitute for Flk1 deficiency in vascular development *in vivo*. *Blood* 2004; **103**: 912–20.
32 McCafferty DM, Craig AW, Senis YA, Greer PA. Absence of Fer protein-tyrosine kinase exacerbates leukocyte recruitment in response to endotoxin. *J Immunol* 2002; **168**: 4930–5.
33 Laux V, Seiffge D. Mediator-induced changes in macromolecular permeability in the rat mesenteric microcirculation. *Microvasc Res* 1995; **49**: 117–33.

34 Levitt RC, Mitzner W. Expression of airway hyperreactivity to acetylcholine as a simple autosomal recessive trait in mice. *FASEB J* 1988; **2**: 2605–8.

35 Wang SJ, Greer P, Auerbach R. Isolation and propagation of yolk-sac-derived endothelial cells from a hypervascular transgenic mouse expressing a gain-of-function fps/fes proto-oncogene. *In Vitro Cell Dev Biol Anim* 1996; **32**: 292–9.

36 Craig AW, Greer PA. Fer kinase is required for sustained p38 kinase activation and maximal chemotaxis of activated mast cells. *Mol Cell Biol* 2002; **22**: 6363–74.

37 Margolis B, Rhee SG, Felder S, Mervic M, Lyall R, Levitzki A, Ullrich A, Zilberstein A, Schlessinger J. EGF induces tyrosine phosphorylation of phospholipase C-II: a potential mechanism for EGF receptor signaling. *Cell* 1989; **57**: 1101–7.

38 Detmar M, Brown LF, Schon MP, Elicker BM, Velasco P, Richard L, Fukumura D, Monsky W, Claffey KP, Jain RK. Increased microvascular density and enhanced leukocyte rolling and adhesion in the skin of VEGF transgenic mice. *J Invest Dermatol* 1998; **111**: 1–6.

39 Suri C, McClain J, Thurston G, McDonald DM, Zhou H, Oldmixon EH, Sato TN, Yancopoulos GD. Increased vascularization in mice overexpressing angiopoietin-1. *Science* 1998; **282**: 468–71.

40 Thurston G, Suri C, Smith K, McClain J, Sato TN, Yancopoulos GD, McDonald DM. Leakage-resistant blood vessels in mice transgenically overexpressing angiopoietin-1. *Science* 1999; **286**: 2511–4.

41 Thurston G, Rudge JS, Ioffe E, Zhou H, Ross L, Croll SD, Glazer N, Holash J, McDonald DM, Yancopoulos GD. Angiopoietin-1 protects the adult vasculature against plasma leakage. *Nat Med* 2000; **6**: 460–3.

42 Sato TN, Tozawa Y, Deutsch U, Wolburg-Buchholz K, Fujiwara Y, Gendron-Maguire M, Gridley T, Wolburg H, Risau W, Qin Y. Distinct roles of the receptor tyrosine kinases Tie-1 and Tie-2 in blood vessel formation. *Nature* 1995; **376**: 70–4.

43 Suri C, Jones PF, Patan S, Bartunkova S, Maisonpierre PC, Davis S, Sato TN, Yancopoulos GD. Requisite role of angiopoietin-1, a ligand for the TIE2 receptor, during embryonic angiogenesis. *Cell* 1996; **87**: 1171–80.

44 Andriopoulou P, Navarro P, Zanetti A, Lampugnani MG, Dejana E. Histamine induces tyrosine phosphorylation of endothelial cell-to-cell adherens junctions. *Arterioscler Thromb Vasc Biol* 1999; **19**: 2286–97.

45 Yee SP, Mock D, Maltby V, Silver M, Rossant J, Bernstein A, Pawson T. Cardiac and neurological abnormalities in v-fps transgenic mice. *Proc Natl Acad Sci USA* 1989; **86**: 5873–7.

46 Dhein S, van Koppen CJ, Brodde OE. Muscarinic receptors in the mammalian heart. *Pharmacol Res* 2001; **44**: 161–82.

47 Brodde OE, Michel MC. Adrenergic and muscarinic receptors in the human heart. *Pharmacol Rev* 1999; **51**: 651–90.

48 Cines DB, Pollak ES, Buck CA, Loscalzo J, Zimmerman GA, McEver RP, Pober JS, Wick TM, Konkle BA, Schwartz BS, Barnathan ES, McCrae KR, Hug BA, Schmidt AM, Stern DM. Endothelial cells in physiology and in the pathophysiology of vascular disorders. *Blood* 1998; **91**: 3527–61.

49 Ferrell JE Jr, Machleder EM. The biochemical basis of an all-or-none cell fate switch in Xenopus oocytes. *Science* 1998; **280**: 895–8.

50 Koshland DE Jr. The era of pathway quantification. *Science* 1998; **280**: 852–3.

51 Kim L, Wong TW. The cytoplasmic tyrosine kinase FER is associated with the catenin-like substrate pp120 and is activated by growth factors. *Mol Cell Biol* 1995; **15**: 4553–61.

52 Fong GH, Rossant J, Gertsenstein M, Breitman ML. Role of the Flt-1 receptor tyrosine kinase in regulating the assembly of vascular endothelium. *Nature* 1995; **376**: 66–70.

53 Miquerol L, Langille BL, Nagy A. Embryonic development is disrupted by modest increases in vascular endothelial growth factor gene expression. *Development* 2000; **127**: 3941–6.

54 Jones N, Voskas D, Master Z, Sarao R, Jones J, Dumont DJ. Rescue of the early vascular defects in Tek/Tie2 null mice reveals an essential survival function. *EMBO Rep* 2001; **2**: 438–45.

55 Hirschi KK, D'Amore PA. Pericytes in the microvasculature. *Cardiovasc Res* 1996; **32**: 687–98.

56 Lindahl P, Hellstrom M, Kalen M, Betsholtz C. Endothelial-perivascular cell signaling in vascular development: lessons from knockout mice. *Curr Opin Lipidol* 1998; **9**: 407–11.

57 Lindahl P, Bostrom H, Karlsson L, Hellstrom M, Kalen M, Betsholtz C. Role of platelet-derived growth factors in angiogenesis and alveogenesis. *Curr Top Pathol* 1999; **93**: 27–33.

58 Morikawa S, Baluk P, Kaidoh T, Haskell A, Jain RK, McDonald DM. Abnormalities in pericytes on blood vessels and endothelial sprouts in tumors. *Am J Pathol* 2002; **160**: 985–1000.

59 Esser S, Lampugnani MG, Corada M, Dejana E, Risau W. Vascular endothelial growth factor induces VE-cadherin tyrosine phosphorylation in endothelial cells. *J Cell Sci* 1998; **111**: 1853–65.

60 Arregui C, Pathre P, Lilien J, Balsamo J. The nonreceptor tyrosine kinase fer mediates cross-talk between N-cadherin and beta1-integrins. *J Cell Biol* 2000; **149**: 1263–74.

61 Piedra J, Miravet S, Castano J, Palmer HG, Heisterkamp N, Garcia de Herreros A, Dunach M. p120 Catenin-associated Fer and Fyn tyrosine kinases regulate beta-catenin Tyr-142 phosphorylation and beta-catenin–alpha-catenin interaction. *Mol Cell Biol* 2003; **23**: 2287–97.

62 Carmeliet P, Ferreira V, Breier G, Pollefeyt S, Kieckens L, Gertsenstein M, Fahrig M, Vandenhoeck A, Harpal K, Eberhardt C, Declercq C, Pawling J, Moons L, Collen D, Risau W, Nagy A. Abnormal blood vessel development and lethality in embryos lacking a single VEGF allele. *Nature* 1996; **380**: 435–9.

63 Craig AW, Zirngibl R, Williams K, Cole LA, Greer PA. Mice devoid of fer protein-tyrosine kinase activity are viable and fertile but display reduced cortactin phosphorylation. *Mol Cell Biol* 2001; **21**: 603–13.

64 Shibata A, Laurent CE, Smithgall TE. The c-Fes protein-tyrosine kinase accelerates NGF-induced differentiation of PC12 cells through a PI3K-dependent mechanism. *Cell Signal* 2003; **15**: 279–88.

65 Carmeliet P. Developmental biology. One cell, two fates. *Nature* 2000; **408**: 5.

66 Moyon D, Pardanaud L, Yuan L, Breant C, Eichmann A. Selective expression of angiopoietin 1 and 2 in mesenchymal cells surrounding veins and arteries of the avian embryo. *Mech Dev* 2001; **106**: 133–6.

67 Holmgren L, Glaser A, Pfeifer-Ohlsson S, Ohlsson R. Angiogenesis during human extraembryonic development involves the spatiotemporal control of PDGF ligand and receptor gene expression. *Development* 1991; **113**: 749–54.

68 Hermanson M, Funa K, Hartman M, Claesson-Welsh L, Heldin CH, Westermark B, Nister M. Platelet-derived growth factor and its receptors in human glioma tissue: expression of messenger RNA and protein suggests the presence of autocrine and paracrine loops. *Cancer Res* 1992; **52**: 3213–9.

69 Heldin CH, Westermark B. Mechanism of action and *in vivo* role of platelet-derived growth factor. *Physiol Rev* 1999; **79**: 1283–316.

70 Kolibaba KS, Druker BJ. Protein tyrosine kinases and cancer. *Biochim Biophys Acta* 1997; **1333**: F217–48.

71 Fleming TP, Saxena A, Clark WC, Robertson JT, Oldfield EH, Aaronson SA, Ali IU. Amplification and/or overexpression of platelet-derived growth factor receptors and epidermal growth factor receptor in human glial tumors. *Cancer Res* 1992; **52**: 4550–3.

72 Fleming TP, Matsui T, Aaronson SA. Platelet-derived growth factor (PDGF) receptor activation in cell transformation and human malignancy. *Exp Gerontol* 1992; **27**: 523–32.

73 Leon SP, Zhu J, Black PM. Genetic aberrations in human brain tumors. *Neurosurgery* 1994; **34**: 708–22.

74 Weinmaster G, Zoller MJ, Smith M, Hinze E, Pawson T. Mutagenesis of Fujinami sarcoma virus: evidence that tyrosine phosphorylation of P130gag-fps modulates its biological activity. *Cell* 1984; **37**: 559–68.

ELSEVIER

EXPERIMENTAL HEMATOLOGY

Experimental Hematology 31 (2003) 1259–1267

The *fps/fes* proto-oncogene regulates hematopoietic lineage output

Waheed Sangrar[a], Yan Gao[a], Ralph A. Zirngibl[a,b], Michelle L. Scott[a,b], and Peter A. Greer[a,c]

[a]*Division of Cancer Biology and Genetics, Queen's University Cancer Research Institute, Kingston, Ontario, Canada; Department of* [b]*Biochemistry and* [c]*Pathology, Queen's University, Kingston, Ontario, Canada*

(Received 16 June 2003; revised 26 August 2003; accepted 4 September 2003)

Objective. **The *fps/fes* proto-oncogene is abundantly expressed in myeloid cells, and the Fps/Fes cytoplasmic protein-tyrosine kinase is implicated in signaling downstream from hematopoietic cytokines, including interleukin-3 (IL-3), granulocyte-macrophage colony-stimulating factor (GM-CSF), and erythropoietin (EPO). Studies using leukemic cell lines have previously suggested that Fps/Fes contributes to granulomonocytic differentiation, and that it might play a more selective role in promoting survival and differentiation along the monocytic pathway. In this study we have used a genetic approach to explore the role of Fps/Fes in hematopoiesis.**

Methods. **We used transgenic mice that tissue-specifically express a mutant human *fps/fes* transgene (fps^{MF}) that was engineered to encode Fps/Fes kinase that is activated through N-terminal myristoylation (MFps). Hematopoietic function was assessed using lineage analysis, hematopoietic progenitor cell colony-forming assays, and biochemical approaches.**

Results. **fps^{MF} transgenic mice displayed a skewed hematopoietic output reflected by increased numbers of circulating granulocytic and monocytic cells and a corresponding decrease in lymphoid cells. Bone marrow colony assays of progenitor cells revealed a significant increase in the number of both granulomonocytic and multi-lineage progenitors. A molecular analysis of signaling in mature monocytic cells showed that MFps promoted GM-CSF-induced STAT3, STAT5, and ERK1/2 activation.**

Conclusions. **These observations support a role for Fps/Fes in signaling pathways that contribute to lineage determination at the level of multi-lineage hematopoietic progenitors as well as the more committed granulomonocytic progenitors.** © **2003 International Society for Experimental Hematology. Published by Elsevier Inc.**

The *fps/fes* proto-oncogene (hereafter called *fps*) encodes a cytoplasmic protein-tyrosine kinase that is abundantly expressed in cells of the hematopoietic lineage [1]. Although the precise molecular role for the Fps kinase is not understood, it has been implicated in signaling downstream from a number of hematopoietic cytokines including interleukin (IL)-3 [2], IL-4 [3,4], granulocyte-macrophage colony-stimulating factor (GM-CSF) [2,5], erythropoietin (EPO) [6,7], and IL-6 [8]. In some cases, a link to PI3′ kinase and cell survival has been made [3,4], and in other studies a connection with activation of signal transducers and activators of transcription (STATs) has been demonstrated [5,6,9–11] which would have implications in both survival and differentiation.

In early studies of *fps*, forced expression in the K562 human erythroleukemic cell line correlated with myeloid differentiation potential [12], and anti-sense blocking experiments suggested that Fps protects human leukemic HL60 or fresh acute promyelocytic leukemia blast cells from programmed cell death during induced granulocytic, but not monocytic, differentiation [13,14]. Transduction of the human bipotential promonocytic leukemic cell line U937 with retrovirus encoding an activated form of Fps was shown to drive differentiation down the monocytic pathway [15]. Interestingly, this appeared to occur at the expense of granulocytic differentiation, and it correlated with enhanced activity of the *ets* family transcriptional regulator, PU.1 [15]. More recently, the same activated Fps-encoding retrovirus promoted survival and granulocytic differentiation of the IL-3-dependent 32D cell line, and this correlated with activation of the transcription factors C/EBPα and STAT3 [16]. These observations suggested that Fps might participate in lineage-determining signaling pathways involving PU.1, C/EBPα, and STAT3 that govern the survival and differentiation of granulomonocytic progenitors.

Offprint requests to: Peter A. Greer, Ph.D., Department of Pathology, Division of Cancer Biology and Genetics, Cancer Research Institute, Botterell Hall, Room A309, Queen's University, Kingston, Ontario, K7L 3N6, Canada; E-mail: greerp@post.queensu.ca

0301-472X/03 $–see front matter.
doi: 10.1016/j.exphem.2003.09.013

Cell culture–based experiments like those described above suggested that loss of *fps* would seriously compromise in vivo myelopoiesis. This hypothesis has recently been addressed by gene targeting in transgenic mice. A mouse knockin mutation that abolished Fps kinase activity without compromising its expression resulted in only a mild defect in cytokine-induced STAT activation in myeloid cells, and there were no substantial defects in myelopoiesis in these $fps^{KR/KR}$ mice [11]. Surprisingly different phenotypes have since been reported in mouse strains targeted with null mutations. In one case enhanced myelopoiesis was reported in *fps*-null mice; and this correlated with increased GM-CSF and IL-6-induced STAT3 and STAT5 activation in cultured myeloid cells [17]. This prompted an interesting model where Fps was hypothesized to compete with Jak2 kinase for access to STAT 3 or STAT5 [17]. However, an independently generated *fps*-null mouse strain displayed no obvious defect in cytokine-induced STAT3 or STAT5 activation [18]. Furthermore, a decrease in circulating granulocytes and monocytes from this second reported $fps^{-/-}$ mouse strain was observed, and this phenotype was corrected by a *fps* transgene in $fps^{-/-;Tg}$ mice [18]. These observations were consistent with the phenotypes observed earlier in $fps^{KR/KR}$ mice, and in the earlier cell culture experiments. Furthermore, they supported the hypothesis that Fps does participate in myelopoiesis, but that its function might be partially redundant with other kinases, such as members of the Jak, Src, or Syk families, or perhaps the Fps-related Fer kinase. It follows that while myelopoiesis might not be seriously compromised in Fps-deficient mice, it might be enhanced in mice expressing an activated Fps kinase.

We have now examined myelopoiesis in a strain of transgenic mice that were engineered to express an activated "gain-of-function" mutant Fps kinase (MFps) in a tissue-specific fashion [19]. The addition of five amino acids immediately after the amino-terminal glycine in Fps created a minimal Src-like myristoylation consensus sequence. This MFps protein was efficiently myristoylated and displayed enhanced kinase and transforming activity in rat fibroblasts [19]. The complete human *fps* locus including this mutation was used as a transgene to generate fps^{MF} transgenic mice which tissue-specifically expressed the active MFps kinase [19]. Analysis of transgene-derived transcripts and Fps protein in a range of tissues from two independent fps^{MF} mouse lines and seven independently generated lines expressing a wild-type version of this *fps* transgene demonstrated that the human genomic DNA fragment used as a transgene included the endogenous *fps* promoter as well as a locus control element capable of protecting the transgene from position effects. An independent study has since mapped a locus control element with the 5′ region of the *fps/fes* gene [20].

In the present study, we show that in vivo expression of activated MFps correlated with a skewing of hematopoiesis, manifested by increased granulomonocytic output and a corresponding decrease in lymphoid cells. Increased numbers of granulomonocytic precursors were detected in the bone marrow using flow cytometry–based lineage analysis and progenitor colony assays. Interestingly, there was also evidence of decreased B cell progenitors in the bone marrow and a block in T-cell maturation. Bone marrow–derived monocytes from fps^{MF} mice displayed enhanced GM-CSF-induced activation of STAT3, STAT5, and ERK. Based upon these observations, we propose a molecular model for Fps involvement in cytokine signaling which is consistent with phenotypes seen in all of our transgenic mouse strains. Furthermore, we propose a role for Fps in regulating lineage determination by multi-potential hematopoietic progenitors.

Experimental procedures

Mice

Derivation of fps^{MF} transgenic mice expressing myristoylated MFps were previously described [19]. The fps^{MF} line is maintained in an out-bred CD-1 background and is housed at the Animal Care Facility at Queen's University, Kingston, Ontario, Canada. All protocols involving animals were approved by the institutional animal care committee in accordance with the guidelines of the Canadian Council on Animal Care.

Peripheral white blood cell analysis

Whole blood was acquired by cardiac puncture as previously described [18].

Flow cytometry

Bone marrow (from femur), spleen, and thymi were obtained from *wt* and fps^{MF} mice and single cell suspensions were prepared for flow cytometry as previously described [11,18]. Cells were incubated with either phycoerythrin (PE)- or fluorescein isothiocyanate (FITC)-conjugated monoclonal antibodies (Pharmingen, Mississauga, ON, Canada unless otherwise specified). Bone marrow cells and splenocytes were incubated with either PE-Ly6G and FITC-CD11b or PE-CD45R/B220 and FITC-IgM (Serotec, Raleigh, NC, USA). Splenocytes were also incubated with PE-CD8 (Leinco Technologies, Inc., St. Louis, MO, USA) and FITC-CD4 (Leinco Technologies, Inc).

Cell colony assays

Methylcellulose progenitor assays were performed as previously described [11]. Methylcellulose was supplemented with two different cocktails of recombinant cytokines (R& D Systems, Minneapolis, MN, USA): One cocktail consisted of 50 ng/mL Steel factor (SF), 5 ng/mL IL-3, 10 ng/mL IL-6, 10 ng/mL thrombopoietin (TPO), 1 U/mL EPO, and 5 ng/mL GM-CSF and the second cocktail consisted of 1 U/mL EPO and 5 ng/mL GM-CSF.

GM-CSF stimulation of bone marrow cultures

Bone marrow–derived macrophages were prepared, cultured, and stimulated with recombinant cytokine as previously described [11]. Stimulations were carried out with 25 ng/mL recombinant GM-CSF (0–30 minutes) (R&D Systems) and soluble cell lysates were prepared for subsequent immunoblotting analysis [11]. Lysates were quantified using a BioRad protein assay kit (BioRad, Hercules, CA, USA) and equal masses of total protein were utilized for Western blotting analyses. Blots were probed with the following antibodies according to manufacturer instructions: Fps/Fer (FpsQE) [21], phospho-(p)STAT3, STAT3, pSTAT5A/B, STAT5A, pJAK2, JAK2, and ERK1/2 (all from Upstate Biotechnology, Charlottesville, VA, USA); pp38, pAKT, and AKT (all from Cell Signaling Technologies, Beverly, MA, USA); and p38, pERK1/2, and pTyr (clone PY99) mAb (all from Santa Cruz Biotechnologies, Santa Cruz, CA, USA). In some instances, SDS-PAGE gels were directly stained with Sypro Ruby Protein fluorescent gel stain (Molecular Probes, Eugene, OR, USA) in order to confirm equal loading of total protein.

Statistical analysis

Student's *t*-tests and means were determined using Microsoft Excel (Microsoft, Mississisauga, ON, Canada) and GraphPad Prism statistical analysis software (GraphPad Software Inc, San Diego, CA, USA). *t*-test analyses of data sets with *p*-values less than or equal to 0.05 were considered statistically significant. Where appropriate, data are expressed as mean ± SEM.

Results

Elevated levels of circulating monocytes and granulocytes in fps^{MF} mice

Fps is highly expressed in myeloid cells and has been implicated in terminal differentiation and survival of myeloid progenitors, suggesting that perturbations in the function of this kinase might affect hematopoietic output. Consistent with this hypothesis, peripheral blood white cell differentials were markedly abnormal in the fps^{MF} transgenic mice. This was reflected by elevations in percentages and absolute levels of circulating neutrophils, monocytes, and basophils and, in contrast, by decreased lymphocytes (Table 1). Indeed, the percentage decrease in lymphocytes closely corresponded to the increase in the percentage of granulomonocytic cells. Perturbations of this extent were not observed in a transgenic line overexpressing a wild-type human *fps* transgene Fps [18] suggesting that the abnormal white blood cell outputs in fps^{MF} mice were not due to Fps overexpression, but were linked to expression of the activated MFps kinase. Interestingly, fps^{MF} mice also displayed decreases in erythroid output (Table 1) and the opposite was observed in $fps^{-/-}$ mice [18]. Taken together, these observations suggested that expression of MFps might skew hematopoietic output toward the granulomonocytic lineage at the expense of both the erythroid and lymphoid lineages. This would be consistent with a contributing role for Fps in the regulation of hematopoietic lineage determination by committed multipotential hematopoietic progenitor cells.

Table 1. Peripheral blood analysis

White Blood Cells	*wild-type (n)*	fps^{MF} *(n/p-value)*
White Blood Cells (10^9/L)	7.0 ± 0.4 (28)	7.5 ± 0.7 (22/0.5)
Neutrophils (10^9/L)	1.3 ± 0.1 (27)	**1.7 ± 0.2** (21/0.02)
Neutrophils (%)	17.6 ± 1.2 (27)	**24.7 ± 1.8** (21/<0.001)
Lymphocytes (10^9/L)	5.6 ± 0.3 (27)	5.3 ± 0.5 (21/0.6)
Lymphocytes (%)	80.9 ± 1.1 (27)	**72.7 ± 0.2** (22/<0.001)
Monocytes (10^6/L)	47.6 ± 8.7 (28)	**152.4 ± 15.3** (21/<10^{-7})
Monocytes (%)	0.7 ± 0.1 (28)	**2.4 ± 0.3** (21/<10^{-6})
Basophils (10^6/L)	6.4 ± 0.9 (28)	**16.7 ± 1.9** (21/<10^{-5})
Basophils (%)	0.09 ± 0.01 (28)	**0.26 ± 0.04** (21/0.02)
Eosinophils (10^6/L)	undetectable (28)	undetectable (21/—)
Red Blood Cells (10^{12}/L)	9.1 ± 0.1 (28)	**7.8 ± 0.1** (22/<10^{-10})

Blood was acquired from *wild-type* (4.5 ± 0.2 mo.) and fps^{MF} (4.3 ± 0.2 mo.) mice by cardiac puncture. Peripheral blood was analyzed using a SYSMEX XE-2100 automated hematological analyzer. Data are presented as mean ± standard error of the mean (S.E.M.) along with *p*-values (*p*) and the number of animals used in the analyses (*n*). Statistically significant parameters are bolded.

Perturbations in undifferentiated myeloid progenitors and mature B cells in fps^{MF} mice

Lineage analyses of bone marrow cells from $fps^{-/-}$ mice had previously shown a statistically significant reduction in Ly-6G$^+$/CD11b$^+$ granulomonocytic cells, and this was rescued by a human *fps* transgene [18]. This was consistent with a positive role for Fps in maturation of granulomonocytic cells in the bone marrow, and suggested that activated Fps might therefore enhance granulomonocytic output. While fps^{MF} mice did not display the expected increase in Ly-6G$^+$/CD11b$^+$ bone marrow cells, there was a statistically significant increase in presumptive granulomonocytic progenitor Ly-6G$^-$/CD11b$^+$ cells in both bone marrow and spleen (Figs. 1 and 2). These observations correlated with the peripheral blood data depicting increased granulocyte and monocyte output (Table 1). We also observed statistically significant decreases in mature B cell populations (B220$^+$IgM$^+$) in the bone marrow of fps^{MF} mice (Fig. 1); this correlated with the reduced output of lymphocytes in the periphery (Table 1). However, no differences were observed in mature B cell levels in the spleens of fps^{MF} mice (Fig. 2).

Increases in bone marrow CFU-GM and CFU-GEMM colonies in fps^{MF} mice

In order to confirm that increases in granulomonocytic output are a result of abnormal hematopoiesis, we performed methylcellulose colony assays to assess the number of bone marrow progenitor cells in *wt* and fps^{MF} mice. These assays were performed using either a cocktail of hematopoietic factors (condition A: Scf, GM-CSF, EPO, TPO, IL-6, IL-3), or a more restricted condition (condition B: EPO and

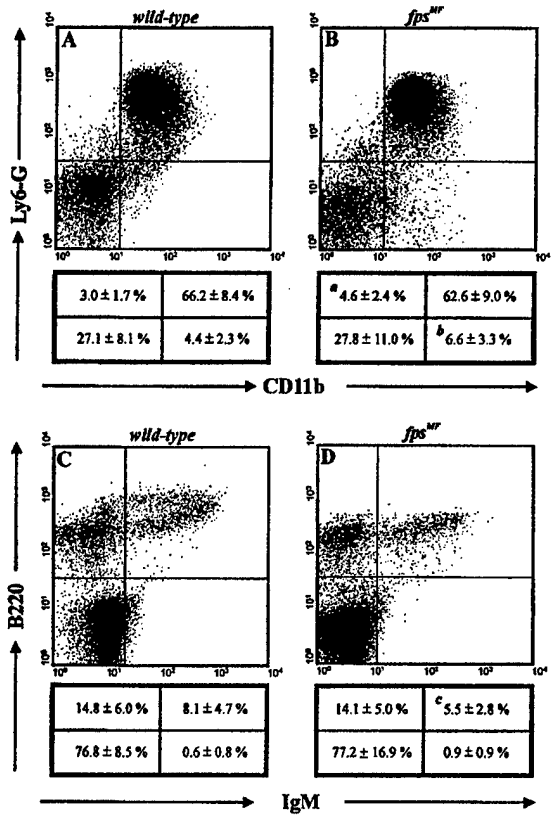

Figure 1. Flow cytometry analysis of myeloid and B cell precursors in bone marrow. **(A,B)**: Bone marrow from *wt* (age = 2.9 mo ± 0.2 mo, n = 24) and fps^{MF} mice (age = 2.9 mo ± 0.2 mo, n = 22) was analyzed for levels of myeloid progenitors using markers for Ly6-G and CD11b. Statistically significant increases were present in undifferentiated granulocyte and monocyte progenitor populations (*a*; $p = 0.015$ and *b*; $p = 0.024$). **(C,D)**: Analysis of B cell precursors using markers for B220 and IgM revealed a statistically significant decrease in immature B cell levels in fps^{MF} mice (age = 2.9 mo ± 0.2 mo, n = 23, *c*; $p = 0.02$) compared to *wt* mice (age = 2.9 mo ± 0.2 mo, n = 25).

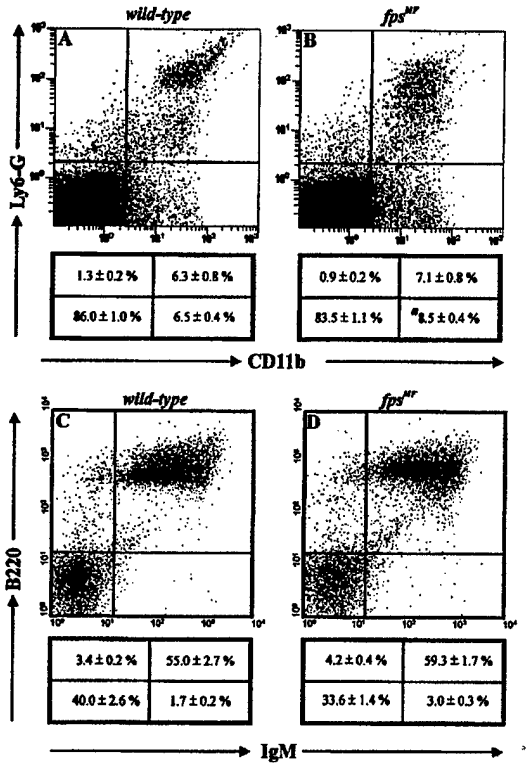

Figure 2. Flow cytometry analysis of myeloid and B cell precursors in spleen. **(A,B)**: Levels of myeloid precursors in spleen suspensions from *wt* (age = 2.8 mo ± 0.04 mo, n = 8) and fps^{MF} (age = 2.8 mo ± 0.04 mo, n = 8) were determined using markers for Ly6-G and CD11b. The data show a statistically significant increase in single-positive CD11b undifferentiated progenitor populations in fps^{MF} mice (*a*: $p = 0.003$). **(C,D)**: Immature B cell levels in spleens of *wt* (age = 3.7 mo ± 0.4 mo, n = 9) and fps^{MF} (age = 3.7 mo ± 0.2 mo, n = 13) mice were assessed using markers for B220 and IgM. The data indicate that splenic B cell precursor population levels are normal in fps^{MF} transgenic mice.

GM-CSF). In condition A, fps^{MF} CFU-GM colonies were increased 1.8-fold ($p = 0.014$) relative to *wt*, while the numbers of other mixed colonies were normal (Fig. 3A). A comparable fold increase of CFU-GM colonies was observed in the more limited cytokine condition B (1.5-fold increase; $p = 0.069$) (Fig. 3B). We also observed a 1.9-fold increase ($p = 0.0281$) in CFU-GEMM mixed colonies in condition B, but the numbers of CFU-GEMM colonies were the same in condition A. These results indicated a selectively enhanced GM-CSF responsiveness of fps^{MF} multi-lineage progenitors cells.

Evidence for T-cell maturation defects in fps^{MF} mice

Splenocytes from transgene-rescued Fps-null mice ($fps^{-/-:Tg}$), which overexpress wild-type Fps, were previously shown to have slight decreases in the CD4 and CD8 single-positive populations [18]. This led us to examine these populations in the spleens and thymi of fps^{MF} mice. Statistically significant decreases of both $CD4^+CD8^-$ and $CD4^-CD8^+$ cells were apparent in the spleen of fps^{MF} mice (Fig. 4C and D). Statistically significant increases in $CD4^+CD8^-$ populations were seen the thymi of fps^{MF} mice (Fig. 4A and B). These data were consistent with the observed decreases of lymphocytes in the periphery in fps^{MF} mice, and suggested a role for Fps in regulating the development and/or maturation of T cells.

Enhanced cytokine-induced STAT3, STAT5, and ERK activation in fps^{MF} macrophages

Given the apparent evidence for enhanced myelopoiesis in fps^{MF} mice, we next examined expression of Fps and MFps in bone marrow–derived macrophages, and cytokine-induced activation of Jak2 kinase, STAT3/5, ERK1/2, and other signaling proteins. Western blotting analysis confirmed that MFps is overexpressed in macrophages from fps^{MF} mice relative to endogenous Fps (Fig. 5A). The relative

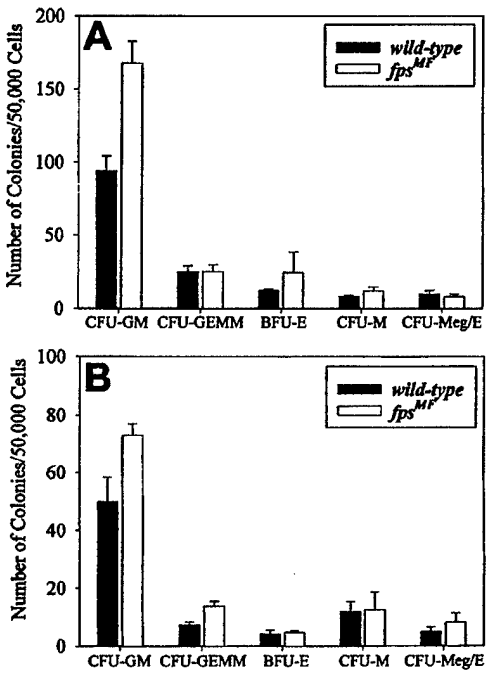

Figure 3. Colony-forming unit assay. Bone marrow from *wt* and fps^{MF} siblings was grown in methylcellulose media containing two different cocktails of recombinant cytokines. **(A)**: 50 ng/mL SCF, 5 ng/mL IL-3, 10 ng/mL IL-6, 10 ng/mL TPO. **(B)**: 1 U/mL EPO and 5 ng/mL GM-CSF. Colonies were counted 8 days postplating and data are expressed as mean ± SEM. The results of three separate experiments indicate increases in the number of CFU-GM colonies with either cocktail in fps^{MF} mice ($p = 0.014$ and $p = 0.069$ respectively). We also observed an increase in CFU-GEMM colonies in fps^{MF} mice with EPO and GM-CSF ($p = 0.0281$).

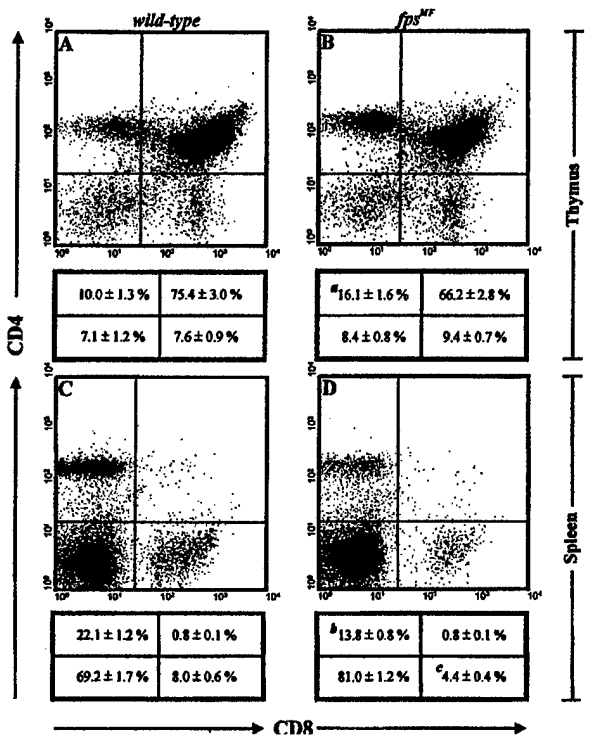

Figure 4. T-cell maturation defects in secondary lymphoid organs of fps^{MF} mice. Flow analysis using markers for CD4 and CD8 were utilized to assess T cell populations in the thymus and spleen. **(A,B)**: Increased levels of $CD4^+/CD8^-$ T cell populations were observed in the thymus of fps^{MF} mice (3.7 mo ± 0.1 mo, n = 16, *a*; $p < 0.006$) relative to *wt* mice (age = 3.8 mo ± 0.2 mo, n = 12). **(C,D)**: $CD4^+/CD8^-$ and $CD4^-/CD8^+$ populations in spleen were reduced in fps^{MF} mice (age = 3.7 mo ± 0.2 mo, n = 16, *b*; $p < 0.006$, *c*; $p < 10^{-4}$) in comparison to *wt* mice (age = 3.7 mo ± 0.2 mo, n = 12).

levels of MFps and Fps in macrophage cultures was consistent with the previously characterized tissue-specific expression of the fps^{MF} transgene, and the estimated 10 transgene copies relative to two endogenous *fps* alleles [19]. The fatty acid modification resulted in MFps migrating between p94Fer and p92Fps (Fig. 5A).

An examination of signaling in bone marrow macrophages from fps^{MF} mice revealed increased STAT3 and STAT5A/B phosphorylation in response to GM-CSF (Fig. 5A). Although the degree of enhanced STAT activation was not dramatic, this was consistently observed in three independent experiments. A quantitative representation of the representative data shown is provided in Figure 5B. These results suggested a positive effect of Fps on STAT signaling downstream of GM-CSF and further suggested that MFps promoted a higher degree of STAT activation. Equal loading was confirmed using antibodies specific for Fps/Fer, STAT3, STAT5A/B, and total protein levels (Fig. 5A). Interestingly, there were no differences in the kinetics of activation of JAK2 between *wt* and fps^{MF} mice, suggesting that Fps affected STAT signaling in a JAK2-independent fashion.

Since the degree of enhanced STAT activation in fps^{MF} macrophages was modest, we also examined the kinetics of GM-CSF-induced activation of several other downstream effectors (Fig. 6A). We were unable to observe significant quantitative differences in the kinetics of activation of p38, AKT, and JNK (Fig. 6 and data not shown). However, we frequently observed increases in the kinetics of ERK1/2 activation (Fig. 6).

Discussion

Although *fps* and *fes* were first identified as retroviral oncogenes capable of causing sarcomas in chickens and cats, respectively, an involvement of the cellular *fps/fes* proto-oncogene in malignancy has not yet been determined. Mutations in *fps/fes* have recently been reported in human colon carcinoma [22]; however, the involvement of these in disease progression was not explored. The oncogenic potential of *fps/fes* was explored in an early transgenic mouse model by expressing a retroviral Gag-Fps protein under the control of

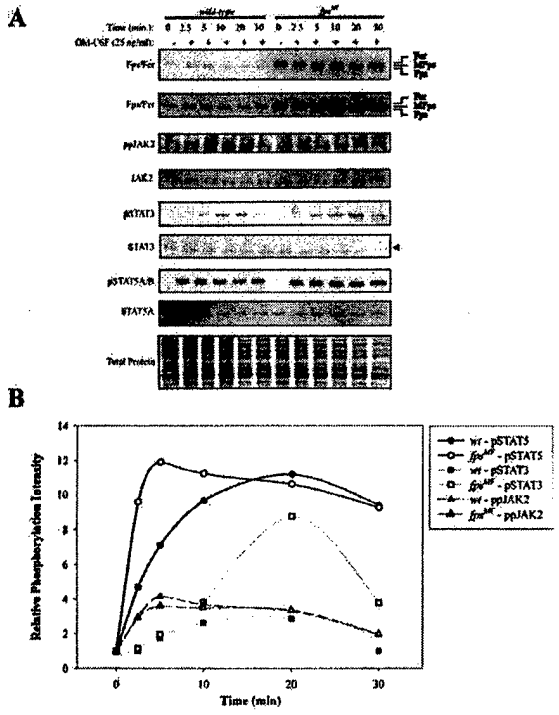

Figure 5. Enhanced STAT3/5 phosphorylation in *fps*^{MF} *macrophages.* **(A):** Bone marrow–derived macrophages were stimulated with GM-CSF for 0–25 minutes, lysed, and analyzed with phospho-specific antibodies to JAK2, STAT3, and STAT5. Antibodies to the latter proteins and to Fps and Fer were also used to assess mass levels of the respective proteins during the time course of the stimulation. Total protein content was measured by Sypro Ruby Protein fluorescent gel stain in order to confirm loading in each lane. The upper two panels represent the same blot at low and high exposures and depict the migration profiles of Fer, MFps, and Fps. The data in the panels below show that JAK2 activation is unaffected and that STAT3/5 activation is enhanced in response to GM-CSF in *fps*^{MF} mice. **(B):** Densitometry was used to generate quantitative analysis of the data shown in panel A.

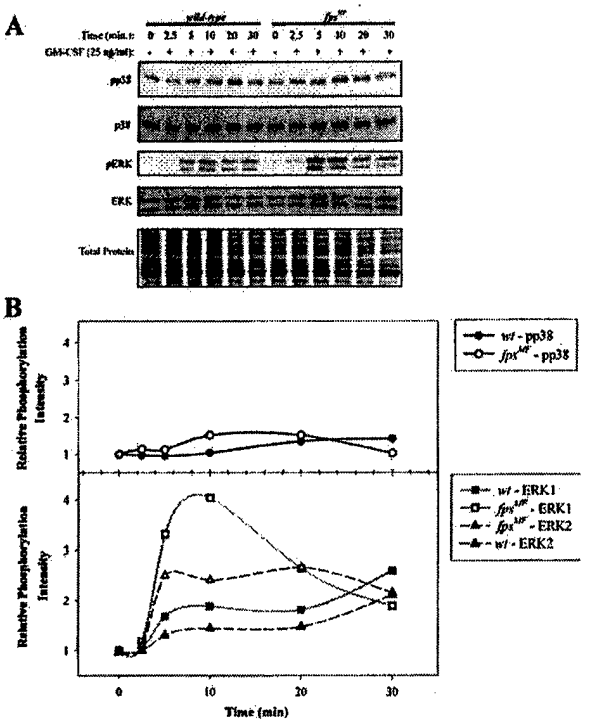

Figure 6. Effect of *fps*^{MF} on downstream effectors of GM-CSF signaling. **(A):** Activation of the downstream signaling proteins p38 and pErk were assessed using phospho-specific antibodies. Mass levels were also assessed by corresponding control antibodies, and equal loading was confirmed by Sypro Ruby Protein fluorescent gel staining of total protein. The data show increased kinetics of Erk activation in response to GM-CSF. No significant differences were observed in the kinetics of activation of p38 and of Akt and Jnk (data not shown). **(B):** Densitometry was used to generate quantitative analysis of the data shown in panel A.

a minimal β-globin promoter [23,24]. These mice developed a range of tumors that were likely determined in large part by the tissue distribution of transgene expression achieved in the specific founder lines. The complete human *fps* locus was next used to generate transgenic mice with tissue-specific overexpression of Fps [25]. The expected high level of myeloid transgene expression was achieved, but no myeloid leukemia or other malignancies were observed, and no hematopoietic defects were observed.

Retroviral Gag is thought to contribute to activation of Fps by enhancing oligomerization and association with the membrane, and cellular Fps is thought to contribute to cytokine receptor signaling, perhaps through phosphorylation of the receptors or associated signaling molecules. We therefore attempted to generate a weaker gain-of-function mutant *fps* allele by introducing coding sequences for amino terminal myristoylation into the context of a genomic *fps* transgene [19]. Our rationale was that myristoylated Fps (MFps) would associate constitutively with lipid bilayers, thereby enhancing interactions with integral membrane proteins, including cytokine receptors. We reasoned that this might lead to Fps-mediated phosphorylation and activation of cytokine receptors or downstream effectors in the presence of subthreshold levels of ligands. Transgenic mice expressing this *fps*^{MF} allele were generated and shown to overexpress MFps in a tissue-specific fashion [19]. The *fps*^{MF} mice have a number of interesting phenotypes that have helped to uncover previously unsuspected biological roles for Fps in the regulation of angiogenesis [19] and thrombosis [18]. However, although a high level of MFps expression was observed in the myeloid lineages, we did not observe any myeloid leukemias in these animals. We now report a hematopoietic phenotype in *fps*^{MF} mice that implicates Fps in the regulation of hematopoietic lineage determination by multi-potential progenitor cells, a role which might extend to the pluripotential hematopoietic stem cell.

Previous studies using cultured human leukemic cell lines that retain the ability to differentiate have suggested that

Fps might preferentially drive hematopoietic commitment along the monocytic lineage [15], and that it might be essential for survival during monocytic, but not granulocytic, differentiation [13,14]. A more recent study using the factor-dependent 32D myeloid leukemic cell line suggested that activated Fps can also promote survival and granulocytic differentiation [16]. Analysis of peripheral blood cell composition provided initial evidence for enhanced myeloid output in the fps^{MF} mice (Table 1). This also pointed to a role for Fps in myelopoiesis, but it did not support a more selective monocytic role, because statistically significant increases were seen in circulating neutrophils, basophils, and monocytes. Furthermore, this effect on myeloid cell output was underscored by the apparent increase in total circulating white blood cells, even though lymphocytes, which represent the majority of circulating white blood cells, were actually decreased by approximately 10% in the fps^{MF} mice. This suggested that Fps might be exerting an affect higher up in the hematopoietic differentiation hierarchy.

In order to determine the level in the hematopoietic differentiation hierarchy where MFps was acting to cause this apparent skewing in lineage output, we next attempted to trace these differences back to hematopoietic tissues. Lineage analysis of bone marrow cells revealed statistically significant increases in the presumptive granulomonocytic progenitor pools (Ly6-G$^-$CD11b$^+$) in the bone marrow (Fig. 1); a similar increase in this population was noted in the spleen (Fig. 2). Mature B cell levels were also reduced in the bone marrow (Fig. 1). These observations are consistent with the hypothesis that Fps was acting on an earlier multipotential progenitor and driving its differentiation toward the myeloid lineages at the expense of the lymphoid lineages. Further analysis using progenitor cell colony assays clearly demonstrated an increase in CFU-GM granulomonocytic progenitor cells in the bone marrow (Fig. 3); interestingly, multi-lineage CFU-GEMM colonies were also significantly higher in response to GM-CSF plus EPO, but not to a more extensive cytokine cocktail (SCF, GM-CSF, EPO, TPO, IL-6, IL-3). The number of CFU-M was not significantly higher in either cytokine condition. These observations suggested that activated Fps was promoting an increase in granulomonocytic progenitors in the bone marrow. However, they did not indicate that this effect extended to more committed monocytic progenitors.

Our observations support the hypothesis that MFps promotes the expansion of multi-lineage progenitors as well as bipotential granulomonocytic progenitors in the bone marrow, but that this effect does not extend to the more committed myelomonocytic progenitors. This would suggest that Fps is expressed in multi-lineage progenitors, and perhaps even in hematopoietic stem cells. In support of this, a *fps*-directed Cre transgene achieved deletion of a loxP flanked PIGA gene in all hematopoietic lineages, including lymphoid cells [26]. Furthermore, bone marrow from these compound transgenic mice established PIGA-deficient long-term hematopoietic repopulation potential [26]. Those observations are consistent with Fps being expressed in the pluripotent hematopoietic stem cell. It remains to be determined if Fps might actually play a significant biological role in the hematopoietic stem cell. This will require isolation and characterization of these cells using hematopoietic reconstitution methods.

While we did not attempt to directly measure lymphoid progenitors, lineage analysis of bone marrow with B cell markers (B220 and IgM) revealed a statistically significant decrease in the double-positive mature B cells (Fig. 1). Similar analysis of T cells in the spleen showed a decrease in both CD4 and CD8 single-positive populations (Fig. 4). However, in the thymus, we observed a reduction in the number of double-positive cells that was accompanied by an interesting increase in the single-positive populations. While these observations are consistent with the reduced T cell output seen in the fps^{MF} mice, they also suggested a potential defect in maturation of T cell progenitors. To our knowledge, there are no published reports suggesting a role for Fps in lymphopoiesis. However, we have recently observed lymphopoiesis defects in mice targeted with kinase-inactivating mutations in both Fps and Fer [27]. It will be interesting to explore whether Fps expression is intrinsic to T cells and contributes to their ontogeny, or alternatively, if Fps expression in supporting stromal cells might provide important extrinsic signals to developing T cells.

Analysis of transgenic and gene-targeted mice are revealing an even wider role for Fps and the related Fer kinase in the regulation of hematopoiesis and the function of mature cells. For example, a role for Fps and Fer in GPVI collagen receptor signaling in platelets has recently been described [28] and mice targeted with kinase-inactivating mutations in both Fps and Fer display hematopoietic defects that are consistent with a redundant role for these kinases in regulation of hematopoiesis [27]. Thus, Fps and Fer may play biologically significant regulatory roles in hematopoietic lineage determination by the earliest uncommitted progenitors, and also by more committed progenitors. In line with this latter possibility, expression of activated Fps (MFps) appears to drive progenitors at several levels toward the granulomonocytic pathway, and this might occur at the expense of lymphoid, erythroid, and megarkaryotic lineages (Fig. 7). The molecular basis of this hypothetical effect remains to be determined and will require the characterization of signaling events in highly enriched preparations of progenitor cells.

A role for Fps in downstream signaling from cytokine receptors in myeloid cells is supported by a number of studies using leukemic cell lines or peripheral while blood cells. We examined signaling in bone marrow–derived macrophages from mice targeted with a kinase-inactivating knockin mutation ($fps^{KR/KR}$). In $fps^{KR/KR}$ macrophages, we reported subtle reductions in both cytokine-induced STAT activation and lipopolysaccharide-induced ERK activation [11]. Others

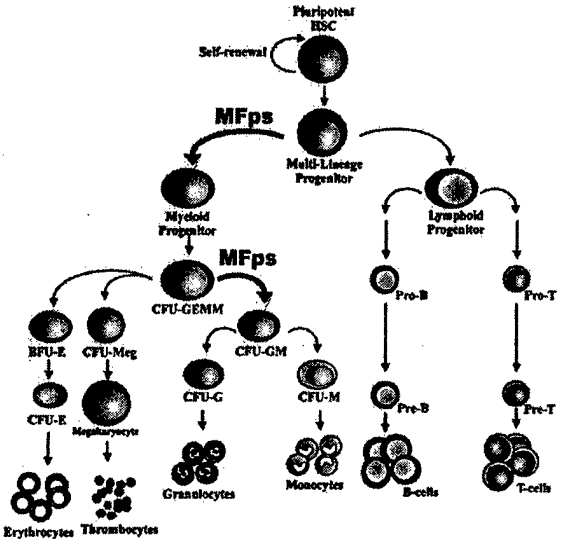

Figure 7. Hypothetical model for Fps involvement in lineage commitment by hematopoietic progenitors. Increased mature circulating granulocytes and monocytes, and decreased lymphoid cells in fps^{MF} mice, suggest a role for Fps at the level of the committed multi-lineage progenitor cell. Increased numbers of CFU-GEMM are also consistent with that role. Increased numbers of CFU-GM suggest this lineage-commitment role extends to the more mature bipotential granulomonocytic progenitor. The lack of a selective increase in monocytic or granulocytic cells argues against a lineage-determining role for Fps beyond this bipotential progenitor.

subsequently reported a striking enhancement of cytokine-induced STAT activation in macrophages from a Fps-knockout model [17]. This led to an attractive model suggesting Fps and JAK2 compete with one another for access to STAT downstream of cytokine-activated receptors. Accordingly, while Fps might be capable of STAT phosphorylation, it would not be as effective as JAK2 in this role and would thus serve to attenuate STAT activation by JAK2. This model predicted that kinase-dead Fps would be an even more effective inhibitor of JAK2-mediated STAT activation. However, in the complete absence of Fps, JAK2 would be unrestrained, leading to hyperactivation of STAT. This model was consistent with results from $fps^{KR/KR}$ mice [11] and the $fps^{-/-}$ mice described by those investigators [17]. However, we have since generated an independent line of $fps^{-/-}$ mice which did not display cytokine-induced hyperactivation of STAT [18]. We have now further complemented our in vivo analysis of Fps/STAT signaling using macrophages from the fps^{MF} mice. Slightly enhanced GM-CSF-induced STAT3, STAT5, and ERK1/2 phosphorylation was observed in bone marrow–derived macrophages from these fps^{MF} mice. JAK2 activation was not affected, nor was that of p38 or JNK. These observations further support a direct role for Fps in phosphorylation of STAT. However, our combined genetic mouse models are not consistent with a role for Fps in attenuation of STAT phosphorylation by JAK2. We propose an alternative model whereby Fps, JAK2, SYK, and SRC-family kinases could all contribute to STAT phosphorylation at the activated cytokine receptor (Fig. 8). JAK2 would be the major player; but SYK, LYN, and perhaps other related kinases, as well as Fps and perhaps Fer, could also contribute. Fps might participate by directly phosphorylating STAT, but it might also contribute to STAT activation by phosphorylation of the receptor, or perhaps serve a scaffolding role. According to this model, slightly enhanced or diminished STAT phosphorylation could occur in the presence of MFps or kinase-dead Fps, respectively. But in the complete absence of Fps, JAK2, LYN, or other kinases could compensate, making it difficult to observe any obvious reduction in STAT activation. We cannot exclude the possibility that Fps might play a more dominant regulatory role in cytokine signaling under specific cell culture conditions, and this could explain the differences seen by other investigators using a different Fps-null strain of mice [17]. However, we have never observed hyperactivation of STAT in any primary cells from our $fps^{-/-}$ mice, and in some circumstances we observed reduced activation of STAT, as well as other signaling molecules. We expect that a careful analysis of cytokine and other signaling pathways in myeloid cells from different tissue sources and at different stages of

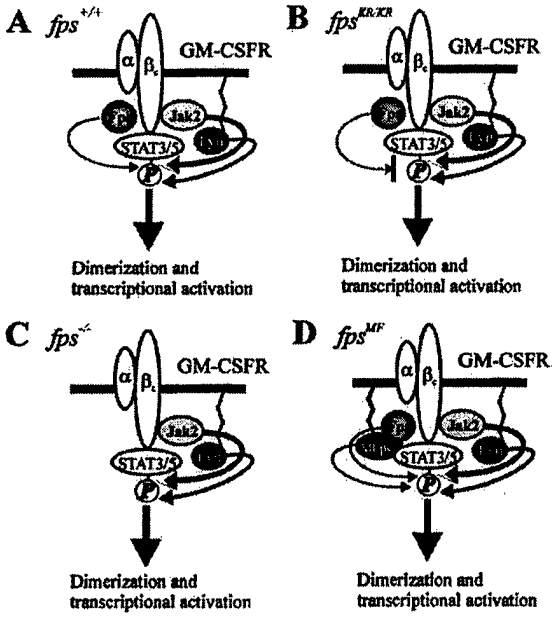

Figure 8. Molecular models supporting a role for Fps in activation of STAT3/5 downstream of GM-CSF. **(A)** ($fps^{+/+}$): in *wild-type* cells, Fps, JAK2, and LYN all participate in STAT3/5 phosphorylation. **(B)** ($fps^{KR/KR}$): in the presence of kinase-inactive Fps, there is some level of interference/competition that reduces the activation of STAT3/5 by JAK2 or LYN. **(C)** ($fps^{-/-}$): in the absence of Fps, there is no apparent effect on STAT3/5 activation, which presumably is mediated predominately by JAK2 and LYN. **(D)** (fps^{MF}): membrane localization of myristoylated Fps (MFps) increases the effective localized concentration near the GM-CSFR β_c resulting in enhanced phosphorylation of STAT3/5.

maturation and activation from our panel of Fps transgenic models will help to unravel this confusion. Clearly, additional biochemical characterization will be required before we have a complete understanding of the molecular function of the Fps kinase in cell signaling.

Acknowledgments

We would like to thank Andrew W.B. Craig for carefully reading the manuscript. W.S. was supported by the United States Department of Defense, Congressionally Directed Medical Research Programs Initiative (Grant ID: BCRP-DAMD17-0110382). This work was supported by the United States Department of Defense, Congressionally Directed Medical Research Programs (Grant ID: BCRP-DAMD17-0110382); the National Cancer Institute of Canada (Grant #012183) with funds from the Canadian Cancer Society; and the Canadian Institute of Health Research (Grant #394294).

References

1. Greer PA. Closing in on the biological functions of Fps/Fes and Fer. Nat Rev Mol Cell Biol. 2002;3:278–289.
2. Hanazono Y, Chiba S, Sasaki K, et al. c-fps/fes protein-tyrosine kinase is implicated in a signaling pathway triggered by granulocyte-macrophage colony-stimulating factor and interleukin-3. EMBO J. 1993;12: 1641–1646.
3. Izuhara K, Feldman RA, Greer P, Harada N. Interleukin-4 induces association of the c-fes proto-oncogene product with phosphatidylinositol-3 kinase. Blood. 1996;88:3910–3918.
4. Jiang H, Foltenyi K, Kashiwada M, et al. Fes mediates the IL-4 activation of insulin receptor substrate-2 and cellular proliferation. J Immunol. 2001;166:2627–2634.
5. Brizzi MF, Aronica MG, Rosso A, et al. Granulocyte-macrophage colony-stimulating factor stimulates JAK2 signaling pathway and rapidly activates p93fes, STAT1 p91, and STAT3 p92 in polymorphonuclear leukocytes. J Biol Chem. 1996;271:3562–3567.
6. Kirito K, Nakajima K, Watanabe T, et al. Identification of the human erythropoietin receptor region required for Stat1 and Stat3 activation. Blood. 2002;99:102–110.
7. Hanazono Y, Chiba S, Sasaki K, et al. Erythropoietin induces tyrosine phosphorylation and kinase activity of the c-fps/fes proto-oncogene product in human erythropoietin-responsive cells. Blood. 1993;81: 3193–3196.
8. Matsuda T, Fukada T, Takahashi-Tezuka M, et al. Activation of Fes tyrosine kinase by gp130, an interleukin-6 family cytokine signal transducer, and their association. J Biol Chem. 1995;270:11037–11039.
9. Nelson KL, Rogers JA, Bowman TL, Jove R, Smithgall TE. Activation of STAT3 by the c-Fes protein-tyrosine kinase. J Biol Chem. 1998;273:7072–7077.
10. Park WY, Ahn JH, Feldman RA, Seo JS. c-Fes tyrosine kinase binds to and activates STAT3 after granulocyte-macrophage colony-stimulating factor stimulation. Cancer Lett. 1998;129:29–37.
11. Senis Y, Zirngibl R, McVeigh J, et al. Targeted disruption of the murine fps/fes proto-oncogene reveals that Fps/Fes kinase activity is dispensable for hematopoiesis. Mol Cell Biol. 1999;19:7436–7446.
12. Yu G, Smithgall TE, Glazer RI. K562 leukemia cells transfected with the human c-fes gene acquire the ability to undergo myeloid differentiation. J Biol Chem. 1989;264:10276–10281.
13. Ferrari S, Manfredini R, Tagliafico E, et al. Antiapoptotic effect of c-fes protooncogene during granulocytic differentiation. Leukemia. 1994;8(suppl 1):S91–S94.
14. Ferrari S, Donelli A, Manfredini R, et al. Differential effects of c-myb and c-fes antisense oligodeoxynucleotides on granulocytic differentiation of human myeloid leukemia HL60 cells. Cell Growth Differ. 1990;1:543–548.
15. Kim J, Feldman RA. Activated Fes protein tyrosine kinase induces terminal macrophage differentiation of myeloid progenitors (U937 cells) and activation of the transcription factor PU.1. Mol Cell Biol. 2002;22:1903–1918.
16. Kim J, Ogata Y, Feldman RA. Fes tyrosine kinase promotes survival and terminal granulocyte differentiation of factor-dependent myeloid progenitors (32D) and activates lineage-specific transcription factors. J Biol Chem. 2003;278:14978–14984.
17. Hackenmiller R, Kim J, Feldman RA, Simon MC. Abnormal Stat activation, hematopoietic homeostasis, and innate immunity in c-fes$^{-/-}$ mice. Immunity. 2000;13:397–407.
18. Zirngibl RA, Senis Y, Greer PA. Enhanced endotoxin-sensitivity in Fps/Fes-null mice with minimal defects in hematopoietic homeostasis. Mol Cell Biol. 2002;22:2472–2486.
19. Greer P, Haigh J, Mbamalu G, et al. The Fps/Fes protein-tyrosine kinase promotes angiogenesis in transgenic mice. Mol Cell Biol. 1994;14:6755–6763.
20. Heydemann A, Warming S, Clendenin C, et al. A minimal c-fes cassette directs myeloid-specific expression in transgenic mice. Blood. 2000; 96:3040–3048.
21. Haigh J, McVeigh J, Greer P. The fps/fes tyrosine kinase is expressed in myeloid, vascular endothelial, epithelial, and neuronal cells and is localized in the trans-golgi network. Cell Growth Differ. 1996;7: 931–944.
22. Bardelli A, Parsons DW, Silliman N, et al. Mutational analysis of the tyrosine kinome in colorectal cancers. Science. 2003;300:949.
23. Yee SP, Mock D, Greer P, et al. Lymphoid and mesenchymal tumors in transgenic mice expressing the v-fps protein-tyrosine kinase. Mol Cell Biol. 1989;9:5491–5499.
24. Yee SP, Mock D, Maltby V, et al. Cardiac and neurological abnormalities in v-fps transgenic mice. Proc Natl Acad Sci U S A. 1989;86: 5873–5877.
25. Greer P, Maltby V, Rossant J, Bernstein A, Pawson T. Myeloid expression of the human c-fps/fes proto-oncogene in transgenic mice. Mol Cell Biol. 1990;10:2521–2527.
26. Keller P, Payne JL, Tremml G, et al. FES-Cre targets phosphatidylinositol glycan class A (PIGA) inactivation to hematopoietic stem cells in the bone marrow. J Exp Med. 2001;194:581–589.
27. Senis YA, Craig AW, Greer PA. Fps/Fes and Fer protein-tyrosine kinases play redundant roles in regulating hematopoiesis. Exp Hematol. 2003;31:673–681.
28. Senis YA, Sangrar W, Zirngibl RA, et al. Fps/Fes and Fer non-receptor protein-tyrosine kinases regulate collagen- and ADP-induced platelet aggregation. J Thromb Haemost. 2003;1:1062–1070.

Journal of Thrombosis and Haemostasis, 1: 1062–1070 APPENDIX 6

ORIGINAL ARTICLE

Fps/Fes and Fer non-receptor protein-tyrosine kinases regulate collagen- and ADP-induced platelet aggregation

Y. A. SENIS,*†[1] W. SANGRAR,† R. A. ZIRNGIBL,‡† A. W. B. CRAIG,† D. H. LEE‡ and P. A. GREER,*†‡§

*Departments of *Pathology; ‡Biochemistry and §Medicine, Queen's University; and †Division of Cancer Biology and Genetics, Queen's University Cancer Research Institute, Kingston, Ontario, Canada*

Summary. Fps/Fes and Fer proto-oncoproteins are structurally related non-receptor protein-tyrosine kinases implicated in signaling downstream from cytokines, growth factors and immune receptors. We show that Fps/Fes and Fer are expressed in human and mouse platelets, and are activated following stimulation with collagen and collagen-related peptide (CRP), suggesting a role in GPVI receptor signaling. Fer was also activated following stimulation with thrombin and a protease-activated receptor4 (PAR4)-activating peptide, suggesting a role in signaling downstream from the G protein-coupled PAR4. There were no detectable perturbations in CRP-induced activation of Syk, PLCγ2, cortactin, Erk, Jnk, Akt or p38 in platelets from mice lacking Fps/Fes, Fer, or both kinases. Platelets lacking Fps/Fes, from a targeted *fps/fes* null strain of mice, showed increased rates and amplitudes of collagen-induced aggregation, relative to wild-type platelets. P-Selectin expression was also elevated on the surface of Fps/Fes-null platelets in response to CRP. Fer-deficient platelets, from mice targeted with a kinase-inactivating mutation, disaggregated more rapidly than wild-type platelets in response to ADP. This report provides the first evidence that Fps/Fes and Fer are expressed in platelets and become activated downstream from the GPVI collagen receptor, and that Fer is activated downstream from a G-protein coupled receptor. Furthermore, using targeted mouse models we show that deficiency in Fps/Fes or Fer resulted in disregulated platelet aggregation and disaggregation, demonstrating a role for these kinases in regulating platelet functions.

Keywords: collagen, glycoprotein VI, platelet, tyrosine kinase.

The primary physiological function of platelets is to arrest bleeding from sites of vascular injury. Fibrillar collagen, found in the basement membrane of blood vessels, is a potent physiological agonist of platelets. The two main collagen receptors on the platelet surface are the integrin GP Ia–IIa (also known as α2β1) and glycoprotein VI (GPVI), which play critical roles in platelet adhesion and activation, respectively [1,2]. The main role of α2β1 is to provide a stable interaction with the site of injury under non-static conditions, whereas the GPVI receptor is an activatory receptor, crucial for the full activation of platelets by collagen [1,2]. GPVI is a type I transmembrane protein belonging to the immunoglobulin (Ig) superfamily, and is most closely related to human FcαR, natural killer cell receptors, and mouse paired Ig-like receptors (PIR) [3]. Signaling proteins activated downstream of GPVI are also activated downstream of T- and B-cell receptors, and Fc receptors [4]. The GPVI-associated Fc receptor (FcR) γ-chain contains an immune receptor tyrosine-based activation motif (ITAM) in its cytoplasmic domain [3]. Tyrosine phosphorylation of the ITAM following receptor engagement is carried out by Src family tyrosine kinases, including Fyn and Lyn [5]. The cytoplasmic tyrosine kinase $p72^{Syk}$ (Syk) is recruited to the tyrosine phosphorylated ITAM and initiates the activation of a number of signaling proteins that mediate changes in platelet properties such as cell adhesion. Some of the major targets downstream of GPVI include the adapters LAT and SLP-76, phosphatidylinositol 3′-kinase (PI3-kinase) and phospholipase Cγ2 (PLCγ2) [6].

The *fps/fes* proto-oncogene (hereafter referred to as *fps*) encodes a non-receptor protein-tyrosine kinase (PTK) expressed in macrophages and monocytes, as well as endothelial, epithelial and neuronal cells [7]. Efforts to determine the biological roles of Fps have focused on myelopoiesis and signaling downstream from cytokine receptor superfamily members, including receptors for granulocyte macrophage-colony stimulating factor (GM-CSF), interleukin (IL)-3, IL-4, IL-6, IL-11, erythropoietin (Epo), and leukemia inhibitory factor (LIF) [7]. Interestingly, several of these cytokines act synergistically to promote growth and maturation of megakaryocytes in the bone marrow (BM) [8]. Fps has also recently been suggested to play a role in inflammation and the innate immune response [9–11].

Fer is the only other known PTK structurally related to Fps. Unlike Fps, Fer appears to be ubiquitously expressed. Fps and Fer kinases share common domain structures, including an N-terminal Fps/Fer/CIP-4 (Cdc42 interacting protein-4) homology (FCH) domain, followed by a region containing three

Correspondence: Peter A. Greer, Queen's University Cancer Research Institute, Botterell Hall, Room A309, Kingston, Ontario, K7L 3 N6, Canada. Tel.: +613 5332813; fax: +613 5336830; e-mail: greerp@post.queensu.ca
[1]Present address: University of Oxford, Department of Pharmacology, Mansfield Road, Oxford OX1 3QT, UK.

Received 21 October 2002, accepted 26 November 2002

predicted coiled-coil (CC) motifs which mediate oligomerization, a central Src homology 2 (SH2) domain, and a C-terminal catalytic domain [7]. The SH2 domains of Fps and Fer are believed to mediate interactions with phosphorylated tyrosine residues on putative substrates, and/or regulate intramolecular or intermolecular interactions. Fer has been previously implicated in FcεRI receptor signaling in a mast cell line [12]. Both Fps and Fer were recently shown to be tyrosine phosphorylated following FcεRI receptor cross-linking on mast cells, and Fer is required for maintaining maximal p38 kinase activation and chemotaxis in response to either stem cell factor or FcεRI receptor cross-linking [13]. Interestingly, a consensus-binding sequence for the Fps SH2 domain is contained within the α-chain of the mouse high affinity receptor for the Fc region of IgG (FcγRI) [14], a receptor that shares the same FcR γ-chain homodimer with the FcεRI receptor on mast cells and the GPVI collagen receptor on platelets. These observations suggested a possible involvement of Fps and Fer kinases in signaling downstream from these related receptors.

In this study we wished to determine if Fps and Fer were expressed in platelets; and if so, to determine if they played a role in signaling downstream from the GPVI collagen receptor or other receptors found on the platelet surface, and if their activities were involved in regulating platelet functions.

Methods

Materials

Prostaglandin E_1 (PGE_1), potato apyrase grade VII, Gly-Pro-Arg-Pro (GPRP) tetrapeptide, porcine heparin, leupeptin, aprotinin, phenylmethylsulfonyl fluoride, vanadate, and indomethacin were purchased from Sigma-Aldrich Canada Inc. (Oakville, ON, Canada). Human thrombin IIa was kindly provided by Dr Mike Nesheim (Queen's University, Canada). CRP was kindly provided by Dr Steve Watson (University of Oxford, UK). PAR4-activating peptide, AYPGKF, was synthesized by Dr Sook Shen (Queen's University, Peptide Synthesis Laboratory). Recombinant human thrombopoietin (Tpo) was purchased from R & D Systems (Minneapolis, MN, USA). Native collagen fibrils (type I) from equine tendon and adenosine diphosphate (ADP) were purchased from Chrono-Log (Havertown, PA, USA). Antiphosphotyrosine mouse monoclonal antibody (PY99), anti-Erk1/2 rabbit polyclonal (K-23) antibody and antiphosphoErk1/2 (E-4) mouse monoclonal antibody were purchased from Santa Cruz Biotechnology Inc. (San Diego, CA, USA). Anti-Fps/Fer rabbit polyclonal antiserum (anti-FpsQE) was raised against Fps, but is equally reactive with Fps and Fer [15]. Anti-Fer rabbit polyclonal antiserum (anti-FerLA) is specific for Fer [15]. Anti-Syk rabbit polyclonal antiserum (738) was kindly provided by Drs Karen Zoller and Joan Brugge [16] (Ariad Pharmaceuticals Inc., Cambridge, MA, USA). Anti-PLCγ2 rabbit polyclonal antiserum (anti-PLCγRI) was kindly provided by Drs Christine Ellis and Tony Pawson [17] (Samuel Lunenfeld Research Institute, Toronto, Canada). Anticortactin mouse monoclonal antibody (4F11) was purchased from Upstate Biotechnology Inc. (Lake Placid, NY, USA). Horseradish peroxidase (HRP)-conjugated goat antirabbit IgG was purchased from Chemicon International Inc. (Temecula, CA, USA). GammaBind Plus Sepharose and HRP-conjugated sheep antimouse IgG was purchased from Amersham Pharmacia Biotechnology Canada, Baie d'Urfe, QU. FITC-conjugated rat antimouse P-selectin monoclonal antibody (CD62P, RB40.34) was purchased from BD PharMingen Canada Inc. (Mississauga, ON, Canada).

Transgenic mouse lines $fps^{-/-}$ and $fer^{DR/DR}$ transgenic mice were generated in-house and genotyped as previously described [11,18]. $fps^{-/-}$ mice are null for Fps, while $fer^{DR/DR}$ mice express only a catalytically inactive and unstable Fer protein. All mice were maintained at the Queen's University Animal Care Facility, according to guidelines of the Canadian Council on Animal Care.

Preparation of washed platelets

Washed platelets were prepared as described by Law *et al.* [19], with a few minor modifications. Platelets were resuspended at a concentration of $3 \times 10^8\ mL^{-1}$ for P-selectin expression assays, or at a concentration of $5 \times 10^8\ mL^{-1}$ for immunoprecipitation and Western blot analysis.

Immunoprecipitation and Western blot analysis

The protocol used was the same as that described by Asselin *et al.* [20]. Platelets ($1 \times 10^8\ mL^{-1}$) were stimulated with $30\ \mu g\ mL^{-1}$ collagen, $3\ \mu g\ mL^{-1}$ CRP, $10\ U\ mL^{-1}$ IIa, $500\ \mu M$ AYPGKF, $50\ \mu M$ ADP and $100\ ng\ mL^{-1}$ thrombopoietin (Tpo). Soluble cell lysates (SCL) or immunoprecipitated proteins were resolved on 7.5% sodium dodecyl sulfate–polyacrylamide gel electrophoresis and transferred to Immobilon-P membrane (Millipore Canada Corp., Mississauga, ON, Canada) with a Trans-Blot Semi-Dry Transfer Cell (Bio-Rad Laboratories Canada Ltd, Mississauga, ON, Canada) and immunoblotted. Immobilized proteins were visualized with Western Lightning Chemiluminescence Reagent Plus (PerkinElmer Life Sciences Inc., Boston, MA, USA) and exposing to Kodak X-Omat Blue XB-1 Scientific Imgaing Film (NEN Life Science Products Inc., Boston, MA, USA). Antibodies were stripped from membranes with two 8-min washes in $0.2\ mol\ L^{-1}$ NaOH.

Platelet aggregation in whole blood

Platelet aggregation in whole blood was measured using a Chrono-Log two-channel whole blood aggregometer (Chrono-Log, Havertown, PA, USA). Nine parts blood was collected into one part 3.2% sodium citrate ($Na_3C_6H_5O_7 \cdot 2H_2O$) by cardiac puncture. Five hundred microliters of blood was diluted with an equal volume of Lactated Ringer's buffer, pH 6.2 ($102.7\ mmol\ L^{-1}$ NaCl, $27.7\ mmol\ L^{-1}$ $C_3H_5NaO_3$, $4\ mmol\ L^{-1}$ KCl, $1.4\ mmol\ L^{-1}$ $CaCl_2 \cdot 2H_2O$) and continuously stirred at 1000 r.p.m. at 37 °C. Platelet aggregation was induced by the addition of $2\ \mu g\ mL^{-1}$ collagen or $10\ \mu mol\ L^{-1}$ ADP.

FACS analysis of P-selectin surface expression on activated platelets

Reactions consisted of 1.5×10^6 platelets suspended in 50 μL stimulation buffer containing 2.5 mmol L^{-1} GPRP peptide, and 0.1 μg of FITC-conjugated rat antimouse CD62P monoclonal antibody. Ten microliters of the desired concentration of IIa or collagen was added to each platelet sample. All stimulations were carried out at room temperature and were terminated by the addition of 300 μL of ice-cold 1% paraformaldehyde in cacodylate buffer, pH 7.2. Samples were analyzed with a Beckman Coulter Epics Altra flow cytometer (Beckman Coulter Inc., Miami, FL, USA).

Statistical analysis

Significant differences were calculated using Student's *t*-test (Prism software package, GraphPAD Software for Science, San Diego, CA, USA).

Results

Fps and Fer are expressed in mouse and human platelets

Immunoblotting analysis was first performed on mouse and human platelet lysates using a rabbit polyclonal antiserum that recognizes both Fps and Fer. A tight doublet of 92 and 94 kDa immunoreactive peptides was observed in both murine and human platelets (Fig. 1a,c), consistent with expression of both p94Fer and p92Fps. Mouse platelets expressed higher levels of Fer than Fps, compared with human platelets, which expressed approximately equal amounts of both kinases. As expected, there was no detectable Fps protein in platelets from $fps^{-/-}$ mice, Fer was not detectable in platelets from $fer^{DR/DR}$ mice, which express catalytically inactive Fer that is rapidly degraded [18], and platelets from compound mutant $fps^{-/-}$ $fer^{DR/DR}$ mice did not express detectable levels of either Fps or Fer. Fer was also detected in *wild-type* and $fps^{-/-}$ platelets with Fer-specific rabbit polyclonal antiserum (anti-Fer) (Fig. 1b).

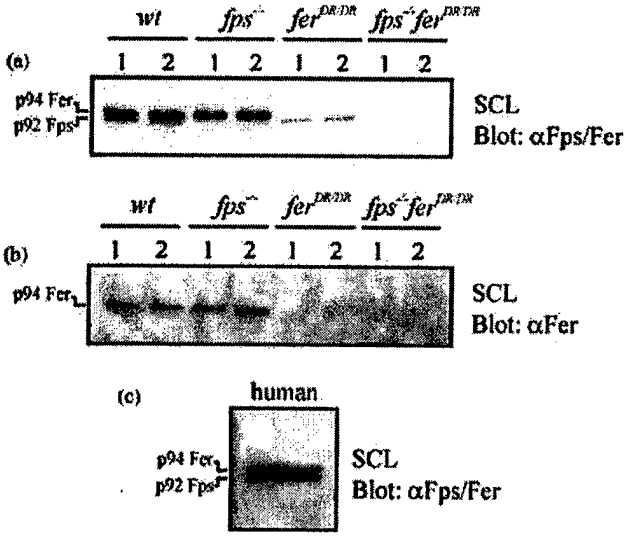

Fig. 1. Fps and Fer expression in platelets. Platelet soluble cell lysates (SCL) from $fps^{-/-}$, $fer^{DR/DR}$, and $fps^{-/-}$ $fer^{DR/DR}$ mice (a and b) or humans (c) were analyzed by immunoblotting with anti-Fps/Fer (αFps/Fer) (a and c) or anti-Fer (αFer) antisera (b). The positions of p94Fer and p92Fps are indicated.

Platelet activation resulted in tyrosine phosphorylation of Fps and Fer

Wild-type murine platelets were stimulated with known platelet agonists, including collagen, CRP, IIa, AYPGKF, ADP and Tpo. Soluble cell lysates were first immunoblotted with antiphosphotyrosine antibody (anti-PY) to confirm that agonists were active. Collagen and CRP stimulations resulted in the most robust activation of tyrosine phosphorylation (Fig. 2a). Fps and Fer were also immunoprecipitated from stimulated platelets and immunoblotted with anti-PY antibody to determine if they became activated in stimulated platelets. Fps and Fer were inducibly phosphorylated following stimulation with collagen

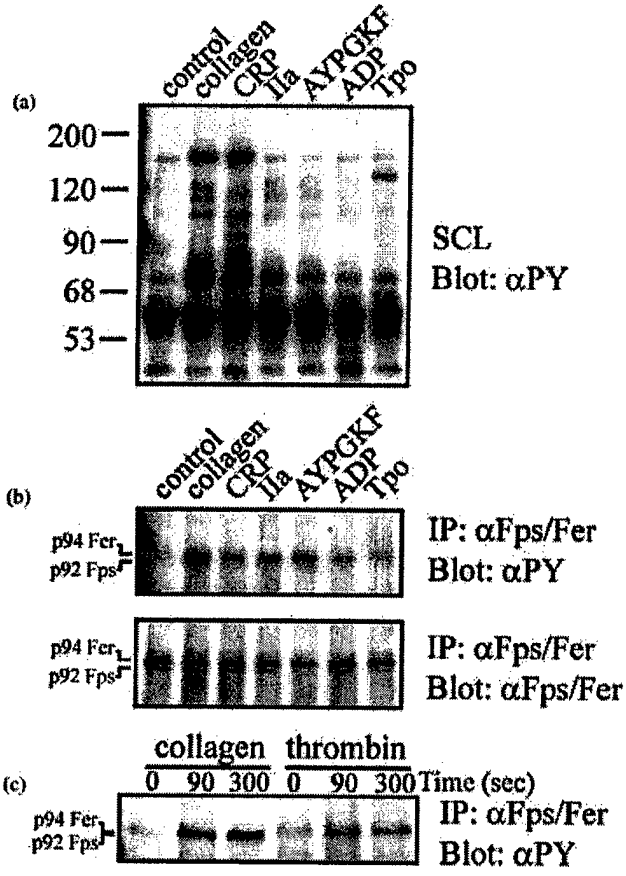

Fig. 2. Tyrosine phosphorylation of Fps and Fer in mouse platelets. *Wild-type* mouse platelets were stimulated for 5 min with PBS (control), 30 μg mL^{-1} collagen, 3 μg mL^{-1} CRP, 10 U mL^{-1} IIa, 500 μM AYPGKF, 50 μM ADP and 100 ng mL^{-1} thrombopoietin (Tpo) (a and b), or with either 30 μg mL^{-1} collagen or 10 U mL^{-1} thrombin (IIa) for 0, 90 and 300 s. SCL were then immunoblotted (blot) directly with antiphosphotyrosine antiserum (αPY) (a), or immunoprecipitated (IP) with αFps/Fer and immunoblotted sequentially with αPY and αFps/Fer (b and c).

and CRP (Fig. 2b). Fer also became detectably tyrosine phosphorylated post stimulation with IIa and AYPGKF, whereas Fps phosphorylation was not consistently detectable with these agonists (Fig. 2b). High levels of tyrosine phosphorylation of Fps and Fer were observed 90 s post stimulation with collagen, and with IIa in the case of Fer (Fig. 2c). In contrast, only low levels of tyrosine phosphorylated Fps and/or Fer were observed following stimulation with ADP or Tpo (Fig. 2b). These results suggested that Fps and Fer might signal downstream from the GPVI and PAR4 receptors.

A time course of collagen-induced tyrosine phosphorylation of Fps and Fer revealed a detectable increase in the phosphorylation of both kinases within 90 s of addition of collagen (Fig. 3a,b). A CRP dose–response analysis revealed tyrosine phosphorylation of both kinases at 3 $\mu g\,mL^{-1}$ of CRP (Fig. 4), and in some experiments this was apparent at doses as low as 0.3 $\mu g\,mL^{-1}$. The kinetics of activation of Fps and Fer were similar with collagen and CRP (Figs 3b and 4b).

Due to the cross-reactivity of the anti-Fps/Fer antisera, and the close migration of Fps and Fer, we next repeated the collagen stimulations using platelets from *fer*$^{DR/DR}$ mice, which contain very little detectable Fer. Collagen-induced changes in global tyrosine phosphoproteins were indistinguishable between *wild-type* and *fer*$^{DR/DR}$ platelets (Fig. 5a), suggesting that Fer is not itself a major phosphoprotein, nor are any potential Fer substrates. Anti-PY immunoblotting of anti-Fps/Fer immunoprecipitates from *fer*$^{DR/DR}$ platelets provided compelling evidence that Fps is also tyrosine phosphorylated in response to collagen stimulation (Fig. 5b). In *fer*$^{DR/DR}$ platelets tyrosine phosphorylated Fps was not overshadowed by Fer, as it was in *wild-type* platelets. However, a residual faint band migrating at the position of Fer was still observed in *fer*$^{DR/DR}$ platelets,

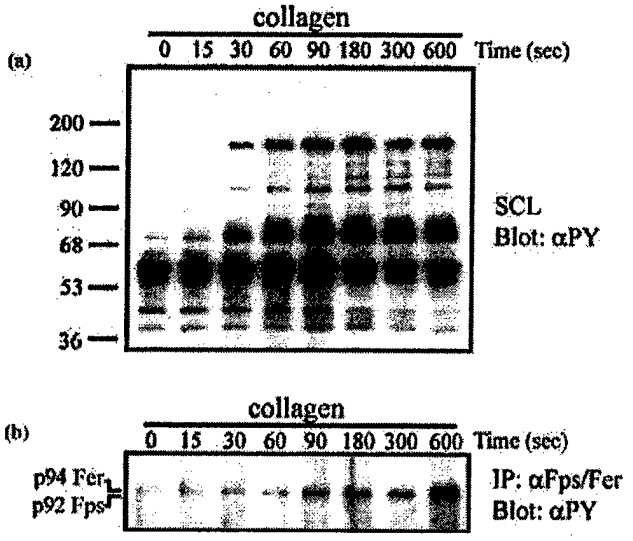

Fig. 3. Time course of collagen-induced tyrosine phosphorylation of Fps and Fer. *Wild-type* mouse platelets were stimulated with 30 $\mu g\,mL^{-1}$ collagen for the indicated times and SCL were either immunoblotted directly with αPY (a), or immunoprecipitated with αFps/Fer and immunoblotted with αPY (b), followed by striping and reprobing with αFps/Fer to confirm loading (not shown).

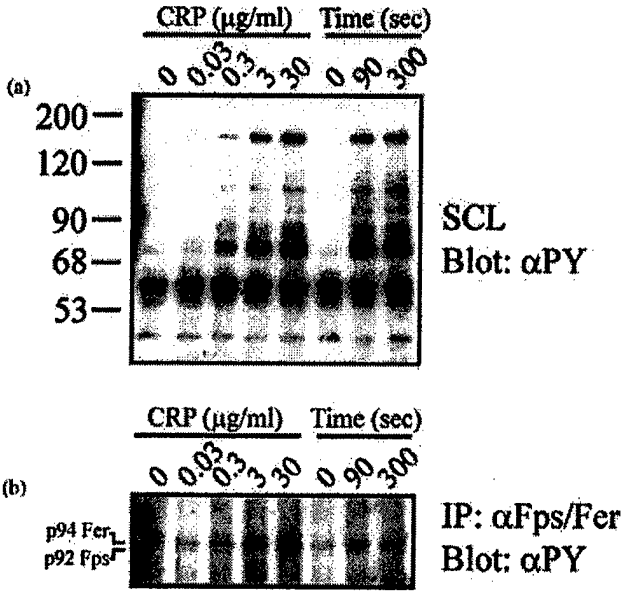

Fig. 4. Time course and dose–response of CRP-induced tyrosine phosphorylation of Fps and Fer. *Wild-type* mouse platelets were stimulated for 300 s with 0, 0.03, 0.3, 3 or 30 $\mu g\,mL^{-1}$ CRP, or with 3 $\mu g\,mL^{-1}$ CRP for 0, 90 or 300 s. SCLs were analyzed directly by immunoblotting with αPY (a), or Fps and Fer were immunoprecipitated and then analyzed by immunoblotting with αPY (b), followed by striping and reprobing with αFps/Fer to confirm loading (not shown).

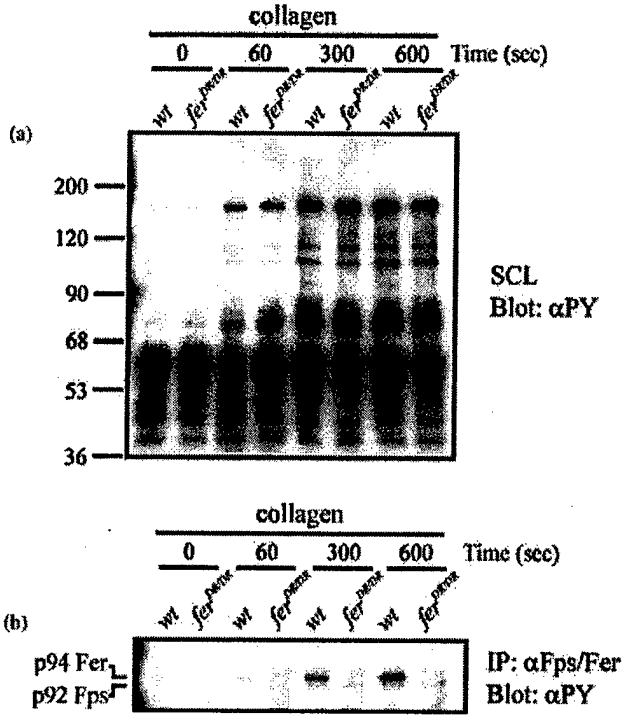

Fig. 5. Collagen-induced tyrosine phosphorylation of Fps in platelets. Platelets from *wild-type* or *fer*$^{DR/DR}$ mice were stimulated with 30 $\mu g\,mL^{-1}$ collagen for the indicated times. SCL were then analyzed directly by immunoblotting with αPY (a), or Fps and Fer was immunoprecipitated with αFps/Fer and immunoblotted with αPY (b), followed by striping and reprobing with αFps/Fer to confirm loading (not shown).

suggesting that Fer might be a substrate of another kinase in collagen-stimulated platelets. In support of this, phosphorylation of kinase-inactive Fer was also described downstream of platelet-derived growth factor (PDGF) receptor [18].

Inhibition of collagen-induced tyrosine phosphorylation of Fps and Fer

Platelets undergo a dramatic shape change during activation, followed by formation of filopodia and lamellopodia, requiring extensive cytoskeletal remodeling [21]. This remodeling is dependent upon PI3-kinase activity and many key signaling proteins become associated with the cytoskeleton during platelet activation [22]. We therefore examined the effect of PI3-kinase inhibitors, wortmannin and LY294002, and the actin polymerization inhibitor, cytochalasin D, on collagen-mediated Fps and Fer activation. Pretreatment of platelets with cytochalasin D abolished collagen-induced tyrosine phosphorylation of many proteins (Fig. 6a). Likewise, Fps and Fer phosphorylation was blocked by cytochalasin D (Fig. 6b), suggesting their phosphorylation is dependent upon actin polymerization.

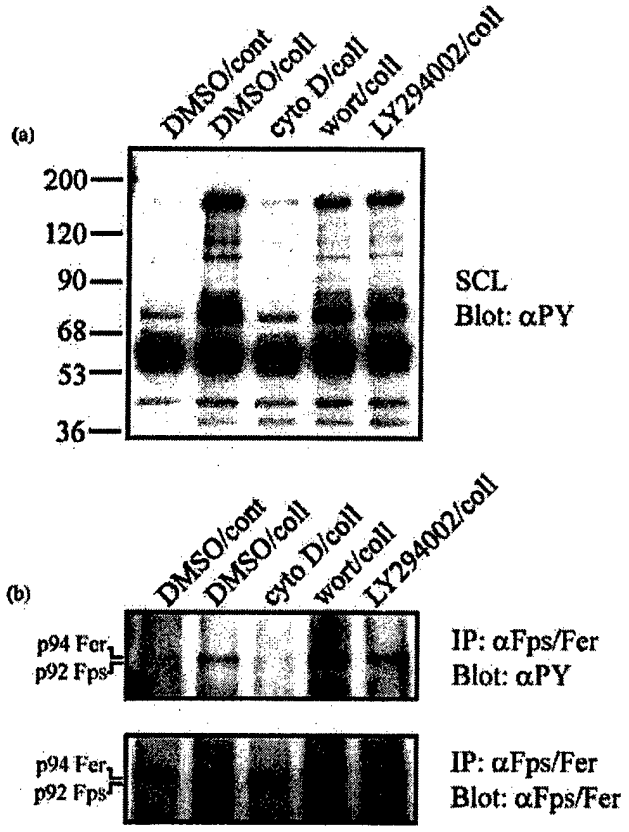

Fig. 6. Collagen-induced tyrosine phosphorylation of Fps and Fer is inhibited with cytochalasin D, but not with wortmannin or LY294002. *Wild-type* mouse platelets were preincubated with either 0.1% DMSO (control), 10 μM cytochalasin D, 100 nM wortmannin or 16 μM LY294002 for 10 min, then stimulated with PBS (control) or 30 μg mL^{-1} collagen for 5 min. SCL were then analyzed directly by immunoblotting with αPY (a), or Fps and Fer was immunoprecipitated with αFps/Fer and immunoblotted sequentially with αPY and αFps/Fer (b).

Despite the ability of the PI3-kinase inhibitors wortmannin and LY294002 to partially inhibit the global tyrosine phosphorylation profile (Fig. 6a), this treatment had no obvious effect on the extent of tyrosine phosphorylation of Fps or Fer (Fig. 6b), suggesting that Fps and Fer activation downstream from collagen signaling in platelets does not require PI3-kinase activity.

Tyrosine phosphorylation of collagen-inducible signaling proteins

To explore the role of Fps and Fer downstream from collagen receptors in platelets, we compared the tyrosine phosphorylation status of a number of known signaling molecules in collagen-stimulated platelets from *wild-type*, *fps*$^{-/-}$, *fer*$^{DR/DR}$ and compound *fps*$^{-/-}$ *fer*$^{DR/DR}$ mice. There were no obvious differences in total tyrosine phosphoproteins between the different genotypes at the agonist concentration tested (Fig. 7a).

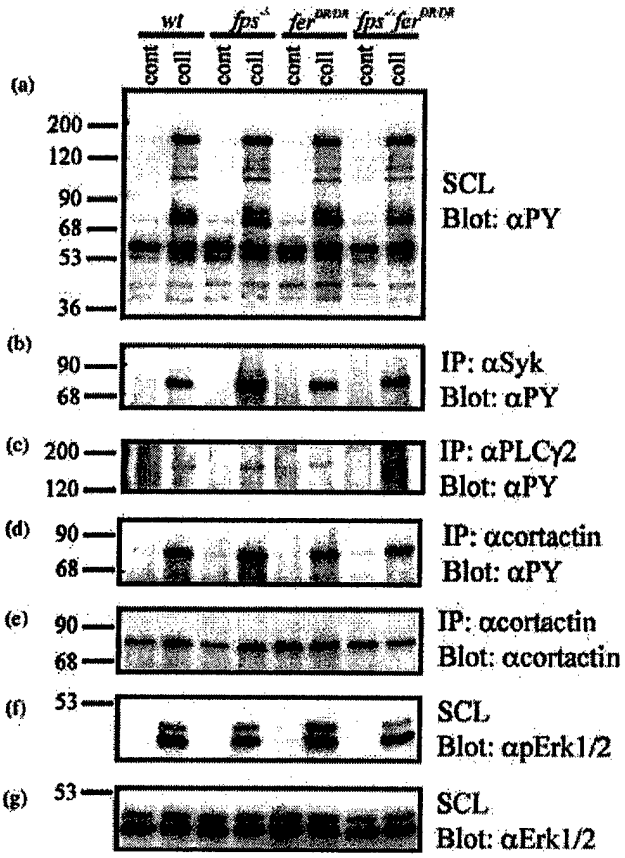

Fig. 7. Activation of signaling proteins in collagen-stimulated platelets from *wild-type*, *fps*$^{-/-}$, *fer*$^{DR/DR}$, and *fps*$^{-/-}$ *fer*$^{DR/DR}$ mice. Platelets were treated with either PBS (cont) or 30 μg mL^{-1} collagen (coll) for 5 min. SCL were prepared and analyzed directly by immunoblotting with αPY (a), antiphospho Erk1/2 (αpErk1/2) (f), or anti-Erk1/2 (αErk1/2) (g). Alternatively lysates were immunoblotted with αPY after immunoprecipitation with anti-Syk (αSyk) (b), anti-PLCγ2 (αPLCγ2) (c), or anticortactin (αcortactin) (d); or immunoblotted with αcortactin after immunoprecipitation with αcortactin (e). Blots shown in (b and c) were subsequently stripped and reprobed with anti-Syk or anti PLCγ2 to confirm loading (not shown).

Immunoprecipitation followed by anti-PY blotting of some of the main signaling proteins acting downstream of GPVI, including Syk, PLCγ2 and cortactin, also revealed no significant differences in their collagen-induced tyrosine phosphorylation status (Fig. 7b–e). We next checked the activation status of other signaling proteins that may play a role in GPVI receptor signaling in platelets, including Jnk, Akt, p38 (data not shown), and Erk1/2 (Fig. 7f,g). No differences were observed between *wild-type and* $fps^{-/-}$, $fer^{DR/DR}$ or $fps^{-/-}$ $fer^{DR/DR}$ platelets. A similar analysis performed with IIa-induced platelets also revealed no differences (data not shown). Therefore, Fps and Fer are not required for tyrosine phosphorylation of these known targets, and their substrates remain to be identified.

Platelet aggregation in whole blood

We next evaluated aggregation of platelets in whole blood from *wild-type*, $fps^{-/-}$ or $fer^{DR/DR}$, mice in response to collagen or ADP. Platelets from $fps^{-/-}$ mice exhibited elevated rates ($P = 3.5 \times 10^{-6}$) and amplitudes ($P = 0.025$) of collagen-induced aggregation relative to *wild-type* mice (Fig. 8a). However, platelets from $fer^{DR/DR}$ mice aggregated almost identically to *wild-type* mice. When ADP was used as an agonist, platelets from $fps^{-/-}$ mice aggregated with a higher rate ($P = 0.032$) relative to *wild-type* platelets, and although the apparent amplitude was also higher, this did not reach statistical significance ($P = 0.127$). While ADP-stimulated $fer^{DR/DR}$ platelets aggregated with a similar rate to *wild-type* platelets, they displayed a more rapid onset of disaggregation ($P = 0.023$) relative to *wild-type* platelets (Fig. 8b). This difference in disaggregation kinetics was not observed in ADP stimulated $fps^{-/-}$ platelets.

P-Selectin expression on the surface of activated platelets

P-Selectin is a membrane-associated cell adhesion molecule that is stored in platelet α-granules, and becomes rapidly exocytosed to the platelet surface upon stimulation with various agonists [23]. As Fps has been implicated in regulating vesicular trafficking [24], we assessed whether there were any defects in P-selectin expression on the surface of $fps^{-/-}$ and $fer^{DR/DR}$ platelets following IIa- or CRP-mediated activation. Higher levels of P-selectin were detected on the surface of $fps^{-/-}$ platelets stimulated with a low dose of IIa (0.15 nM), however, no differences were noticed at the higher doses tested (Fig. 9a). Interestingly, $fps^{-/-}$ platelets displayed a more gradual dose–response curve than *wild-type* platelets, but the EC_{50} values were the same. There was no apparent difference in the response to IIa between *wild-type* and $fer^{DR/DR}$ platelets (data not shown), suggesting that Fer does not participate in the degranulation response to IIa.

When CRP was used as an agonist, $fps^{-/-}$ platelets showed a higher amplitude ($P = 0.030$) of P-selectin expression relative to *wild-type* platelets (Fig. 9b). While $fer^{DR/DR}$ platelets also showed elevated CRP-induced rate of P-selectin expression compared with *wild-type* platelets, this did not reach a statistically significant difference (data not shown).

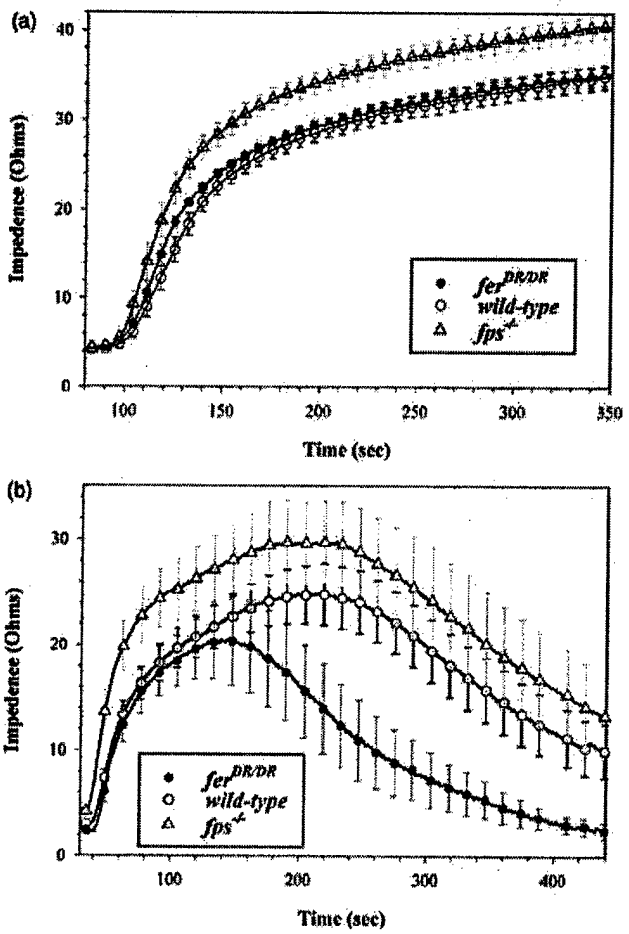

Fig. 8. Platelet aggregation in whole blood. Platelet aggregation was induced in whole blood with 2 μg mL^{-1} collagen (a) or 10 μM ADP (b). The curves represent averaged plots (± SEM) based on *wild-type* ($n = 18$), ○; $fps^{-/-}$ ($n = 12$), ; or $fer^{DR/DR}$ ($n = 6$), ●. Non-linear regressions were performed for each data set.

Conclusions

In this study we demonstrate for the first time that Fps and Fer are expressed in human and mouse platelets, and that both become tyrosine phosphorylated, and thus activated in response to collagen and CRP. Fer was also activated following IIa and PAR4-specific stimulation of platelets. Activation of Fps and Fer following collagen stimulation could be inhibited by pretreating platelets with cytochalasin D, suggesting that formation of cytoskeleton-associated signaling complexes is necessary for regulating both kinases. In preliminary fractionation experiments we have not been able to detect an agonist-inducible change in the distribution of Fps or Fer from the cytosolic to cytoskeletal fraction (data not shown).

Using gene targeted mice we revealed defects in aggregation and activation of Fps- or Fer-deficient platelets. These phenotypes were consistent with a negative regulatory role for Fps in collagen-induced aggregation and activation, but paradoxically suggested opposing roles for Fps and Fer in ADP-induced signaling. The proposed inhibitory role for Fps is further substantiated by the recent analysis of transgenic mice (fps^{MF})

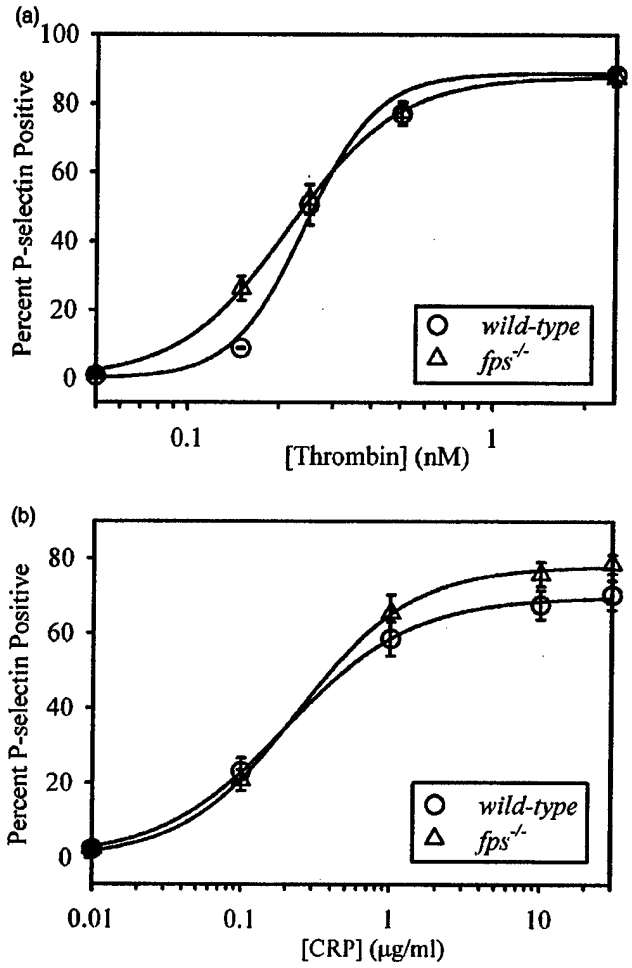

Fig. 9. P-Selectin expression on the surface of activated platelets. Washed platelets were stimulated with serial dilutions of thrombin (a) or CRP (b) and surface P-selectin levels were quantitated by flow cytometry. The curves represent averaged plots (± SEM) based on *wild-type* ($n = 7$), ○; or $fps^{-/-}$ ($n = 5$), △; or $fer^{DR/DR}$ ($n = 6$), ●. Non-linear regressions were performed for each data set.

that express an activated mutant Fps kinase (Sangrar, Senis, Richardson and Greer, manuscript submitted). The fps^{MF} mice displayed the expected opposite phenotype to the $fps^{-/-}$ mice; specifically, they showed reduced platelet aggregation and activation, and even more compelling, fps^{MF} mice displayed significantly increased clotting times. It will be interesting to determine whether $fps^{-/-}$ mice are more susceptible to disseminated intravascular coagulation (DIC) in response to septicemia or traumatic shock.

Fps and Fer were minimally tyrosine phosphorylated in resting platelets, but inducibly phosphorylated by several classical agonists. The majority of tyrosine phosphorylation we observed following collagen stimulation was probably the result of engagement of the GPVI receptor as these experiments were done in the presence of Ca^{2+} chelators to inhibit signaling from collagen integrin α2β1 [25]. Also, use of the GPVI-specific agonist CRP, and platelets from Fer-deficient mice clearly demonstrated that both kinases were activated downstream from this receptor. To determine whether Fps and Fer also become phosphorylated downstream from the α2β1 collagen integrin will require the use of α2β1-specific agonists or the use of either human or mouse platelets deficient in GPVI or FcR γ-chain [3,26]. Although Fer has been shown to associate with the β1 integrin subunit in neurites [27], we could not demonstrate collagen-induced interactions between Fps or Fer with either α2 or β1 (data not shown).

It has been difficult to identify the relevant physiological agonists of non-receptor PTKs, which generally become activated downstream of other receptors, including receptor PTKs. Modest activation of Fps and Fer kinases have been demonstrated downstream from a number of cytokine and growth factor receptors, and more recently both kinases have been shown to become activated upon engagement of the FcεRI receptor on mast cells [13]. The GPVI collagen receptor provides the most dramatic example to date of an effective upstream activator for both the Fps and Fer PTKs.

The kinetics of collagen-induced tyrosine phosphorylation of Fps and Fer was slower than Fyn, Lyn and Syk, which have clearly defined biochemical roles in the early stages of GPVI receptor signaling [2]. This suggests that Fps and Fer may be involved in later stages of platelet activation. Deletion of Fyn, Lyn or Syk greatly affected the ability of platelets to activate properly [2]. However, neither Fps nor Fer appeared to be involved in regulating tyrosine phosphorylation of Syk or PLCγ2, two of the main signal transducers downstream from the GPVI receptor. As phosphorylation of Syk and PLCγ2 was also normal in compound *fps/fer* mutant platelets, it appears that Fps and Fer must function further downstream in the GPVI signaling pathway. Cortactin plays a pivotal role in cytoskeletal reorganization in activated platelets [28,29], and we have recently reported a defect in PDGF-induced cortactin phosphorylation in fibroblasts from $fer^{DR/DR}$ mice [18]. However, we did not observe a defect in collagen-induced tyrosine phosphorylation of cortactin in platelets from $fps^{-/-}$, $fer^{DR/DR}$, or compound $fps^{-/-}$ $fer^{DR/DR}$ mice, suggesting that a redundant mechanism must exist in this cell system. However, high stoichiometry of cortactin phosphorylation mediated by Syk and Src-family kinases might mask a defect in phosphorylation of specific tyrosine residues in cortactin by Fer or Fps. Collagen-induced activation of several other downstream signaling proteins, including Jnk, Akt, p38, and Erk1/2 were apparently normal in Fps and Fer deficient platelets.

Cytochalasin D inhibits collagen-induced tyrosine phosphorylation of many signaling proteins including Syk [30], focal adhesion kinase (Fak) [31] and the actin reorganizing Wiskott–Aldrich syndrome protein (WASP) [32], presumably by preventing the formation of cytoskeleton associated signaling complexes. Cytochalasin D also inhibited activation of Fps and Fer in collagen treated platelets, indicating a requirement for actin polymerization in their activation. In contrast, PI3-kinase inhibitors wortmannin and LY294002 had no effect on tyrosine phosphorylation of Fps or Fer.

None of the mutant mouse lines analyzed in this study demonstrated overt bleeding tendencies. However, increases

were observed in the rates and amplitudes of collagen-induced platelet aggregation in whole blood from $fps^{-/-}$ mice, suggesting that Fps might negatively regulate collagen-induced platelet aggregation. In light of the proposed role for Fer in cross-talk between adherens junctions and focal adhesions [27] and Fps in semaphorin3A-induced growth cone collapse [33] we suggest that Fps and Fer might also participate in a cytoskeleton-based inside-out signaling pathway from GPVI to the collagen and fibrinogen integrins. Their involvement in this pathway might be to regulate tyrosine phosphatases such as PTP1B or SHP1 that in turn might regulate the tyrosine phosphorylation status of the integrins or associated cytoskeletal proteins. Based upon the hyperaggregation phenotype observed in Fps-deficient platelets, we suggest that these kinases might activate tyrosine phosphatases which in turn inhibit inside-out signaling to the integrins. In support of this hypothesis, decreased collagen-induced aggregation has been observed in transgenic mice expressing activated Fps [34], and these fps^{MF} mice have dramatically reduced platelet aggregation responses relative to *wild-type* controls [35].

Paradoxically, $fer^{DR/DR}$ platelets disaggregated more rapidly following ADP stimulation. This suggests an additional positive regulatory role for Fer in ADP-induced platelet aggregation that is distinct from any inhibitory role it or Fps might play in collagen-induced aggregation.

Several of the Src family kinases present in platelets are localized around vesicles, and are believed to regulate vesicular trafficking [5,36,37]. Fps and Fer have also been detected around vesicular structures [24]. This raised the possibility that Fps and/or Fer may also regulate some aspect of α-granule trafficking. The more gradual dose–response to IIa and higher CRP-induced maximum levels of P-selectin expression in $fps^{-/-}$ mice were again consistent with some inhibitory or modulatory role for Fps in α-granule trafficking. In $fer^{DR/DR}$ platelets, the P-selectin expression in response to IIa was identical to *wild-type* controls, however, the increased response to CRP again argued for a negative regulatory role for Fer in α-granule trafficking. These P-selectin expression phenotypes further support the hypothesis that Fps and Fer kinases participate in signaling pathways that regulate cytoskeletal reorganization.

In summary, these results introduce Fps and Fer as two novel players in the GPVI and PAR4 signaling pathways. More work is required to identify the physiologically relevant substrates of these kinases in these pathways; however, the phenotypes observed in Fps- and Fer-deficient mice provide important clues and suggest inhibitory roles for these kinases acting further downstream at the level of cross-talk between GPVI or PAR4 and the integrins or other cytoskeleton-based functions.

Acknowledgements

We thank Dr Walter Emrich and Jeanette Dick who kindly collected the human blood samples to initiate this study; Jessica Palmer, Michelle Scott, Nichole Peterson, and Shuguang Cao for technical assistance; and Derek Schulze for his help with the FACS analysis. We also thank Dr Steve Watson for helpful suggestions in preparing this manuscript.

Supported by grant no. 012183 from the National Cancer Institute of Canada with funds from the Canadian Cancer Society, and grant no. MOP-11627 from the Canadian Institutes of Health Research.

References

1 Clemetson KJ, Clemetson JM. Platelet collagen receptors. *Thromb Haemost* 2001; **86**: 189–97.

2 Watson SP, Asazuma N, Atkinson B, Berlanga O, Best D, Bobe R, Jarvis G, Marshall S, Snell D, Stafford M, Tulasne D, Wilde J, Wonerow P, Frampton J. The role of ITAM- and ITIM-coupled receptors in platelet activation by collagen. *Thromb Haemost* 2001; **86**: 276–88.

3 Nieswandt B, Bergmeier W, Schulte V, Rackebrandt K, Gessner JE, Zirngibl H. Expression and function of the mouse collagen receptor glycoprotein VI is strictly dependent on its association with the FcRgamma chain. *J Biol Chem* 2000; **275**: 23998–4002.

4 Asazuma N, Wilde JI, Berlanga O, Leduc M, Leo A, Schweighoffer E, Tybulewicz V, Bon C, Liu SK, McGlade CJ, Schraven B, Watson SP. Interaction of linker for activation of T cells with multiple adapter proteins in platelets activated by the glycoprotein VI-selective ligand, convulxin. *J Biol Chem* 2000; **275**: 33427–34.

5 Quek LS, Pasquet JM, Hers I, Cornall R, Knight G, Barnes M, Hibbs ML, Dunn AR, Lowell CA, Watson SP. Fyn and Lyn phosphorylate the Fc receptor gamma chain downstream of glycoprotein VI in murine platelets, and Lyn regulates a novel feedback pathway. *Blood* 2000; **96**: 4246–53.

6 Gross BS, Melford SK, Watson SP. Evidence that phospholipase C-gamma2 interacts with SLP-76, Syk, Lyn, LAT and the Fc receptor gamma-chain after stimulation of the collagen receptor glycoprotein VI in human platelets. *Eur J Biochem* 1999; **263**: 612–23.

7 Greer P. Closing in on the Fps/Fer and Fer protein-tyrosine kinases. *Nat Rev Mol Cell Biology* 2002; **3**: 278–89.

8 Avraham H, Price DJ. Regulation of megakaryocytopoiesis and platelet production by tyrosine kinases and tyrosine phosphatases. *Methods* 1999; **17**: 250–64.

9 Hackenmiller R, Kim J, Feldman RA, Simon MC. Abnormal Stat activation, hematopoietic homeostasis, and innate immunity in c-fes−/− mice. *Immunity* 2000; **13**: 397–407.

10 Senis Y, Zirngibl R, McVeigh J, Haman A, Hoang T, Greer PA. Targeted disruption of the murine fps/fes proto-oncogene reveals that Fps/Fes kinase activity is dispensable for hematopoiesis. *Mol Cell Biol* 1999; **19**: 7436–46.

11 Zirngibl R, Senis YA, Greer PA. Enhanced endotoxin-sensitivity in Fps/Fes-null mice with minimal defects in hematopoietic homeostasis. *Mol Cell Biol* 2002: **22**: 2472–86.

12 Penhallow RC, Class K, Sonoda H, Bolen JB, Rowley RB. Temporal activation of nontransmembrane protein-tyrosine kinases following mast cell Fc epsilon RI engagement. *J Biol Chem* 1995; **270**: 23362–5.

13 Craig AWB, Greer PA. Fer kinase is required for sustained p38 kinase activation and maximal chemotaxis of activated mast cells. *Mol Cell Biol* 2002; **22**: 6363–74.

14 Songyang Z, Shoelson SE, McGlade J, Olivier P, Pawson T, Bustelo XR, Barbacid M, Sabe H, Hanafusa H, Yi T, Ren R, Baltimore D, Ratnofsky S, Feldman RA, Cantley LC. Specific motifs recognized by the SH2 domains of Csk, 3BP2, fps/fes, GRB-2, HCP, SHC, Syk, and Vav. *Mol Cell Biol* 1994; **14**: 2777–85.

15 Haigh J, McVeigh J, Greer P. The fps/fes tyrosine kinase is expressed in myeloid, vascular endothelial, epithelial, and neuronal cells and is localized in the trans-golgi network. *Cell Growth Differ* 1996; **7**: 931–44.

16 Zoller KE, MacNeil IA, Brugge JS. Protein tyrosine kinases Syk and ZAP-70 display distinct requirements for Src family kinases in immune response receptor signal transduction. *J Immunol* 1997; **158**: 1650–9.
17 Sultzman L, Ellis C, Lin LL, Pawson T, Knopf J. Platelet-derived growth factor increases the *in vivo* activity of phospholipase C-gamma 1 and phospholipase C-gamma 2. *Mol Cell Biol* 1991; **11**: 2018–25.
18 Craig AW, Zirngibl R, Williams K, Cole LA, Greer PA. Mice devoid of fer protein-tyrosine kinase activity are viable and fertile but display reduced cortactin phosphorylation. *Mol Cell Biol* 2001; **21**: 603–13.
19 Law DA, Nannizzi-Alaimo L, Ministri K, Hughes PE, Forsyth J, Turner M, Shattil SJ, Ginsberg MH, Tybulewicz VL, Phillips DR. Genetic and pharmacological analyses of Syk function in alphaIIbbeta3 signaling in platelets. *Blood* 1999; **93**: 2645–52.
20 Asselin J, Gibbins JM, Achison M, Lee YH, Morton LF, Farndale RW, Barnes MJ, Watson SP. A collagen-like peptide stimulates tyrosine phosphorylation of syk and phospholipase C gamma2 in platelets independent of the integrin alpha2beta1. *Blood* 1997; **89**: 1235–42.
21 Fox JE. Cytoskeletal proteins and platelet signaling. *Thromb Haemost* 2001; **86**: 198–213.
22 Rittenhouse SE. Phosphoinositide 3-kinase activation and platelet function. *Blood* 1996; **88**: 4401–14.
23 Escolar G, White JG. Changes in glycoprotein expression after platelet activation: differences between *in vitro* and *in vivo* studies. *Thromb Haemost* 2000; **83**: 371–86.
24 Zirngibl R, Schulze D, Mirski SE, Cole SP, Greer PA. Subcellular localization analysis of the closely related Fps/Fes and Fer protein-tyrosine kinases suggests a distinct role for Fps/Fes in vesicular trafficking. *Exp Cell Res* 2001; **266**: 87–94.
25 White JG, Escolar G. EDTA-induced changes in platelet structure and function. adhesion and spreading. *Platelets* 2000; **11**: 56–61.
26 Moroi M, Jung SM, Okuma M, Shinmyozu K. A patient with platelets deficient in glycoprotein VI that lack both collagen-induced aggregation and adhesion. *J Clin Invest* 1989; **84**: 1440–5.
27 Arregui C, Pathre P, Lilien J, Balsamo J. The nonreceptor tyrosine kinase fer mediates cross-talk between N-cadherin and beta1-integrins. *J Cell Biol* 2000; **149**: 1263–74.
28 Ozawa K, Kashiwada K, Takahashi M, Sobue K. Translocation of cortactin (p80/85) to the actin-based cytoskeleton during thrombin receptor-mediated platelet activation. *Exp Cell Res* 1995; **221**: 197–204.
29 Ichinohe T, Takayama H, Ezumi Y, Arai M, Yamamoto N, Takahashi H, Okuma M. Collagen-stimulated activation of Syk but not c-Src is severely compromised in human platelets lacking membrane glycoprotein VI. *J Biol Chem* 1997; **272**: 63–8.
30 Asazuma N, Yatomi Y, Ozaki Y, Qi R, Kuroda K, Satoh K, Kume S. Protein-tyrosine phosphorylation and p72syk activation in human platelets stimulated with collagen is dependent upon glycoprotein Ia/IIa and actin polymerization. *Thromb Haemost* 1996; **75**: 648–54.
31 Lipfert L, Haimovich B, Schaller MD, Cobb BS, Parsons JT, Brugge JS. Integrin-dependent phosphorylation and activation of the protein tyrosine kinase pp125FAK in platelets. *J Cell Biol* 1992; **119**: 905–12.
32 Oda A, Ochs HD, Druker BJ, Ozaki K, Watanabe C, Handa M, Miyakawa Y, Ikeda Y. Collagen induces tyrosine phosphorylation of Wiskott–Aldrich syndrome protein in human platelets. *Blood* 1998; **92**: 1852–8.
33 Mitsui N, Inatome R, Takahashi S, Goshima Y, Yamamura H, Yanagi S. Involvement of Fes/Fps tyrosine kinase in semaphorin3A signaling. *EMBO J* 2002; **21**: 3274–85.
34 Greer P, Haigh J, Mbamalu G, Khoo W, Bernstein A, Pawson T. The Fps/Fes protein-tyrosine kinase promotes angiogenesis in transgenic mice. *Mol Cell Biol* 1994; **14**: 6755–63.
35 Sangrar W, Senis YA, Richardson M, Greer PA. Transgenic mice expressing an activated mutant Fps/Fes nonreceptor protein-tyrosine kinase are characterized by bleeding defects, thrombocytopenia and increased platelet volume. *Blood*, in press.
36 Stenberg PE, Pestina TI, Barrie RJ, Jackson CW. The Src family kinases, Fgr, Fyn, Lck, and Lyn, colocalize with coated membranes in platelets. *Blood* 1997; **89**: 2384–93.
37 Pestina TI, Stenberg PE, Druker BJ, Steward SA, Hutson NK, Barrie RJ, Jackson CW. Identification of the Src family kinases, Lck and Fgr in platelets. Their tyrosine phosphorylation status and subcellular distribution compared with other Src family members. *Arterioscler Thromb Vasc Biol* 1997; **17**: 3278–85.